African Journal of Biotechnology

Volume 15 Number 45, 9 November 2016

ISSN 1684-5315

Academic Journals

ABOUT AJB

The African Journal of Biotechnology (AJB) (ISSN 1684-5315) is published weekly (one volume per year) by Academic Journals.

African Journal of Biotechnology (AJB), a new broad-based journal, is an open access journal that was founded on two key tenets: To publish the most exciting research in all areas of applied biochemistry, industrial microbiology, molecular biology, genomics and proteomics, food and agricultural technologies, and metabolic engineering. Secondly, to provide the most rapid turn-around time possible for reviewing and publishing, and to disseminate the articles freely for teaching and reference purposes. All articles published in AJB are peer-reviewed.

Contact Us

Editorial Office: ajb@academicjournals.org

Help Desk: helpdesk@academicjournals.org

Website: http://www.academicjournals.org/journal/AJB

Submit manuscript online http://ms.academicjournals.me/

Editorial Board

African Journal of Biotechnology

Table of Content: Volume 15 Number 45 9 November, 2016

ARTICLES

academicJournals

Vol. 15(45), pp. 2530-2537, 9 November, 2016
DOI: 10.5897/AJB2015.14539
Article Number: 1030AB061537
ISSN 1684-5315

http://www.academicjournals.org/AJB

African Journal of Biotechnology

Full Length Research Paper

Characterization of mutant cowpea [*Vigna unguiculata* (L) Walp] lines using random amplified polymorphic DNAs (RAPDs) and amplified fragment length polymorphism (AFLP) markers

Olufisayo Atinuke Kolade[1]*, Mercy Oluremi Olowolafe[2] and Iyiola Fawole[3]

[1]Africa Rice Center, Nigeria.
[2]IAR & T, Moor plantation Ibadan, Nigeria.
[3]Department of Biological Science, College of Natural and Applied Science, Bells University of Technology, Ogun State, Nigeria.

Received 3 March, 2015; Accepted 24 October, 2016

Phylogenetic relationship and polymorphism was detected in 10 cowpea lines comprising of leaf, flower and stem mutants, their putative parents and an exotic accession using 10 random amplified polymorphic DNAs (RAPDs) and three primer combinations of amplified fragment length polymorphism (AFLP) markers. These mutants were earlier obtained through the probable activities of transposable elements. The RAPD and AFLP markers revealed a genetic diversity of 47 and 31%, respectively, within the cowpea lines used. Genetic distance ranged from 0.05 to 0.30 based on AFLP markers, while it ranged between 0.13 and 0.44 for RAPD markers. Cluster analysis indicated that there are differences in RAPD markers between the various mutants and it grouped an exotic genotype separately. OPC-14 primer had the highest discriminatory capacity (11 polymorphic fragments). The AFLP analysis was able to group two of the flower mutants, leaf mutants and wild types separately. A combined analysis of the two markers gave a similar grouping as was obtained from the AFLP analysis. AFLP was more discriminatory in grouping the plant samples and the exotic line was distinguished based on both markers. Useful heterotic prediction can be done based on the genetic distance between the mutants and their parents. This will further broaden the genetic base of cowpea and enhance the use of these mutants which have some evolutionary significance. In addition, unique allele RAPD_OPC15-500bp can be harnessed in genetic identification of reduced petal mutant. This study further corroborates the discriminatory power of AFLP over RAPDs.

Key words: *Vigna unguiculata*, amplified fragment length polymorphism (AFLP), randomly amplified polymorphic DNA (RAPD), mutants, transposable elements.

INTRODUCTION

Genetic diversity studies are usually done to assess the variation and the similarity within plant species. In breeding programs, this helps in determining the plant materials that can be crossed in order to obtain recombinants with the most favourable combination of desirable traits. Several mutants were obtained among

Table 1. List of the mutants and wild types and their sources.

Name	Description	Source
Ife brown	Non mutant cultivar	University of Ibadan , Ibadan Nigeria
Ife BPC	Non mutant cultivar derived from Ife Brown	IITA
Tvu1	Wild type	IITA
Tvu1509	Wild type	IITA
LM1	Unifoliate leaf form mutant	University of Ibadan , Ibadan Nigeria
LM2	Non petiolate and non-branching mutant	University of Ibadan , Ibadan Nigeria
RFM	Rose-like flower mutant	University of Ibadan , Ibadan Nigeria
RPM1	Reduced petal mutant	University of Ibadan , Ibadan Nigeria
RPM2	Reduced petal mutant	University of Ibadan , Ibadan Nigeria
Tvu 94051	Non mutant line/exotic line	University of California Davis, Davis CA USA

the progenies from crosses made by previous workers on cowpea. These mutants, with genetic evidence used in this study, have shown to be under the influence of transposable elements. Mutants are sources of variation, which may be useful in introducing unique and useful alleles to new populations. Genetic variation is required for crop improvement, hence the need to broaden the genetic base of any crop. This study was done in order to further enhance this in cowpea.

While assessing diversity and phylogenetic relationship with other mutants and their parents, each unique mutant was also characterized. Randomly amplified polymorphic DNA (RAPD) developed by Williams et al. (1990) has been successfully used in assessing diversity in many crops including cassava (Marmey et al., 1994), tropical pumpkin (Gwanama et al., 2000), somatic mutants of grapes (Maia et al., 2009) and more recently to assess diversity in Faba bean (Yahia et al., 2014) and cowpea (Anatala et al., 2014). It is an efficient marker for fingerprinting, evaluation of gene flow and studying traits such as pest resistance. Among PCR based assays, RAPD is more effective and easier than specific PCR based assays because they neither require sequence information nor any previous knowledge of the target genome, and moreover, they are relatively simple and rapid to perform (Mumtaz et al., 2009).

These cowpea lines were further characterized using amplified fragment length polymorphism (AFLP) developed by Vos et al. (1995). This PCR based marker, which has been widely used in genetic diversity studies, is reportedly more discriminatory in assessing diversity than the other markers like RAPDs and simple sequence repeats SSRs (Powell et al., 1996). Liu and Hou (2010) and Ojuederie et al. (2014) used AFLP in the assessment of genetic diversity of pigeon pea and African yam bean, respectively.

Baker et al. (1990), Garcia et al. (2004), Baraket et al. (2010) Ikechukwu et al. (2014) and Anatala et al. (2014) also used a combination of two or more molecular markers to assess more robust diversity or to compare the effectiveness of one marker relative to the other. The objectives of this study were to (i) compare the information provided by these markers in characterizing mutants and parents, (ii) compare the genetic distance information of these mutants and parents and (iii) show if there are unique alleles which can distinguish the mutant lines from their wild types (parents).

MATERIALS AND METHODS

Plant materials

Five mutants lines out of the 10 cowpea samples used for this study were obtained from the Department of Crop Protection and Environmental Biology, University of Ibadan. The mutants were obtained and selected from the progenies from crosses between several cowpea lines. They are namely: reduced petal mutant 1 (RPM-1), reduced petal mutant 2 (RPM-2), Rosa flower mutant (RFM), leaf mutants (LM-1) and LM-2. Their parents/wild types: Tvu 1509, Tvu 1, Ife brown, Ife BPC were obtained from the Gene bank of the International Institute of Tropical Agriculture and Tvu 94051 an 'exotic' cowpea cultivar (DNA) was obtained from University of California Davies. Ife Brown is the putative parent of Ife BPC (Table 1). The mutants are progenies of crosses between Ife brown and other lines.

DNA extraction

The seeds of the mutants and their parents were planted out in pots in the screen house, and young leaves were harvested from them at two weeks. DNA was extracted from these samples using the CTAB method (Dellarporta et al., 1983). The entire study was carried out at the Central Biotech Laboratory of International Institute of Tropical Agriculture (IITA) Ibadan, Nigeria.

*Corresponding author. E-mail: o.kolade@cgiar.org.

Table 2. List of RAPD primers used for this study and their sequences.

Primer name	Sequence	No. of fragments	No. of polymorphic fragments
OPQ1	GGGACGATGG	10	7
OPQ15	GGGTAACGTG	10	6
OPP1	GTAGCACTCC	8	4
OPP13	GGAGTGCCTC	7	4
OPP15	GGAAGCCAAC	6	5
OPB06	TGCTCTGCCC	9	6
OPI20	AAAGTGCGGG	9	6
OPC10	TGTCTGGGTG	9	8
OPI04	CCGCCTAGTC	6	5
OPC14	TGCGTGCTTG	11	11
	Mean	81	62 (76%)

PCR amplification

For the RAPD study, OPERON primers OPQ1, OPQ15, OPP1, OPP13, OPP15, OPB06, OPI20, OPC10, OPI04 and OPC14 of 10mer oligonucleotides were used in this study (Table 2). Reactions were carried out in a total volume of 25 µl containing 1X buffer, 50 mM KCl, 1.5 mM $MgCl_2$, 0.1% Tween 20, 2.5 mM each of dNTPs (Promega), 50 ng of genomic DNA and 1 unit of Taq polymerase (Bioline). PCR reactions were carried out in a thermal cycler (MJ Research). The samples were subjected to an initial denaturation at 94°C for 4 min, 45 cycles of 1 min at 94°C, one min at 37°C and 2 min at 72°C and then a final extension at 72°C for 5 min. Amplification products were analyzed on 1.5% agarose gels in 1X Tris Acetate EDTA (TAE) buffer at 100 V for 2 h and detected by staining with ethidium bromide.

AFLP marker analysis

PCR was carried out with genomic DNA obtained by using the same extraction protocol as used above. 400 ng DNA was digested with Mse and EcoR1 enzymes (5 u/µl) in a total volume of 25 µl. Ligations were carried out for 2 h using specific adapters. Pre-selective amplification was carried out on a 1:10 dilution of the ligated product in 10 µl following manufacturer's instructions. The mix was amplified using the following program: denaturation at 94°C for 2 min, 25 cycles of 2 min at 94°C, 1 min at 56°C and 1 min at 72°C and then a final extension at 72°C for 5 min. For selective amplification, 1:50 dilutions of pre amplification product was made and thereafter used as template for the reaction with the '+3' primers namely EAACMCAG, EAACMCAG and EAACMCTG.

The PCR was done using a modified touch down progam as follows: 94°C for 2 min, 12 cycles of 2 min at 94°C, one min at 65°C (-0.7°C per cycle) and 1 min at 72°C after which there were 23 cycles of 2 min at 94°C, 1 min at 56°C and 1 min at 72°C and then a final extension at 72°C for 5 min.

Gel electrophoresis

An aliquot of 5 µl of the product was mixed with equal volume of formamide dye, denatured for 5 min at 94°C and snap-chilled on ice. These products were separated on 6% PAGE gels. Electrophoresis was carried out in 1X TBE buffer at a constant power of 70 W for 2½ h at 50°C. Silver staining was carried out to visualize the bands on the gels.

Data analysis

Presence and absence of bands were scored using binary code of 1 or 0, respectively. Matrixes of distances were generated using SIMQUAL program of Numerical and Taxonomy system software (NTSYS) 2.0 (Rohlf, 1998). Clustering was done using the SAHN algorithm of the unweighted pair group method using average linkages (UPGMA) and a tree was obtained using the tree plot option of NTSYS, a rooted tree was also generated from the DARwin software version 4 (Perrier and Jacquemoud-Collet, 2006).

RESULTS

DNA fingerprints were obtained for all the mutants and their parents using both RAPDs and AFLP markers. Plate 1 shows the amplification obtained using RAPD primer OPP13 and Plate 2 shows the amplification obtained for the 10 samples using AFLP marker EAACMCAG. Based on the RAPD analysis, the total number of fragments obtained from the 10 primers on the 10 samples was 81 while the total number of polymorphic fragment was 62 (76%). The number of fragments for each primer varied from 6 to 11 fragments among the primers, with an average of 6.8, whereas OPC-14 primer showed the greatest capacity for discriminating polymorphism in the population studied (Table 2). From the DARwin analysis, a diversity of 31% was obtained from RAPD markers for these lines. Three mini groups were obtained from the use of the RAPD markers, while the exotic line Tvu 94051 and Reduced petal mutant 2 (RPM2) were grouped separately. Cluster I consisted of LM1 and RFM, cluster II consisted of Ife BPC, Ife brown and LM2, while cluster III consisted of Tvu1, Tvu1509 and RPM1. Line Tvu94051 from California was grouped alone in group II (Figure 1).

Conversely, a diversity of 47% was obtained from the AFLP analysis. Reduced petal mutant: RPM2, Tvu1 and Tvu 94051 clustered, separately. One cluster consisted of Ife BPC and Tvu1509 while another cluster consisted of RFM and RPM1, both flower mutants. In addition, the leaf

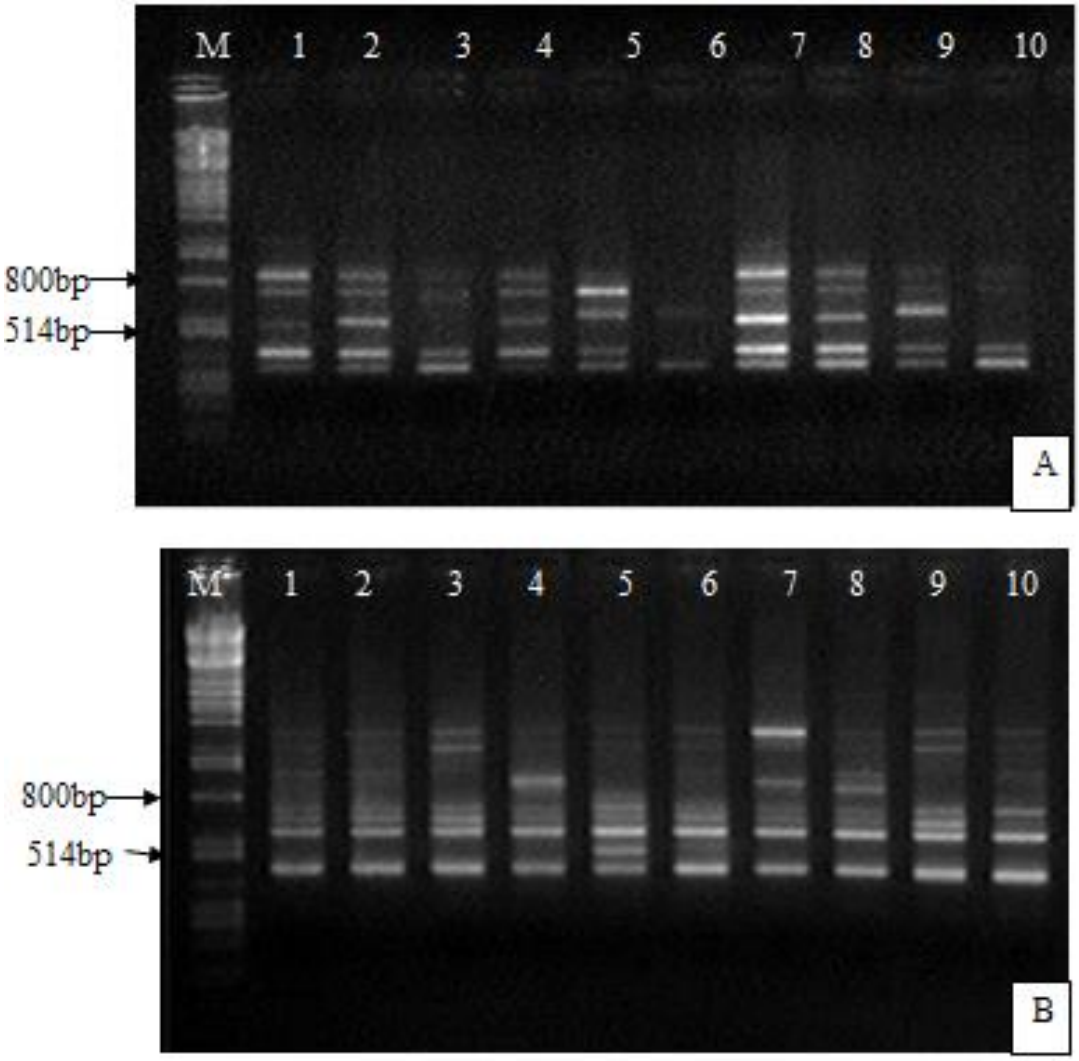

Plate 1. Amplification obtained from the mutant cowpea lines and parents using RAPD primers OPP13 (A) and OPQ15 (B). M is Lambda DNA pst1 digest. 1 = Ife Brown, 2 = Ife BPC, 3 = Tvu 1, 4 = LM1, 5 = RPM1, 6 = RPM2, 7 = RFM, 8 = LM2, 9 = Tvu1509, 10 = Tvu 94051 (arrow points at a band ca 520 bp distinguishing RPM1 from others).

mutants LM1 and LM2 clustered together with Ife brown (Figure 2). It was observed that the RAPD analysis was able to group the parental types together and the exotic line separately as compared to AFLP. For instance, the two cultivated parental lines, Ife Brown and Ife BPC clustered together while the wild types Tvu1 and Tvu 1509 were also found together in another cluster. However, in the case of AFLP, two of the flower mutants, were clustered together, while the two leaf mutants were in the same cluster along with Ife brown. Both RPM2 and Tvu 94051 (exotic line) were in a class of their own in both analyses. The AFLP analysis was more discriminatory as it gave a higher genetic distance among the lines and gave more separation based on the grouping of the mutants. It also gave a similar pattern to the combined analysis of the two markers.

The genetic distance ranged between 0.05 and 0.30, the lower value was obtained between Ife BPC and LM2, while the highest values were obtained between RFM and RPM2 and between LM2 and RPM2 based on RAPD analysis (Table 3). However, for the AFLP analysis, the genetic distance ranged between 0.13 and 0.44 which were obtained between LM2 and Ife brown and between RPM2 and Ife BPC, respectively (Table 4). A combined analysis of both AFLP and RAPD however gave a similar pattern to the AFLP in terms of grouping but a different genetic distance. The distance ranged from 0.13 to 0.36 with many pairs having the higher value. All the mutants and parents except RPM1 and exotic line had a genetic distance of 0.36 with RPM2. In addition, Tvu 94051 had the same distance of 0.36 with RFM, LM2 and Tvu 1509 (Table 5).

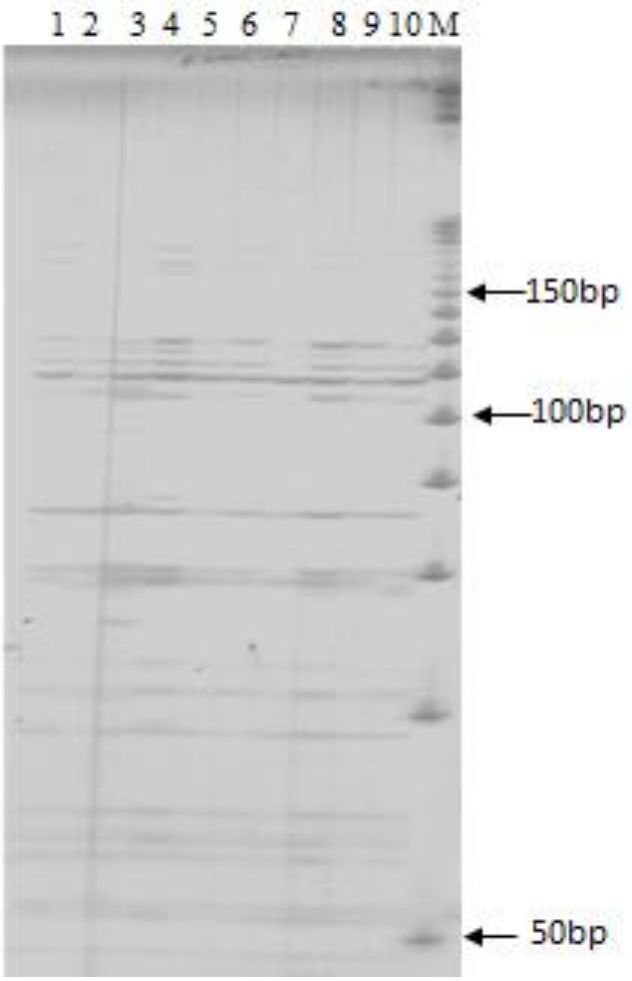

Plate 2. AFLP amplification of the mutant cowpea lines and their parents using primer EAACMCAG. Marker is 30 to 330 bp marker.1 = Ife Brown, 2 = Ife BPC, 3 = Tvu 1, 4 = LM1, 5 = RPM1, 6 = RPM2, 7 = RFM, 8 = LM2, 9 = Tvu1509, 10 = Tvu 94051.

The search for unique alleles revealed that there were no many bands distinguishing certain mutants from the other. A unique allele was however observed in the RAPD OPQ15_ 500 (about 500 bp) which distinguished the RPM1 from the others (Figure 1b).

DISCUSSION

The levels of differences obtained from the two molecular markers are relatively low; this is because they share a similar background but for the mutations on all the mutants which are derivatives of Ife Brown and Ife BPC. These are mutants that were obtained due to activities of transposable elements (TEs) and obtained from previous studies (Fawole, 1988a, 1997, 1998b, 2001, 2010). They have increased the genetic base of cowpea as additional sources of variation for future breeding work. The TEs have been characterized using molecular markers by Kolade et al. (2015).

The RAPD analysis gave a similar level of polymorphism, 62 out of 81 (76%) from 10 primers as compared to a previous study by Anatala et al. (2014) on cowpea genetic diversity which gave 67%, 81 out of 120 fragments. The clustering, which appeared to be based on the type of mutation or origin is an interesting observation. In this case, the fact that the leaf mutants, the flower mutants clustered close to each other and the wild species were found in the same cluster, while the exotic variety was found in separate cluster, indicated the usefulness of the markers for grouping based on the kind of mutation that exists in the sample and where the samples originated from. This has been observed by many authors, while using RAPD markers in population genetic analysis of biodiversity, relationships among species at different levels, to identify cultivars and to reveal phylogenetic relationships among them (Ba et al., 2004; Malviya and Yadav, 2010; Motagi et al., 2013; Anatala et al., 2014).

The more discriminatory power of the AFLP has been shown (Archak et al., 2003) for comparative analysis while using RAPD, ISSR and AFLP in Cashew (*Anachardium occidentalis*). This study also corroborates it but further showed that a combination of RAPD and AFLP is also slightly more discriminatory than when either is used singly. The reduced flower mutant, RPM2, might have clustered differently from the other flower mutants, because it is an unstable mutant. In addition, discrimination of the flower mutants from that of the wild types and the leaf mutants as revealed by AFLP analysis than RAPDs in the present studies agree with previous reports that compared two types of molecular markers (Barker et al., 1999; Garcia et al., 2004; Baraket et al., 2010).

Conclusion

This study reveals the phylogenetic relationship between these mutants and their parents. The exotic line was different from the rest with the two molecular markers, indicating the difference in their pedigree and geographical origin. AFLP analysis was found to be more discriminatory in characterizing the mutants than the RAPD analysis and gave a similar grouping pattern as obtained from the combined analysis. The result obtained here will be useful for breeders who are willing to explore the possibility of pyramiding genes that are responsible for rose like flower mutations, reduced petal mutation and others studied. The level of diversity as evident in these mutants can be harnessed in breeding for better varieties as the divergent genotypes are expected to result in high heterosis. The unique allele can be harnessed for genotype identity.

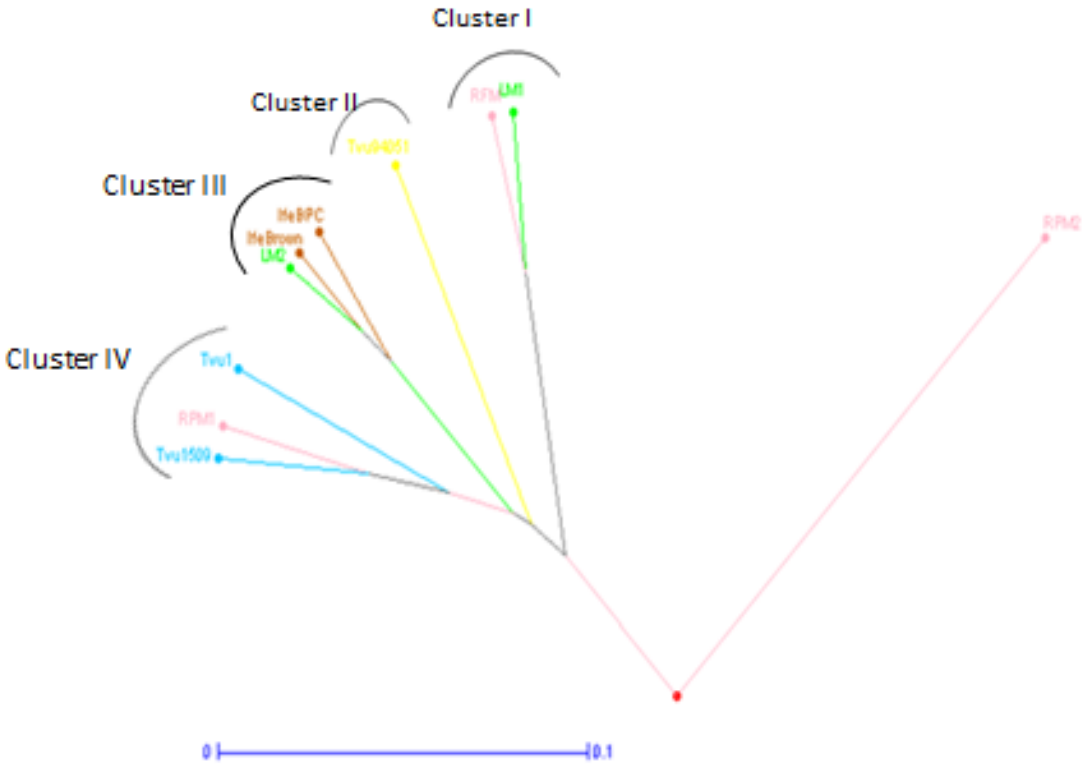

Figure 1. Rooted diagram (axial) obtained from the analysis of the mutant lines and parents using RAPD markers (DARwin) (pink represents flower mutants, blue represents wild type, green represents leaf mutants and yellow, exotic line).

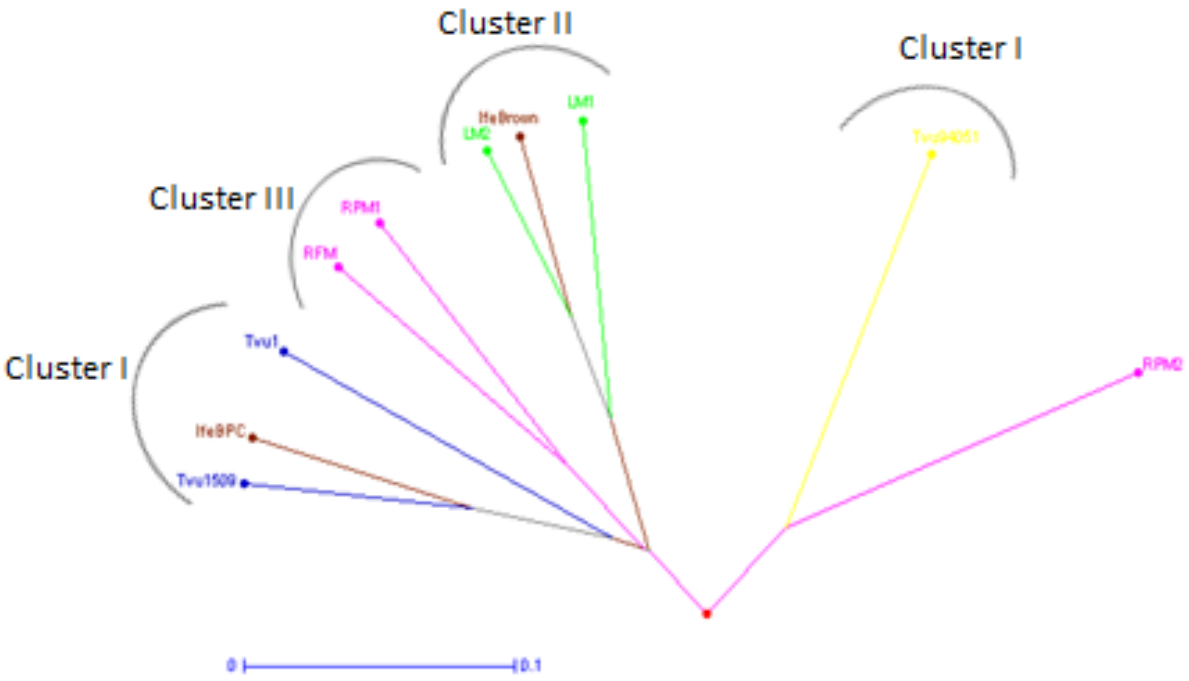

Figure 2. Rooted diagram (axial) obtained from the analysis of the mutant lines and parents using RAPD and AFLP markers (DARwin) (pink represents flower mutants, blue represents wild type, green represents leaf mutants and yellow, exotic line).

Table 3. Genetic distance matrix revealed by RAPD analysis.

Variables	Ife Brown	Ife BPC	Tvu1	LM1	RPM1	RPM2	RFM	LM2	TVu1509
Ife BPC	0.06								
Tvu1	0.13	0.17							
LM1	0.17	0.21	0.16						
RPM1	0.18	0.22	0.15	0.22					
RPM2	0.26	0.3	0.23	0.29	0.19				
RFM	0.17	0.22	0.17	0.07	0.23	0.3			
LM2	0.07	0.05	0.17	0.21	0.23	0.3	0.22		
Tvu1509	0.13	0.17	0.1	0.16	0.08	0.16	0.17	0.17	
Tvu94051	0.15	0.19	0.16	0.2	0.21	0.29	0.21	0.20	0.16

Table 4. Genetic distance matrix revealed by AFLP analysis.

Variables	Ife Brown	Ife BPC	Tvu1	LM1	RPM1	RPM2	RFM	LM2	Tvu1509
Ife BPC	0.33								
Tvu1	0.30	0.31							
LM1	0.19	0.34	0.31						
RPM1	0.26	0.31	0.28	0.28					
RPM2	0.33	0.44	0.41	0.35	0.37				
RFM	0.30	0.35	0.32	0.31	0.22	0.41			
LM2	0.13	0.36	0.33	0.22	0.29	0.36	0.33		
Tvu1509	0.26	0.17	0.24	0.28	0.25	0.37	0.28	0.29	
Tvu 94051	0.30	0.41	0.38	0.31	0.34	0.28	0.38	0.33	0.34

Table 5. Genetic distance matrix from combined RAPD and AFLP analyses.

Variables	Ife brown	Ife BPC	Tvu1	LM1	RPM1	RPM2	RFM	LM2	Tvu1509
Ife BPC	0.30								
Tvu1	0.30	0.27							
LM1	0.21	0.30	0.30						
RPM1	0.30	0.30	0.30	0.30					
RPM2	0.36	0.36	0.36	0.36	0.36				
RFM	0.30	0.30	0.30	0.30	0.22	0.36			
LM2	0.13	0.30	0.30	0.21	0.30	0.36	0.30		
Tvu1509	0.30	0.17	0.27	0.30	0.30	0.36	0.30	0.30	
Tvu 94051	0.36	0.36	0.36	0.36	0.36	0.28	0.36	0.36	0.36

Conflicts of Interests

The authors have not declared any conflict of interests.

REFERENCES

Anatala TJ, Gajera HP, Savaliya DD, Domadiya RK, Patel SV, Golakiya BA (2014). Molecular Diversity Analysis of Cowpea (*Vigna unguiculata* L.) Genotypes Determined by ISSR and RAPD Markers. Int. J. Agric. Environ. Biotechnol. 7(2):269.

Archak S, Gaikwad AB, Gautam D, Rao EV, Swamy KR, Karihaloo JL (2003). Comparative assessment of DNA fingerprinting techniques (RAPD, ISSR and AFLP) for genetic analysis of cashew (*Anacardium occidentale* L.) accessions of India. Genome 46(3):362-369.

Ba FS, Pasquet RS, Gepts P (2004). Genetic diversity in cowpea (*Vigna unguiculata* (L.) Walp) as revealed by RAPD markers. Gen. Res. Crop Evol. 51:539-550.

Baraket G, Chatti K, Saddoud O, Abdelkarim AB, Mars M, Trifi M, Hannachi AS (2010). Comparative Assessment of SSR and AFLP Markers for Evaluation of Genetic Diversity and Conservation of Fig, Ficus carica L., Genetic Resources in Tunisia. Plant Mol. Biol. Rep. 29(1):171-184

Barker JHA, Matthes M, Arnold GM, Edwards KJ, Ahman I, Larsson S, Karp A (1999). Characterisation of genetic diversity in potential biomass willows (*Salix spp*.) by RAPD and AFLP analyses. Genome 42:173-183.

Dellarporta SF, Wood J, Hicks JB (1983). A plant DNA minipreparation version two. Plant Mol. Biol. Rep. 1:19-21.
Fawole I (1988a). A non-petiolate leaf mutant in Cowpea [*Vigna unguiculata* (L.) Walp.] J. Hered. 16:484-487.
Fawole I (1998b). Two unstable dominant genes in cowpea, Vigna unguiculata (L.) Walp. Eighteenth International Congress of Genetics, Beijing, China, August 10-15. Chinese Academy of Sciences and the Genetics Society of China; 29.
Fawole I (1997). Inheritance of crinkled leaf in cowpea [*Vigna unguiculata* (L) Walp.]. Niger. J. Sci. 31:35-40.
Fawole I (2001). Genetic analysis of mutations at loci controlling leaf form in cowpea (*Vigna unguiculata*) J. Hered. 1:43-50.
Fawole I (2010). Origin, Morphology & Inheritance of Dominant Mutations affecting Flower form and Colour in Cowpea. Niger. J. Sci. 44:77-87
Garcia AAF, Benchimol LL, Barbosa AMM, Geraldi IO, Souza Jr. CL, de Souza AP (2004). Comparison of RAPD, RFLP, AFLP and SSR markers for diversity studies in tropical maize inbred lines. Genet. Mol. Biol. 27(4):579-588.
Gwanama C, Labuschagne MT, Botha AM (2000). Analysis of genetic variation in *Cucurbita moschata* by randomly amplified polymorphic DNA (RAPD) markers. Euphytica 113:19-24.
Ikechukwu A, Prakash P, Sabhojit D, Nadarajan N (2014). Comparative efficiency of SRAP, SSR and AFLP-RGA markers in resolving genetic diversity in Pigeon Pea (Cajanus sp). Ind. J. Biotechnol. 14:486-495.
Kolade O, Raji A, Fawole I, Ingelbrecht I (2015). Molecular Characterization of transposable elements in cowpea (*Vigna unguiculata* (L.) Walp. Am. J. Plant Sci. 6:767-776.
Liu Y, Hou W (2010). Genetic Diversity of Faba Bean Germplasms in Qinghai and Core Germplasm Identified based on AFLP Analysis. Legume Genom. Genet. 11:1.
Maia SHZ, Mangolin CA, Collet SAO, Machado MFPS (2009). Genetic diversity in somatic mutants of grape (*Vitis vinifera*) cultivar Italia based on random amplified polymorphic DNA. Genet. Mol. Res. 8(1):28-38.
Malviya N, Yadav D (2010). RAPD Analysis among Pigeon pea [*Cajanus cajan* (L.) Mill sp.] Cultivars for their Genetic Diversity. Genet Eng. Biotechnol. J.1:1-9.
Marmey P, Beeching JR, Hamon S, Charrier A (1994). Evaluation of cassava (*Manihot esculenta* Crantz) germplasm collections using RAPD markers. Euphytica 74:203-209.
Motagi BN, Angadi CC, Naidu GK, Shashidhar TR (2013). Genetic diversity analysis of cowpea [Vigna unguiculata (L.) Walp] genotypes using RAPD markers. Int. J. Agric. Sci. 9:320-322.
Mumtaz S, Khan IA, Ali S, Zeb B, Iqbal A, Shah Z, Swati ZA (2009). Development of RAPD based markers for wheat rust resistance gene cluster (*Lr37-Sr38-Yr17*) derived from *Triticum ventricosum* L. Afr. J. Biotechnol. 8(7):1188-1192.
Ojuederie BO, Balogun OM, Fawole I, Igwe OD, Olowolafe OM (2014). Assessment of the genetic diversity of African Yam bean (Sphenostylis stenocarpa Hochst ex. A Rich Harms) accessions using Amplified Fragment Length Polymorphism (AFLP) markers. Afr. J. Biotechnol. 13(18):1850-1858.
Perrier X, Jacquemoud-Collet JP (2006). DARwin software, http://darwin.cirad.fr
Powell W, Morgante M, Andre C, Hanafey M, Vogel J, Tingey S, Rafalski A (1996). The comparison of RFLP, RAPD, AFLP and SSR (microsatellite) markers for germplasm analysis. Mol. Breed. 2:225-238.
Rohlf FJ (1998). Numerical Taxonomy and Multivariate Analysis System (NTSYSpc ver 2.0.).
Vos P, Hogers R, Bleeker M, Reijans M, Van de Lee T, Hornes M. Frijters A, Pot J, Peleman J, Kuiper M, Zabeau M (1995). AFLP: a new technique for DNA fingerprinting, Nucleic Acid Res. 23:4407-4414.
Williams JGK, Kubelik AR, Livak KJ, Rafalski JA, Tingey SS (1990). DNA polymorphisms amplified by arbitrary primers are useful as genetic markers. Nucleic Acid Res. 18:6531-6535.
Yahia Y, Hannachi H, Ferchichi A (2014). Genetic diversity of Vicia faba L. based on random amplified polymorphic DNA and simple sequence repeat markers. Acta Bot. Gall. 161(2):151-158.

academicJournals

Vol. 15(45), pp. 2538-2546, 9 November, 2016
DOI: 10.5897/AJB2016.14902
Article Number: 0A64E6961539
ISSN 1684-5315

http://www.academicjournals.org/AJB

African Journal of Biotechnology

Full Length Research Paper

Pan-genome analysis of Senegalese and Gambian strains of *Bacillus anthracis*

M. Mbengue[1*], F. T. Lo[1], A. A. Diallo[1], Y. S. Ndiaye[1], M. Diouf[1] and M. Ndiaye[2]

[1]National Laboratory for Research on Animal Diseases (LNERV – ISRA) - Hann – Dakar – P. O Box 2057, Senegal.
[2]Biocellular laboratoty for Research on Microbiology and Rickettssiology, Faculty for Sciences and Technology - Dakar University (UCAD) – Senegal.

Received 4 August, 2015; Accepted 10 October, 2016

Bacillus anthracis **is the causative agent of anthrax, and it is classified as "category A" biological weapon. There were six available complete genomes (A0248, Ames, Ames Ancestor, CDC684, H0491 and Sterne). Here, one Gambian and two Senegalese strains (Gmb1, Sen2Col2 and Sen3) were added. In this work, the pan-genome of *B. anthracis* was studied based on nine strains and using bioinformatics tools as Cluster of Orthologous Groups (COG) and Kyoto Encyclopedia of Genes and Genomes (KEGG). Thereafter, *B. anthracis* pan-genome having 2893 core genes and 85 accessory genes was estimated. With Mauve method, the pan-genome of *B. anthracis* was verified and it was found to be very narrow and clonal. To have confidence in this study, different tools were used to compare and validate the results. All of the tools yielded the same results; the addition of the Senegalese and Gambian strains did not change the nature of the *B. anthracis* pan-genome (2893 core genes and 85 accessory genes), which had a core/pan-genome ratio of 99%. The closed nature of the pan-genome of *B. anthracis* (the core genome) represents 99% of the pan-genome size. The hypothesis that *B. anthracis* had a closed pan-genome was hereby validated.**

Key words: *Bacillus anthracis,* Senegalese, Gambian strains, pan-genome.

INTRODUCTION

Anthrax was the first disease to be attributed to a specific microbe, thanks to Davaine in 1863 (Scarlata et al., 2010) and the first animal infection for which we had a vaccine by Pasteur in 1881 (Scarlata et al., 2010). In 1876, Koch discovered for the first time a bacterium which has the capacity to transform into spores: *Bacillus anthracis* (Scarlata et al., 2010). *B. anthracis*, in the Firmicutes phylum and belonging to the *Bacillus cereus* group (Kuroda et al., 2010), is a Gram positive spore-forming bacterium (Wang et al., 2012), which is able to survive in extreme and unfriendly environmental conditions as high levels of radiation or extreme temperature (Wang et al., 2012) and can stay viable in the soil for a long time (Sweeney et al., 2011). *B. anthracis* is the causative agent of anthrax (Kuroda et al., 2010), a zoonosis. Cattle and horses are mainly sensitive (Scarlata et al., 2010).

*Corresponding author. E-mail: mbenguem@yahoo.fr.

Humans can be infected by various routes: ingestion, inhalation of spores or through the skin (Kuroda et al., 2010). There are four clinical syndromes for anthrax disease (Sweeney et al., 2011): cutaneous anthrax (95% of the reported cases), gastrointestinal anthrax (due to contaminated food), inhalational anthrax, and injectional anthrax. *B. anthracis* is classified as a "Category A" potential biothreat (Wang et al., 2012). Indeed, due to the stability of its spores, the high level pathogenicity and lethality and its capacity to be infected by the inhalational route (Rasko et al., 2011), this bacterium represents a bioterrorism weapon. In these days, one bioterrorist attack was done in 2001 in the United States (Scarlata et al., 2010) using a strain of *B. anthracis*, the potential source of which was identified based on genomic analysis. Earlier, they had an attack in USSR in 1979, with an anthrax epidemic through an atmospheric contamination from a military laboratory (Guillemin, 2002; Scarlata et al., 2010). The 2001 event led to an increase of the research about *B. anthracis* and anthrax (Imperiale and Casadevall, 2011) and allows the emergence of new detection system (Wang et al., 2012).

The first genome sequencing study of multiple stains was published in 2005 on *Streptococcus agalactiae* (Tettelin et al., 2005) and, since then, such pangenomic studies have increased quickly. On working on pan-genomes, allowed a comparison between different species or strains, and it is defined like the pool of all the genes present in all the studied genomes. This can be divided into different parts: the core genome (genes present in all the genomes), accessory genes which are present in some genomes and unique genes (genes present only in one of the studied genomes). A pan-genome can be closed or open, depending of the capacity of the species to acquire new genes (Tettelin et al., 2005) and of the age of the initial clone.

Senegalese and Gambian strains of *B. anthracis* have not been compared to the other strains (Read et al., 2002). In this study, analysis of the *B. anthracis* pan-genome was carried out based on three African strains (two from Senegal and one from Gambia) and on six reference genomes [Ames (Read et al., 2003), Ames Ancestor (Ravel et al., 2009), A0248, CDC684 (Okinaka et al., 2011), H9401 (Chun et al., 2012), and Sterne]. The present study shows that African strains were very closely related to the other strains and presented a closed pan-genome, as already shown in previous studies.

MATERIALS AND METHODS

Bacteriological studies

Cells from various organs were cultured in a liquid medium consisting of ordinary broth. After seeding, the medium was incubated at 37°C for 24 h. The isolation ensues on sheep blood agar (blood culture) which was incubated as earlier stated. Gram stain is performed from isolates, as well as the study of biochemical characteristics.

Sequencing

The sequencing strategies of the three strains *B. anthracis* Sen2col2, Sen3 and Gmb1 were carried out through the SOLiD 4_Life technologies in New Generation Sequencing (NGS) technologies (Figure 2). Sequencing of the Sen2col2, Sen3 and Gmb1 strains of *B. anthracis* were performed using the SOLiD 4_Life Technology's New Generation Sequencing technology. The paired end library was constructed from 1 lg of purified genomic DNA from each strain. The sequencing was carried out to 50935 base pairs (bp) using SOLiDTM V4 chemistry on one full slide associated with 96 other projects on an Applied Biosystems SOLiD 4 machine (Applied Biosystems, Foster City, CA, USA). All 96 genomic DNA samples were barcoded with the module 1 to 96 barcodes provided by Life Technologies (Paisley, UK). The libraries were pooled in equimolar ratios, and emPCR (PCR by emulsion) was performed according to the manufacturer's specifications, using templated bead preparation kits on the EZ bead automated Emulsifier, Amplifier and Enricher E80 system for full-scale coverage. A total of 708 million P2-positive beads were loaded onto the flow cell for the run and the output read length was 85 bp, as expected (50935 bp). The three *B. anthracis* genomes (Sen2col, Sen3 and Gmb1) were sequenced through 3.2^{E} + 6, 3.1^{E} + 6 and 3.9^{E} + 6 barcode reading which led to 273, 262, and 382 Mb of data, respectively. The global sequencing of these three genomes resulted in 917 Mb of data.

Basic genomic data

The complete genomic sequences of the six references strains are available on the NCBI: Ames (NC_003997.3), Ames Ancestor (NC_007530.2), A0248 (NC_012659.1), CDC684 (NC_012581.1), H9401 (NC_017729.1), and Sterne (NC_005945.1). Our strains of interest came from Senegal (Sen2Col2 and Sen3) and from Gambia (Gmb1). They were isolated in 2010. The first one (Sen2Col2) was isolated from lungs of a 6 years old ostrich. The second one (Sen3) came from lungs, liver, spleen and blood of a Touabire race sheep. The last one, Gmb1, was isolated on trypanotolerant zebu cattle's blood (Table 1). The sequences of these three Senegalese and Gambian strains (Sen2Col2, Sen3 and Gmb1) were obtained in reference to SOLiD data.

Genomic analysis

Cluster of Orthologous Groups (COG) and Kyoto Encyclopedia of Genes and Genomes (KEGG)

CAMERA (Sun et al., 2011) is a bioinformatics portal where several kind of analysis can be done. It was used to generate the COG data. COG (Tatusov et al., 2001) is a common tool, used to assign functional annotations to proteins. These proteins were classified into categories (the list is available at http://www.ncbi.nlm.nih.gov/COG/old/palox.cgi?fun=all). To get KEGG (Ogata et al., 1999) data and to investigate metabolic pathways, the KAAS (Moriya et al., 2007) (KEGG automatic annotation server) online tool was used. In KEGG, the proteins were classified into classes and subclasses.

Alignments, pan-genome

First of all, two kinds of alignments were performed: a global genome alignment with MAUVE (Darling et al., 2010). With MAUVE (Figure 1) and its backbone output file (Sheppard et al., 2013), the proportion of core genome depending on the pan-genome size was calculated to evaluate the close or open nature of the pan-genome.

Table 1. Characteristics of *Bacillus anthracis strains* (samples).

Code	Strains	Country	Host	Samples origin
G192	Sen2Col2	Senegal	Ostrich 6 Years old	Lungs
G193	Sen3	Senegal	Mouton de race Touabire	Lungs, blood
G194	Gmb1	Gambia	Bovin de race Ndama Trypanotolérante	Blood
Ref strains	Ames	USA	Vache morte	/
Ref strains	Ames Ancestor	USA	Beefmaster female 14 years old	/
/	A0248	USA	Human	/
/	H9401	Korea	Human	/
/	CDC684	USA	Human	/
/	Sterne	UK	/	/

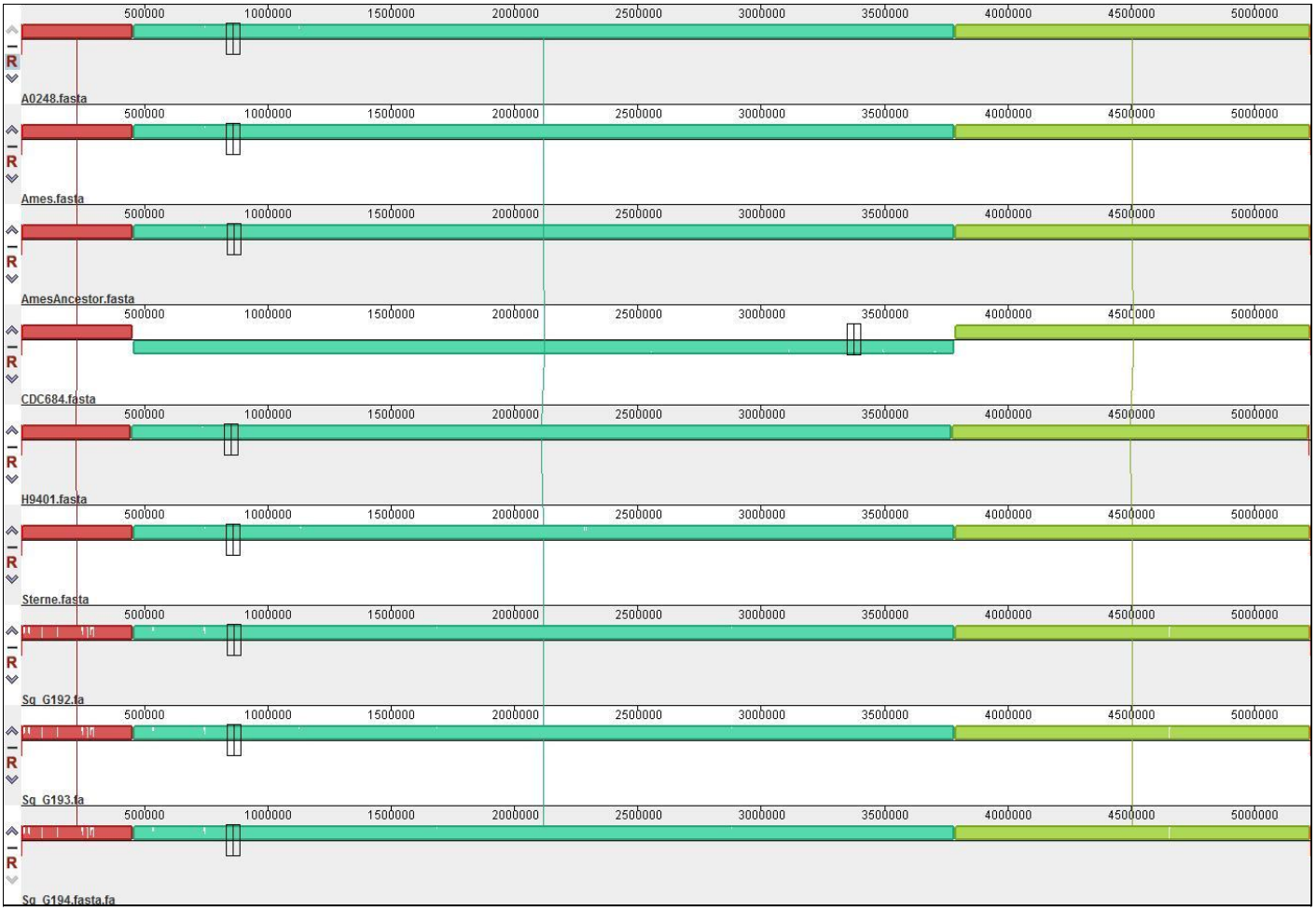

Figure 1. MAUVE global alignement.

Then, OrthoMCL (Chen et al., 2006) was used to obtain a list of orthologs to determine the pan-genome composition (core, accessory and unique genes). MeV (Saeed et al., 2006, 2003) (Multi Experiment Viewer) was used to best visualize the accessory genes distribution and to perform a hierarchical clustering (Figure 7). Clustering of the strains was based on the distribution of all the Cluster of Orthologous Groups categories: J, translation, ribosomal structure and biogenesis; K, transcription; L, replication, recombination and repair; B, chromatin structure and dynamics; D, cell cycle control, cell division, chromosome partitioning; O, post-translational modification, protein turnover, chaperones; M, cell wall/membrane/envelope biogenesis; N, cell motility and secretion; P, inorganic ion transport and metabolism; T, signal transduction mechanisms. SNPs contained in the core genome were also worked on.

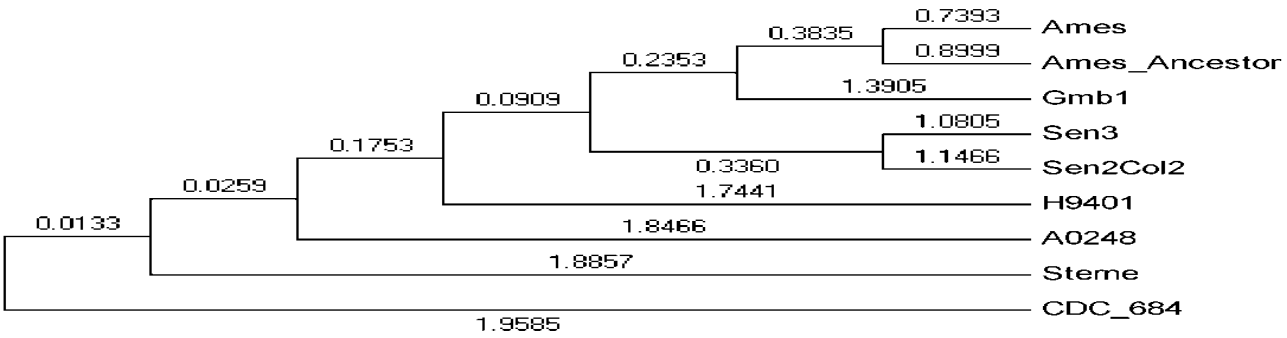

Figure 2. Phylogeny based on complete genome.

Table 2. General characteristics for strains.

Strain	Plasmid	Size (Mb)	GC (%)	Proteins
B*acillus anthracis* str. Ames	/	5.23	35.4	5,328
Bacillus anthracis str. CDC 684	pX01, pX02	5.23	35.4	5,579
Bacillus anthracis str. Sterne	/	5.23	35.4	5,289
Bacillus anthracis str. 'Ames Ancestor'	pX01, pX02	5.23	35.4	5,208
Bacillus anthracis str. A0248	pX01, pX02	5.23	35.4	5,041
Bacillus anthracis str. H9401	BAP1, BAP2	5.22	35.4	5,479
Bacillus anthracis str.Sen2Col2 (G192)	pX01,pX02	5.23	35,2	5,487
Bacillus anthracis str.Sen3 (G193)	pX01,pX02	5.23	35,2	5,493
Bacillus anthracis str.Gmb1 (G194)	pX01,pX02	5.23	35,3	5,502
Bacillus anthracis str.Sen1 (G195)	/	/	/	/

Therefore, we get back the sequences of all the core genes (based on the OrthoMCL part), thanks to a Perl script and used SNPs finder (Song et al., 2005) for the core genome tree.

RESULTS

Culture of *B. anthracis*

On ordinary broth after 24 h of incubation at 37°C, the appearance of flakes at the bottom of the tube was observed, leaving a supernatant clear enough. Mobile bacilli in long chains Gram-positive was not observed after examination. The pathogenicity test on Balb/C mouse was confirmed after 6 h strains inoculation; all of them were dead. Cultural, morphological and biochemical characteristics were studied in detail using conventional methods.

Pan-genome analysis: The obtention of genomic sequences results and their bio informatic analysis has allowed knowing the structure for pan-genome

The pan-genome is composed of 2893 core genes, 7 unique genes, and 85 accessory genes (Figure 6). First, we looked at unique genes. Five in Sterne (2 not found, one conserved hypothetical protein, EmrB/QacA family drug resistance transporter and zinc-binding dehydrogenase), 1 in CDC 684 (not found on the NCBI) and 1 in H9401 (yfeT DNA-binding transcriptional regulator) were found. Then, we looked in details on the 85 accessory genes (Figure 6). The three African strains and CDC684 possessed almost all the accessory genes, whereas A0248 owned only 20 accessory genes out of 85. The half of the accessory genes was annotated as hypothetical proteins (Figure 6). It was noticed that Ames Ancestor owned 42 accessory genes, whereas, its non-virulent version, Ames, owned more (59). The hierarchical clustering (Figure 6) showed again the same two groups found, thanks to COG (Table 3, Figures 3 and 5) and KEGG (Figure 4) (one with Ames, Ames ancestor and A0248, the second with all the other strains). Moreover, the core/pan-genome ratio was done and core genome represented 99% of the pan-genome (Table 2), was found showing again the high rate of conservation between the nine strains. Finally, the SNPs at core genome level were studied. We found 896 SNPs, that is, 32% of the total number of SNPs (2786 SNPs found in comparing all the genomes); and a transition/transversion bias of 0.32. The very small rate of SNPs, the low transition/transversion bias and the very high proportion of the core genome function as the pan-genome (Table

Table 3. COG distribution between various *B. anthracis* strains.

Categories	Ames ancestor	A0248	Ames	Sterne	CDC684	H9401	Sen2Col2	Sen3	Gmb1	Class description
J	209	208	210	211	211	210	210	211	212	Translation ribosomal Structure
K	381	376	383	393	391	387	391	391	391	Transcription
L	155	156	156	159	160	160	159	162	162	Replication and transcription
B	1	1	1	1	1	1	1	1	1	Chromatin structure and dynamics
D	40	40	40	44	44	44	44	45	45	Cell cycle control, cell division
O	101	100	101	103	102	103	102	102	102	Posttranslational modification, protection
M	206	203	215	246	241	241	246	247	251	Cell wall/membrane/ envelope biogenesis
N	48	47	50	60	59	59	224	61	61	Cell motility and secretion
P	226	222	224	246	246	246	54	245	245	Defense mechanism
T	203	202	204	225	224	223	106	224	224	Signal translation mechanism
U	47	46	46	52	54	54	54	55	54	Intracellular traficknng
V	93	93	94	107	106	105	106	106	107	Defense mechanisms
W	0	0	0	0	1	1	0	0	0	Extracellular structure
Z	1	1	1	1	1	1	1	1	1	Cytoskeleton
C	198	198	198	206	205	207	205	205	207	Energy production and conversion
G	248	247	249	268	268	267	270	270	270	Carbohydrate transport and metabolism
E	377	373	375	407	405	403	409	410	409	Amino acide transport and metabolism
F	121	120	122	130	130	131	131	131	131	Nucleotide transport and metabolism
H	169	168	169	173	175	175	175	175	175	Coenzyme transport and metabolism
I	123	121	123	128	129	126	129	126	130	Lipid transport and metabolism
Q	72	72	73	78	82	81	82	81	83	Secondary metabolites biosynthesis
R	543	541	552	587	582	580	582	580	588	General function prediction only
S	427	420	431	442	444	439	444	439	468	Function unknown

4) showed that *B. anthracis* is an ancient protein (probably very older than 150 years). It was believed that the lack of gene transfer and defense mechanisms (CRISPRs) observed in intracellular bacteria suggests that *B. anthracis* multiplies only as a pathogen and that its life in soil is exclusively dormant.

DISCUSSION

In comparing the three African strains to the others, it was noticed that all the Senegalese and Gambian strains are closer from CDC684. In this work, a validation of that was given as previously shown (Tettelin et al., 2005); the pan-genome of *B. anthracis* is narrow. To have confidence in our study, different tools were used in order to compare and validate the results. All go in the same sense: the addition of the Senegalese and Gambian strains did not change the closed nature of this pan-genome (2893 core genes and 85 accessory genes), with a core/pan-genome ratio of 99%. This core/pan-genome ratio is very close from the other human clonal pathogens (Table 1) as *Rickettsia rickettsii.* However, there is discordance between the presence of a mobilome; which is a structure localized in the pXO1 and pXO2 plasmids and contained five transposases, one phage and no CRISPRs and the fact to have a closed pan-genome. Nevertheless, *B. anthracis* derived from *B. cereus* group, a sympatric species that is not intracellular. Therefore, *B. anthracis* may become allopatric (Table 4). This can be explained by the fact that *B. anthracis* is an ancient bacterium (at least 150

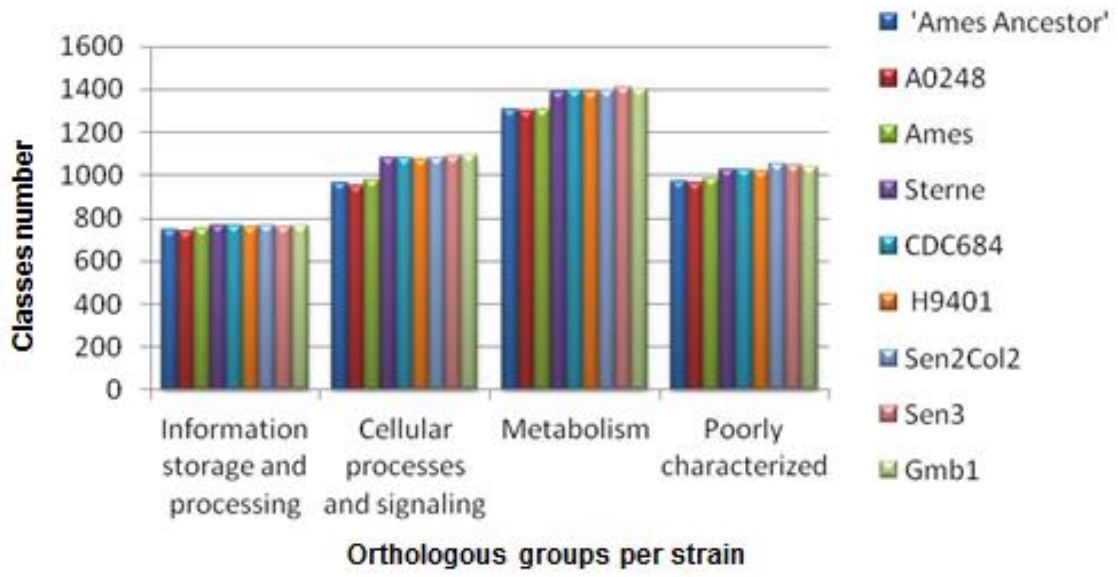

Figure 3. Cluster of Orthologous Groups (COG) classes distribution between *B. anthracis* strains.

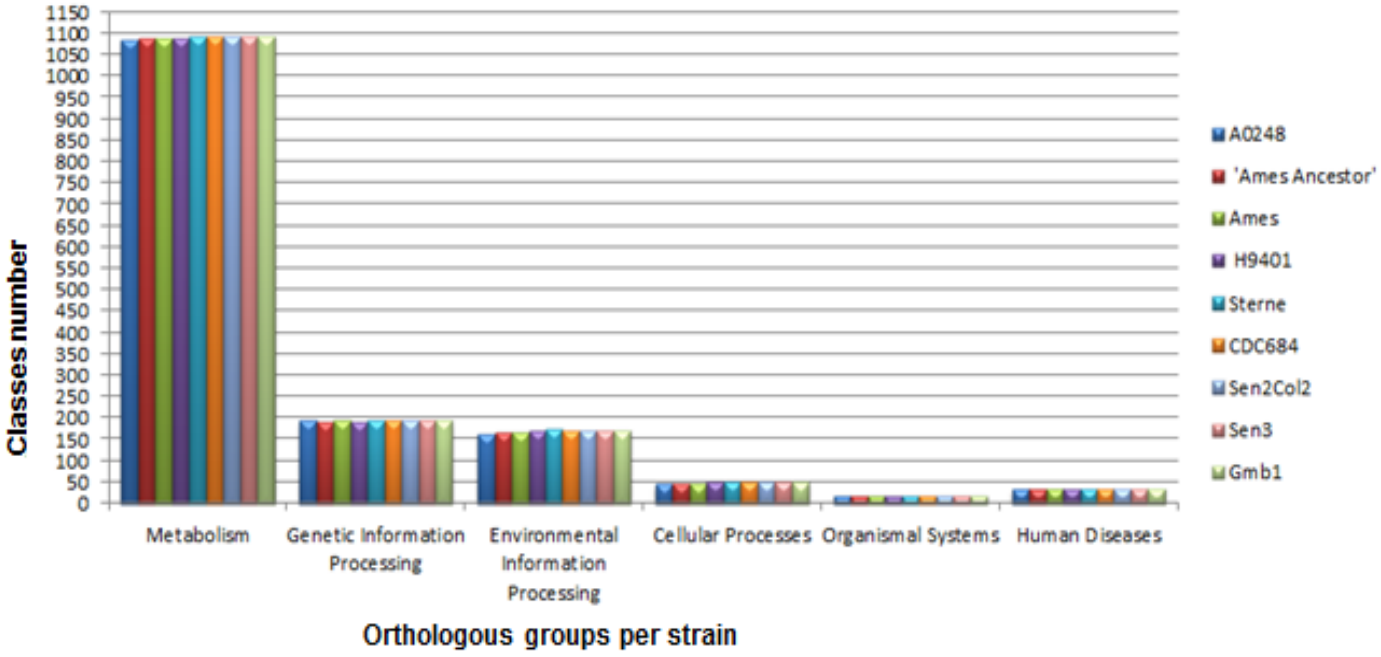

Figure 4. Distribution of KEEG *B. anthracis* classes.

years) which evolve. This hypothesis was tested in studying SNPs based on the core genome content. Only 2786 SNPs in total with 896 in the core genome were found. Moreover, the transition/transversion process is very small (0.32). This lack of SNPs may validate our hypothesis of the evolution of this species. *B. anthracis* is an ancient clone which is stabilized with the time and which present a conserved pan-genome.

Conclusion

B. anthracis was discovered 150 years ago, but kept the same genomic content. We are in a case of a very closed pan-genome with species which do not live in the environment. Due to the lengthy spore phase of its life cycle, *B. anthracis* evolved very slowly and has a very narrow pan-genome, despite its apparent soil ecological

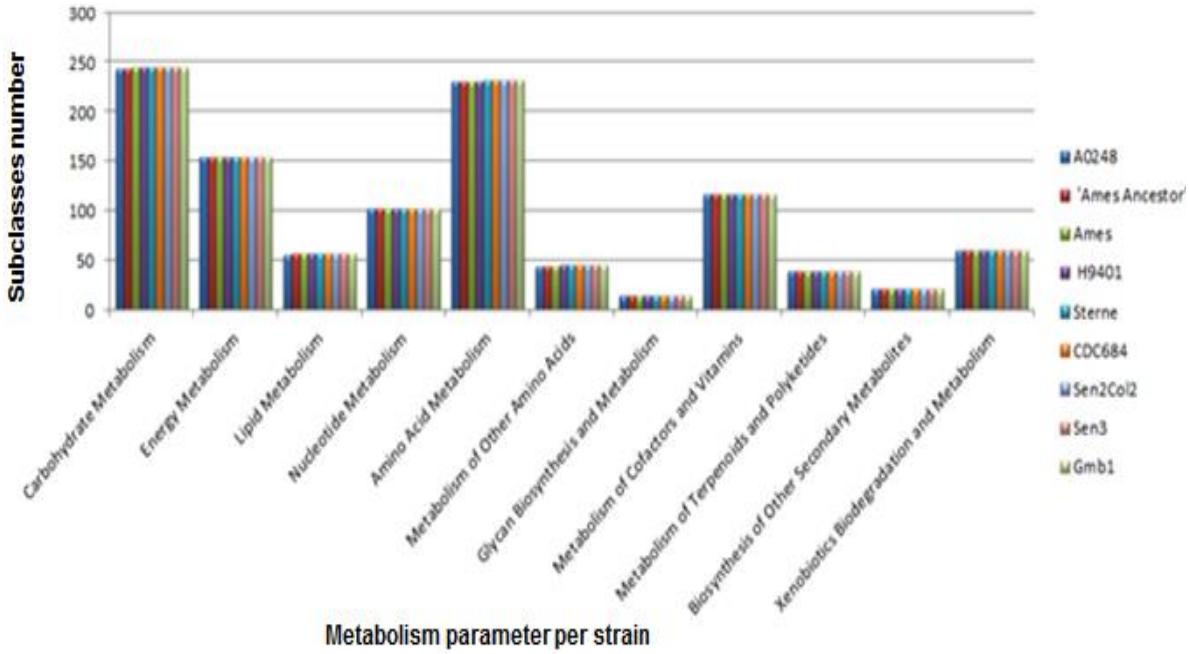

Figure 5. Distribution of metabolisms *B. anthracis* subclasses for various strains.

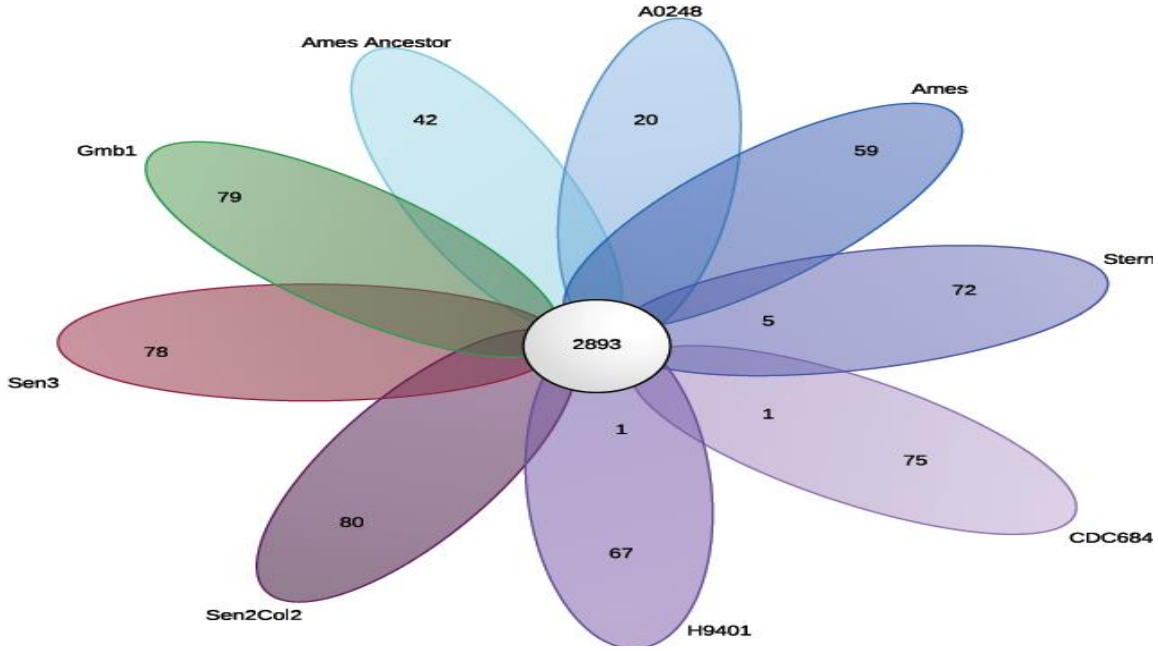

Figure 6. *B. anthracis* pan-genome: Flower pot showing *B. anthracis.* Pan - genome: The number in the center circle is the basic genome. The numbers in the upper part of the petals is the number of accessory genes present in each strain (about 85 in total). The numbers in the lower part of the petals is the number of unique genes in each strain.

niche. It was found out that the three African strains examined belong to lineage A (worldwide lineage), specifically lineage A4, similar to CDC684 and another previously characterized African strain. Pan-genome analysis allowed us to assess the lifestyle of this pathogen and confirmed its allopatric, highly specialized

Figure 7. Hierarchic clustering.

Table 4. Pan-genome for human pathogen strains with colum percentages corresponding to the ratio core/pan genome.

Species	Genome used	Life style	Intracellular	Niche	Pan genome size	Core genome size	%
B .anthracis	9	Allopatric	Non	Animal	47041887	46513801	99
Rickettsia rickettsi	8	Allopatric	Non	Ticks	10129221	100112432	99
Chlamydia trachomatis	20	Allopatric	Non	Human	20960000	20689197	99
Rickettsia prowazeki	8	Allopatric	Non	Human	8888959	8869530	100

lifestyle.

Conflict of Interests

The authors have not declared any conflict of interests.

REFERENCES

Chen F, Mackey AJ, Stoeckert CJ Jr, Roos DS (2006). OrthoMCL-DB: querying a comprehensive multi-species collection of ortholog groups. Nucleic Acids Res. 34(suppl 1):D363-D368.

Chun JH, Hong KJ, Cha SH, Cho MH, Lee KJ, Jeong DH, Yoo CK, Rhie GE (2012). Complete genome sequence of *Bacillus anthracis* H9401, an isolate from a Korean patient with anthrax. J. Bacteriol. 194:4116-4117.

Darling AE, Mau B, Perna NT (2010.) progressiveMauve: multiple genome alignment with gene gain, loss and rearrangement. PLoS.One. 5:e11147.

Grissa I, Vergnaud G, Pourcel C (2007.) CRISPRFinder: a web tool to identify clustered regularly interspaced short palindromic repeats. Nucleic Acids Res. 35:W52-W57.

Guillemin J (2002). The 1979 anthrax epidemic in the USSR: applied science and political controversy. Proc.Am.Philos.Soc. 146:18-36.

Holden MT, Hsu LY, Kurt K, Weinert LA, Mather AE, Harris SR, Strommenger B, Layer F, Witte W, de Lencastre H, Skov R (2013). A genomic portrait of the emergence, evolution and global spread of a methicillin resistant Staphylococcus aureus pandemic. Genome Res. 23(4):653-664.

Imperiale MJ, Casadevall A (2011). Bioterrorism: lessons learned since the anthrax mailings. MBio. 2:e00232-11.

Kim K, Cheon E, Wheeler KE, Youn Y, Leighton TJ, ParkC, Kim W, Chung SI (2005) Determination of the most closely related bacillus isolates to *Bacillus anthracis* by multilocus sequence typing. Yale J. Biol. Med. 78:1-14.

Kuroda M, Serizawa M, Okutani A, Sekizuka T, Banno S, Inoue S (2010). Genome-wide single nucleotide polymorphism typing method for identification of *Bacillus anthracis* species and strains among B. cereus group species. J. Clin. Microbiol. 48:2821-2829.

Moriya Y, Itoh M, Okuda S, Yoshizawa AC, Kanehisa M (2007). KAAS: an automatic genome annotation and pathway reconstruction server. Nucleic Acids Res. 35:W182-W185.

Ogata H, Goto S, Sato K, Fujibuchi W, Bono H, Kanehisa M (1999). KEGG: Kyoto Encyclopedia of Genes and Genomes. Nucleic Acids Res. 27:29-34.

Okinaka RT, Price EP, Wolken SR, Gruendike JM, Chung WK, Pearson T, Xie G, Munk C, Hill KK, Challacombe J, Ivins BE (2011). An attenuated strain of *Bacillus anthracis* (CDC 684) has a large chromosomal inversion and altered growth kinetics. BMC Genomics 12:477.

Rasko DA, Worsham PL, Abshire TG, Stanley ST, Bannan JD, Wilson MR, Langham RJ, Decker RS, Jiang L, Read TD, Phillippy AM (2011). *Bacillus anthracis* comparative genome analysis in support of the Amerithrax investigation. Proc. Natl. Acad. Sci. U.S.A 108:5027-5032.

Ravel J, Jiang L, Stanley ST, Wilson MR, Decker RS, Read TD, Worsham P, Keim PS, Salzberg SL, Fraser-Liggett CM, Rasko DA (2009). The complete genome sequence of *Bacillus anthracis* Ames "Ancestor". J. Bacteriol. 191:445-446.

Read TD, Salzberg SL, Pop M, Shumway M, Umayam L, Jiang L, Holtzapple E, Busch JD, Smith KL, Schupp JM, Solomon D (2002). Comparative genome sequencing for discovery of novel polymorphisms in *Bacillus anthracis*. Science 296:2028-2033.

Read TD, Peterson SN, Tourasse N, Baillie LW, Paulsen IT, Nelson KE, Tettelin H, Fouts DE, Eisen JA, Gill SR, Holtzapple EK (2003). The genome sequence of *Bacillus anthracis* Ames and comparison to closely related bacteria. Nature 423:81-86.

Saeed AI, Bhagabati NK, Braisted JC, Liang W, Sharov V, Howe EA, Li J, Thiagarajan M, White JA, Quackenbush J (2006). TM4 microarray software suite. Methods Enzymol. 411:134-193.

Saeed AI, Sharov V, White J, Li J, Liang W, Bhagabati N, Braisted J, Klapa M, Currier T, Thiagarajan M, Sturn A (2003.) TM4: a free, open-source system for microarray data management and analysis. Biotechniques 34:374-378.

Scarlata F, Colletti P, Bonura SI, Trizzino M, Giordano S, Titone L (2010). [The return of anthrax. From bioterrorism to the zoonotic cluster of Sciacca district]. Infez. Med. 18:86-90.

Sheppard SK, Didelot X, Jolley KA, Darling AE, Pascoe B, Meric G, Kelly DJ, Cody A, Colles FM, Strachan NJ, Ogden ID (2013). Progressive genome-wide introgression in agricultural Campylobacter coli. Mol. Ecol. 22:1051-1064.

Song J, Xu Y, White S, Miller KW, Wolinsky M (2005). SNPsFinder--a web-based application for genome-wide discovery of single nucleotide polymorphisms in microbial genomes. Bioinformatics 21:2083-2084.

Sun S, Chen J, Li W, Altinatas I, Lin A, Peltier S, Stocks K, Allen EE, Ellisman M, Grethe J, Wooley J (2011). Community cyberinfrastructure for Advanced Microbial Ecology Research and Analysis: the CAMERA resource. Nucleic Acids Res. 39:D546-D55.

Sweeney DA, Hicks CW, Cui X, Li Y, Eichacker PQ (2011). Anthrax infection. Am. J. Respir. Crit. Care Med. 184:1333-1341.

Tatusov RL, Natale DA, Garkavtsev IV, Tatusova TA, Shankavaram UT, Rao BS, Kiryutin B, Galperin MY, Fedorova ND, Koonin EV (2001). The COG database: new developments in phylogenetic classification of proteins from complete genomes. Nucleic Acids Res. 29:22-28.

Tettelin H, Masignani V, Cieslewicz MJ, Donati C, Medini D, Ward NL, Angiuoli SV, Crabtree J, Jones AL, Durkin AS, DeBoy RT(2005). Genome analysis of multiple pathogenic isolates of *Streptococcus agalactiae*: implications for the microbial "pan-genome". Proc. Natl. Acad. Sci. U.S.A 102:13950-13955.

Wang DB, Tian B, Zhang ZP, Deng JY, Cui ZQ, Yang RF, Wang XY, Wei HP, Zhang XE (2012). Rapid detection of *Bacillus anthracis* spores using a super-paramagnetic lateral-flow immunological detection system. Biosens. Bioelectron. 42:661-667.

academicJournals

Vol. 15(45), pp. 2547-2557, 9 November, 2016
DOI: 10.5897/AJB2016.15611
Article Number: 0B4787F61541
ISSN 1684-5315

http://www.academicjournals.org/AJB

African Journal of Biotechnology

Full Length Research Paper

RNAi-based silencing of genes encoding the vacuolar-ATPase subunits a and c in pink bollworm (*Pectinophora gossypiella*)

Ahmed M. A. Mohammed

Agricultural Genetic Engineering Research Institute (AGERI), Agricultural Research Center, 9 Gamaa St., 12619 Giza, Egypt.

Received 9 August, 2016; Accepted 28 October, 2016

RNA interference is a post- transcriptional gene regulation mechanism that is predominantly found in eukaryotic organisms. RNAi demonstrated a successful gene silencing in insects that led to the development of novel approaches for insect pest management. In the current study, genes encoding vacuolar ATPase (V-ATPase) subunits a and c from the midgut of pink bollworm, *Pectinophora gossypiella*, were cloned and sequenced. The full length of V-ATPase subunits a and c cDNAs are 2526 and 1140 bp, respectively. The silencing effect of RNAi on these two genes was determined by microinjecting three dsRNA fragments into the thoracic region of pink bollworm larvae. Bioassay results revealed that 200 ng of dsRNAs silenced both genes causing mortality of 18.9 to 26.7%.

Key words: RNAi, dsRNA, Pink bollworm, vacuolar ATPase subunit a, vacuolar ATPase subunit c.

INTRODUCTION

RNA interference (RNAi) is a mechanism of post-transcriptional regulation in higher eukaryotes inhibiting gene expression by RNA transcript degradation (Berezikov, 2011). It was first discovered in the nematode *Caenorhabditis elegans* by Fire et al. (1998) and, later, was exploited as an effective technique for a rapid analysis of gene function by phenotypical changes of the target silenced gene. In this technique, exogenous double stranded RNA (dsRNA) is used to significantly reduce the target gene transcript level (Fire et al., 1998). RNAi technology was harnessed in different applications including insect control, thus, was deployed as a powerful tool in biological control for insect pest management (Gordon and Waterhouse, 2007; Price and Gatehouse, 2008; Zhu, 2013). A variety of methods are used to deliver dsRNA inside the cells such as soaking the animals in dsRNA-containing solution, microinjection and oral feeding (Baum et al., 2007; Chen et al., 2010; Liu et al., 2010; Rosa et al., 2012; Tian et al., 2009; Zhang et al., 2010; Zhao et al., 2011; Zhu et al., 2011).

An advanced progress of RNAi exploitation in the field of insect control was developed in 2007, by expressing insect specific-dsRNAs in transgenic plants. Transgenic corn expressing V-ATPase specific-dsRNAs showed a

E-mail: amohoammed00@yahoo.com.

significant reduction in feeding damage caused by western corn rootworm, *Diabrotica virgifera virgifera* (Baum et al., 2007). Also, cotton was modified to harbor dsRNA targeting the cytochrome P450 gene (CYP6AE14) of the cotton bollworm, *Helicoverpa armigera* (Mao et al., 2007). Cotton bollworm larvae fed on transgenic cotton showed a reduction in growth rate and lower levels of CYP6AE14 transcript within the insect midgut. Thereafter, other RNAi-mediated transgenic plants were developed such as transgenic tobacco plants *Nicotiana tabacum*, that showed higher resistance level compared to non-transgenic against *H. armigera* (Xiong et al., 2013; Jin et al., 2015), *Spodoptera exigua* (Zhu et al., 2012) and *Bemisia tabaci* (Thakur et al., 2014).

The vacuolar proton pumps, V-ATPases, are ubiquitous holoenzyme among eukaryotes (Dow, 1999). It is a member of ATPases family (A, F and V) which are mainly responsible for ATP hydrolysis (Forgac, 2007). The main function of V-ATPases is acidifying a wide array of intracellular organelles and pump protons across the plasma membranes of numerous cell types (Nelson et al., 2000). V-ATPases utilize the energy derived from ATP hydrolysis to transport protons across intracellular and plasma membranes of eukaryotic cells. In the midgut of lepidopteran larvae, the V-ATPase in the apical cell membranes of the goblet cells plays a role in amino acid absorption, by energizing the plasma membrane through pumping H^+ ions/proton into the goblet lumen (Beyenbach and Wieczorek, 2006). V-ATPase is composed of two complexes; a peripheral, catalytic V_1 complex with subunits $A3B3CDE_XFG_YH$ and a membrane-bound, proton-conducting V_0 complex with subunits ac_6de (Vitavska et al., 2003). The V-ATPase is down regulated during larval moult and starvation periods by the reversible dissociation of the enzyme into its two complexes (Sumner et al., 1995; Gräf et al., 1996) and, in turn, the V_1 complex level increases in the cytoplasm. Thus, biosynthesis of V ATPase subunits is down regulated and transcript levels of these subunits decrease gradually (Wieczorek et al., 2000).

Knock down of genes encoding different subunits belonging to insect V-ATPase have been reported in different insect species. In the current study, the effect of RNAi on V-ATPase genes encoding subunits a and c was determined in *P. gossypiella* by injecting the larval instar with V-ATPase subunits a and c-specific dsRNA fragments.

MATERIALS AND METHODS

Insect culture

P. gossypiella colony was reared on an artificial diet until pupation, at temperature 25±2°C and photoperiod of light:dark (16:8) hours (Bell and Joachim, 1976). A pair of neonate larvae was added to approximately 5 g diet in 35 ml glass vial covered by cotton plugs and pupae were collected in glass jars covered by filter paper as oviposition site.

cDNA synthesis and target gene cloning

Total RNA was extracted from *P. gossypiella* midgut tissues using Triazol® (Invitrogen) according to manufacturer's instructions. First strand cDNA was prepared from total RNA using the Superscript II cDNA synthesis kit (Invitrogen) according to the manufacturer's instructions. Degenerate primers were designed based on the conserved regions of the V-ATPase subunits a and c sequences in NCBI database using the Vector NTI® software (Life technologies). The nucleotide sequences of degenerate, specific and RACE primers are presented in Table 1. One fragment of subunit a was amplified using degenerate primers; VATPavo2264FD / VATPavo2484RD and two more fragments were amplified using degenerate and specific primer sets VATPavo776FD/ VATPavo1559RS and VATPavo1439FD/VATPavo2416RS, respectively. On the other hand, two fragments of subunit c were amplified using degenerate primer set (VATPcvoFD/ VATPcvoRD) and degenerate primer VATPcvo146FD and specific primer VATPcvo901RS. The template cDNA was denatured at 95°C for 5 min followed by 25 cycles of 95°C for 30 s and annealing temperature at 55ºC for another 30 s followed by 30 s at 72ºC the PCR reaction was extended at 72ºC for 7 min. The PCR product was cloned into a pGEM-T Easy vector (Promega, Madison, WI), sequenced using the Big Tri Dye sequencing kit (ABI Applied Biosystems) at Macrogen, Korea.

Both 5' and 3' ends were synthesized using First Choice® RLM-RACE kit (Ambion life technologies) following manufacturer's procedures. RACE adaptors and specific primers (Table 1) were used for two rounds of PCR to amplify both ends of subunits a and c with annealing temperatures of 57 and 65ºC, respectively. For subunit a; the outer adaptors were mixed with specific primers VATPavo864RS and VATPavo2265 FS to amplify 5'and 3'-end, respectively. The second PCR round was performed using inner adaptors with specific primers VATPavo795 RS and VATPavo2431FS for 5' and 3'-end, respectively. On the other hand, outer and inner adaptors and specific primers VATPcvo244 RS and VATPcvo185 RS were used to amplify the 5'-end of subunit c. The 3'-end was amplified using specific primers VATPcvo819 FS and VATPcvo847 FS.

Sequence, alignment, and phylogenetic analysis

The obtained sequences of V-ATPase subunits a and c were analyzed using the BLAST algorithm at NCBI for comparative analysis. Multiple alignments of both nucleotide and deduced amino acid sequences were performed by Vector NTI® advance 10 (Life Technologies). The deduced amino acid sequences were also scanned for motifs against the PROSITE database. A phylogenetic tree was constructed using the neighbor-joining method in MAGE version 6 (Tamura et al., 2013).

dsRNA synthesis

The dsRNA fragments were generated using MEGA script® RNAi Kit (Ambion) according to manufacturer's instructions. Two dsRNA fragments; a-1 and a-2 (220 and 466 bp) were prepared to target the *P. gossypiella* V-ATPase subunit a transcript using the following primer sets "VATPavo2264F/VATPavo2484R" and "VATPavo1950F/VATPavo2416R". On the other hand, the gene encoding subunit c was knocked down by only one dsRNA fragment (740 bp) that was synthesized by primer set "VATPcvo161F/ VATPcvo901R" (Table 1).

dsRNA injection

RNAi efficiency of gene silencing in *P. gossypiella* was determined

Table 1. Primers used in PCR, RACE and dsRNA synthesis.

Primer	Sequence
Cloning primers	
Subunit a	
VATPavo2264 FD	5'-GTGGGCDYTKTCRCTKGCBC-3'
VATPavo2484RD	5'-GAAYTTRCTCWKGAACTCCACCC-3'
VATPavo1439FD	5'-TTCTTYGSYGGDCGTTACAT-3'
VATPavo2416 RS	5'-GACGAGGATGGCGAGCGTGAA-3'
VATPavo776 FD	5'-GTVTTYGTGGYBTTCTTCCA-3'
VATP avo1559 RS	5'-CGG AATGCGCCACGACGAGC-3'
Subunit c	
VATPcvoFD	5'-GCYCCYGGCGAYAAGACMTG-3'
VATPcvoRD	5'-GCCSAGRTCBGASAGSCCCAC-3'
VATPcvo146 FD	5'-TGGMACDGCCAAGTCVGGMACBGGT-3'
VATPcvo901 RS	5'-CATCCACTATAAGACAGAAAGCT-3'
RACE primers	
Subunit a	
5'-end	
VATPavo864 RS	5'-GTTGGAAGGCGGACACGGGTA-3'
VATPavo795 RS	5'-CTGCTCACCTTGGAAGAACACC-3'
3'-end	
VATPavo2265 FS	5'-CTTTCGCTGGCTCACGCAGAGTTATC-3'
VATPavo2431 FS	5'-TCTCGGCCTTCCTCCACACCCT-3'
Subunit c	
5'-end	
VATPcvo244 RS	5'-ATAATACCCGCCATGACAACG-3'
VATPcvo185 RS	5'-CGACATAGCGGCGATACCCGT-3'
3'-end	
VATPcvo819 FS	5'-ACTGTGTACCACCATCTTTGC-3'
VATPcvo847 FS	5'-GGTAAAACCTGGCTTAAGTAC-3'
dsRNA primers	
Subunit a	
a-1	
VATPavo2264F	5'-TAATACGACTCACTATAGGGCTTTCGCTGGCTCACGCAGAGT-3'
VATPavo2484R	5'-TAATACGACTCACTATAGGGCAGGGTGTGGAGGAAGGCCGA-3'
a-2	
VATPavo1950F	5'-TAATACGACTCACTATAGGGGAAGATGGCTGCCACGAATA-3'
VATPavo2416R	5'-TAATACGACTCACTATAGGGGACGAGGATGGCGAGCGTG-3'
Subunit c	
VATPcvo161F	5'-TAATACGACTCACTATAGGGCGGCACGGGTATCGCCGCTAT-3'
VATPcvo901R	5'-TAATACGACTCACTATAGGGCATCCACTATAAGACAGAAAGC-3'

by microinjection of dsRNA into larval hameolymph. The third larval instars were injected using Neuros Syringe model 1701RN controlled with dispenser (Hamelton). The dsRNA was diluted with injection buffer (0.1mM $NaHPO_4$ pH 6.8, 5 mM KCl) to final concentration of 1 µg/µl and 0.2 µl were injected into larvae between meso and meta-thoracic segments. The injection was repeated three times for each dsRNA fragment, each replica contained a group of 40 to 45 larvae. Control larvae were injected with injection buffer and treated as the same as experimental individuals. Larvae that died within the first for 24 h were removed and not counted. Larval mortality was recorded five days after injection. Statistics of data was performed with Student's t-test in the Excel program.

RESULTS

Sequence analysis of the V-ATPase subunits a and c

The initial sequences of both transcripts were amplified using degenerate primers designed based on

homologous proteins. A partial sequence (220 bp) of V-ATPase subunit a was obtained from *P. gossypiella* by RT-PCR using degenerate primer set (VATPavo2264FD / VATPavo2484RD), and two longer fragments of 977 and 783 bp were isolated using two sets of combined degenerate and specific primers (VATPavo776FD/ VATPavo1559RS and VATPavo1439FD / VATPavo2416RS) (Supplementary Figure S-1). A 150 bp fragment of V-ATPase subunit c was also isolated based on degenerate primer set (VATPcvoFD/ VATPcvoRD) while a longer 755 bp sequence was amplified by degenerate and specific primers (VATPcvo146FD/VATPcvo901RS). However, the full lengths of the two V-ATPase transcripts were identified by cloning and sequencing the 5' and 3' ends (Supplementary Figure S-2). The RACE strategy demands two PCR reactions, the outer and the inner rounds using RACE adaptors with specific primers. Therefore, two specific primers were designed for each end (Table 1). Specific primers VATPavo864RS and VATPavo795 RS were used to amplify the 5'-end of subunit a, while the 3'-end was synthesized using VATPavo2265 FS and VATPavo2431FS primers. Likewise, the 5'-end of subunit c was identified using specific primers VATPcvo244 RS and VATPcvo185 RS and the 3'-end was amplified using specific primers VATPcvo819 FS and VATPcvo847 FS. The products of PCR and 5' and 3' RACE reactions were aligned to form a contig and finally the full lengths were assembled.

Full length sequence of subunit a (accession no. KU550964) consists of 2760 bp including open reading frame of 2526 bp encoding for 842 amino acids (aa) with 88% identical and 92% similarity to subunit a of *B. mori* and *Amyelois transitella*. The calculated molecular mass of the protein is 96.4 kDa with isoelectric point (pI) of 5.67. On the other hand, subunit c (accession no. KU550965) is 1140 bp containing an ORF of 480 bp and encoding a protein of 160aa with molecular weight of 16.2 kDa and pI of 8.96.

Searching the PROSITE database revealed no common motifs for both subunits sequences. The phylogenetic tree analysis shows that the V-ATPase subunit a of both *P. gossypiella* and *Tribolium castaneum* are located on the same branch as *Bactrocera dorsalis* with 94% bootstrap support (Figure 1a). On the other hand, the *P. gossypiella* V-ATPase subunit c is in close proximity with other lepidopteran species; *H. virescens*, *M. sexta* and *Plutella xylostella* by 50% bootstrap with distal scale length of 0.02 (Figure 1b). The similarity of PgVATPase subunit a and other cognate of other insect orders is presented in Figure 2 whereas subunit c belongs to highly conserved proteolipid protein family known as ductin (Pietrantonio and Gill, 1997). The amino acid sequence of PgVATPase subunit c is highly identical with other lepidopteran insects (Figure 3). The amino acid is 95% identical and 97% similar to that of *Heliothis virescens* and *Manduca sexta*.

dsRNA injection

Third larval instars were injected with 200 ng dsRNA in between thoracic segments. Larval mortality within 24 h after injecting the dsRNA was neglected to make sure that mortality was not caused by injury from injections. Larval mortality was recorded between 24 and 96 h post injection. Although two dsRNAs fragments, a-1 and a-2, were designed to target the same site on the V-ATPase subunit a transcript, each caused different mortality to the injected larvae. The first fragment (a-1) is 220 bp in length (nucleotides 2264-2484), whereas the length of the second dsRNA (a-2) is 466 bp from 1950 to 2416 (Supplementary Figure S-3). Injection of a-1 fragment into the haemolymph causes larval mortality of 18.9%, with P value <0.05 compared to control larvae (5.7%). On the other hand, lethal effect of a-2 fragment results in 26.7% and shows significant difference with the control (P <0.05). Likewise, V-ATPase subunit c specific-dsRNA reveals similar effect on pink bollworm larvae with morbidity of 23.5% (P <0.05) (Figure 4a). Statistical analysis revealed no significance difference among the three dsRNAs treatments (P >0.05). Survived larvae from injection bioassays were kept on diet to observe larval development and pupation. Bodies' shrinkage and retardation of larval development are clearly shown of dsRNA-treated larvae due to starvation effect (Figure 4b). Some of these larvae failed to pupate due to deficiency in food absorption.

DISCUSSION

V-ATPase plays a crucial rule in the lepidopteran midgut keeping an alkaline environment in the midgut lumen and energizing secondary amino acid absorption. It is distributed with high density across the plasma membrane of the goblet cell with approximate ratio of 5000 μm^{-2} (Vitavska et al., 2005). The dynamic function of V-ATPase was summarized by Osteresch et al. (2012). The headpiece A3B3 hexamer catalyses ATP binding and hydrolysis and the generated energy rotates the stalk that functions as a structural and functional connection between the V_1 and V_0. The stalk is made of the central shaft "D and F subunits" that fills the central cavity of the headpiece (Ma et al., 2011) and the V_0 subunits d with the proteolipid ring of c isoforms. H^+ proton is translocated across the membrane through entering the proteolipid ring via the cytosolic half channel of subunit a. The proton binds to conserved glutamate of subunit c, upon rotation, it dissociates and leave into the lumen through the outer half channel of subunit a. The role played by V-ATPase in the insect midgut makes it a good candidate for gene silencing by RNAi.

In this study, we cloned genes encoding the membrane-bound V_0 subunits a and c from the *P. gossypiella* midgut and dsRNA was *in vitro* synthesized and injected into the

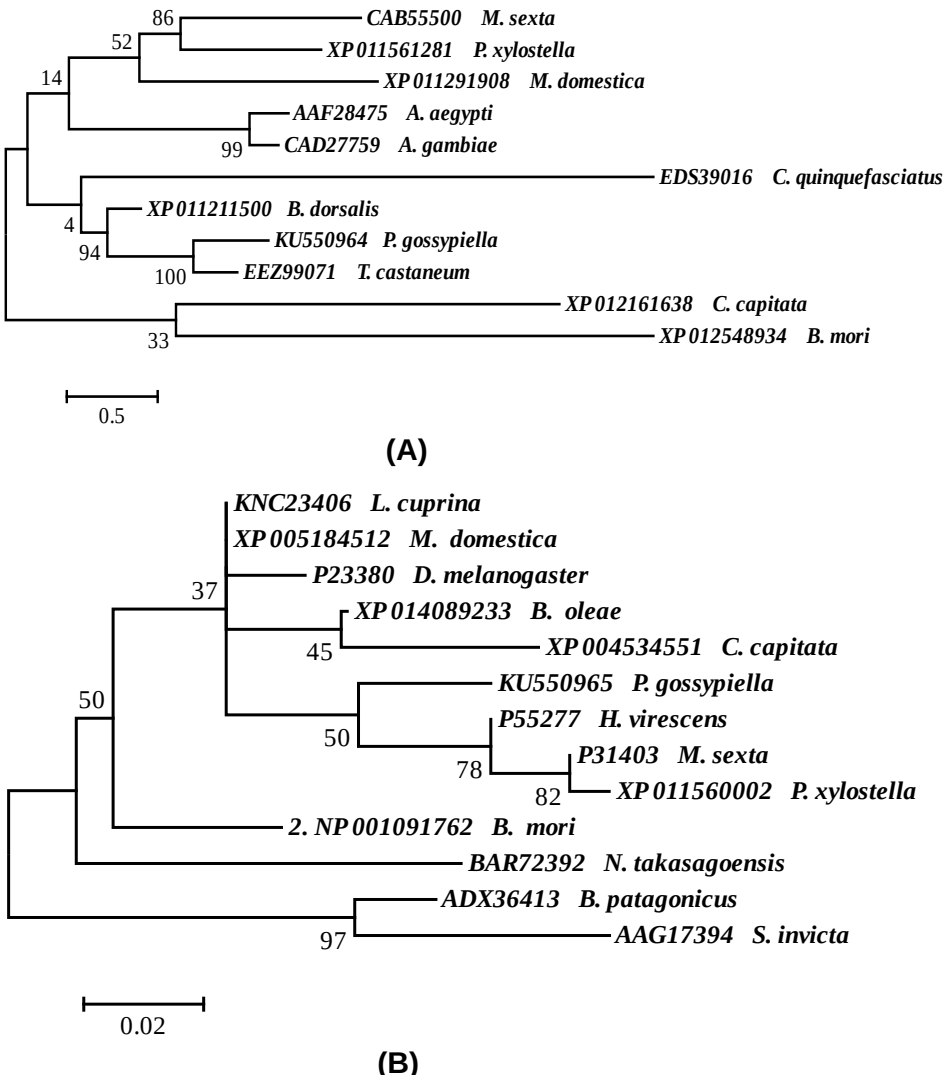

Figure 1. Phylogenetic relationship of V-ATPase subunits. **(A)** V-ATPase subunit a. **(B)** V-ATPase subunit c. This un-rooted phylogenetic tree was constructed by the neighbor-joining method. Nodes indicate bootstrap calculated with 1000 replications support.

third larval instar. RNAi effectiveness depends on multiple factors including the amount of injected dsRNA (Chen et al., 2008). A concentration of 20 ng dsRNA/mg tissue was chosen for the current experiments comparable to previous assessments of dsRNAs on pink bollwormV_1 subunits (Mohammed et al., 2015). Furthermore, high level of silencing is achieved at high doses of dsRNA (0.1 to 1 µg/mg) in some lepidopteran species (Terenius et al., 2011). Direct microinjection is one of the commonly used procedures for delivery of dsRNA into organisms (Bucher et al., 2002; Tomoyasu and Denell, 2004; Chen et al., 2008; Rong et al., 2013; Yao et al., 2013). Nevertheless, microinjection causes pressure on the insect body during injection and may result in wound that reduces insect survival. Therefore, deceased larvae within the first 24 h post injection were not counted. Although the V_0 complex plays a role in translocating the proton, only few reports on targeting V_0 complex subunits were published. We therefore, cloned and targeted V_0 subunits a and c genes and attempted to knockdown these genes by three dsRNA fragments.

Significant mortality was observed in dsRNA treatments compared to control, whereas there were no significant differences in the toxicity of the three dsRNAs. The dsRNA “a-2” was found to be most effective, followed by dsRNA “c” ($P < 0.05$). The dsRNA “a-1” was the least toxic and caused mortality up to 19% only. The observedmortality of pink bollworm larvae by dsRNAs silencing V_0 subunits is consistent with earlier reports with V_1 subunits. Four V_1 subunits (A, B, C and D) of the pink bollworm V-ATPase were knock downed by RNAi with mortality range of 23.5 to 40.5% (Mohammed et al.,

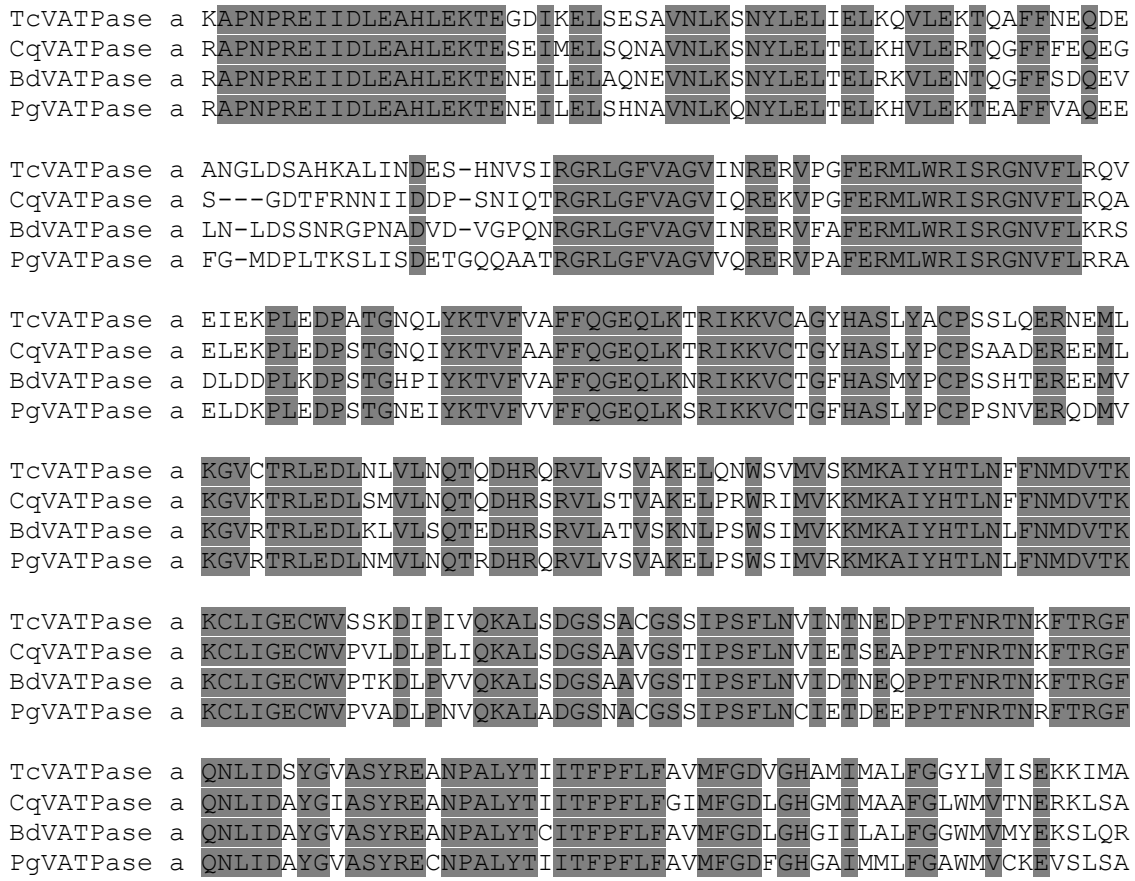

Figure 2. Deduced amino acid sequence between 117-406 aa of PgV-ATPase subunit a and aligned with *Tribolium castaneum* (Gene Bank™ accession number EEZ99071) (TcVATPase a) *Culex quinquefasciatus* EDS39016 (CqVATPase a) and *Bactrocera dorsalis* XP_011211500 (BdVATPase a). The identical amino acids are shaded in black boxes.

Figure 3. Deduced amino acid sequence of PgV-ATPase subunit c and aligned with Heliothesis virescnce (HvVATPase c) and Maduca *sexta* CAB55500 (MsV-ATPase c) and *Plutella xylostella* XP_011561281 (PxVATPase c) (PxV-ATPase c). The identical amino acids are shaded in black boxes.

2015). Current results suggest that silencing either V_1 or V_0 subunits have similar toxicity effects in pink bollworm. However, other reports on other insect species focused on V-ATPase subunit A as a target for RNAi more than

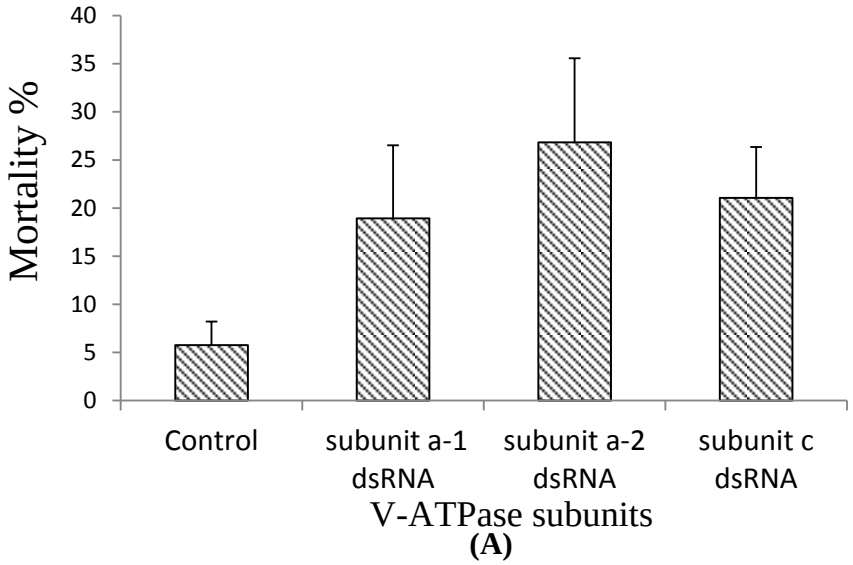

(A)

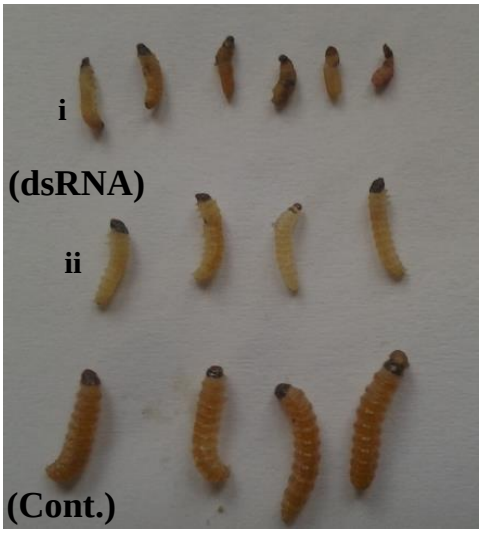

(B)

Figure 4. The lethal effect of injecting dsRNA targeting V-ATPase subunits a and c transcripts into the haemolymph of pink bollworm larvae. The larval mortality was counted 120 h after injection. **(A)** Death bar demonstrate the mortality percentage of the injected larvae against either subunit a or c-specific dsRNAs as well as control larvae. The results are shown as the mean ± SE. **(B)** Image of pink bollworm larvae were injected with V-ATPase specific-dsRNA (dsRNA); "i" dead larvae and "ii" retardation of larval development. Control larvae were injected with buffer showing normal development of control larvae (Cont.).

other subunits. As far as we know, transgenic plant knocking down V-ATPase was exclusively used to silence subunit A gene. Transgenic corn showed significant reduction in root damage by western corn rootworm (Baum et al., 2007). Thakur et al. (2014) developed transgenic tobacco expressing VATpase-A specific dsRNA, resulted in 62% reduction of the V-ATPase A transcripts level within whiteflies midguts. Transgenic plants showed high resistance to heavy infestation of whiteflies compared to control plants. Recently, three genes encoding P450, chitin synthase B and V-ATPase A from the midgut of *H. armigera* were targeted by dsRNAs that are expressed in the chloroplast genome of transplastomic tobacco plants (Jin et al. 2015). The transcripts of these three genes were not detected in the midgut of larvae fed on tobacco leaves expressing dsRNA. As a result, the net weight and growth of fed larvae were retard and pupation rate was significantly

reduced.

Suppression of endogenous V-ATPase subunits genes showed variable results according to targeted subunit and insect species. The V_1 subunits A, D and E genes were targeted by oral feeding of specific dsRNA causing mortality against WCR (Baum et al., 2007). There was no apparent significant difference in the assessed dsRNAs. The V-ATPase A-dsRNA caused variable mortality; 97.5% in *B. tabaci* (Upadhyay et al., 2011), 27.3 to 54.5% in *Tetranychus urticae* (Kwon et al., 2013) and 35% in *B. dorsalis* (Li et al., 2011a). Likewise, the V-ATPase E transcript levels was reduced between 55 and 85% in *Leptinotarsa decemlineata* larvae after ingesting two dsRNA fragments (Ky et al., 2014), low silencing level detected in *M. sexta* (Whyard et al., 2009), and no observed response in *Nilaparvata lugens* (Li et al., 2011b). The V- ATPase B and D transcripts were targeted by both feeding and microinjection of dsRNAs in the corn plant hoper, *P. maidis* (Yao et al., 2013). Quantitative PCR analysis indicated a reduction of 27-fold of V-ATPase transcripts two days post injection, while ingestion of dsRNA resulted in only two fold reduction after six days of feeding. Higher mortality and lower fecundity as well as phenotypic deformation were observed in nymphs injected with 200 ng of either V-ATPase B or D dsRNA.

Different factors influence RNAi efficiency in insects such as; effective dose of dsRNA that efficiently knockdowns target transcripts (Kumar and Sarin, 2013), ability of insect cells to uptake dsRNA molecules and to involve them within the RNAi pathway (Terenius et al., 2011) and RNAi processing machinery within the cells and signal propagation across neighboring cells (Roignant et al., 2003; Miller et al., 2008). Also, length of the dsRNA, life-stage of the insect, and persistence of gene silencing, are important factors for successful RNAi application (Thakur et al., 2014).

Despite the low mortality achieved in the current study, deleterious effects on pink bollworms were noticed. V-ATPase is still a potential target for RNAi and could be deployed in the control of pink bollworm, if multiple genes could be targeted simultaneously by dsRNA, or by targeting different sites on the same target gene(s) causing an increase of larval mortality. RNAi is a promising strategy in insect pest management and further investigation is required to enhance its effect.

Conflicts of Interests

The authors have not declared any conflict of interests.

ACKNOWLEDGMENTS

I would like to thank the Science and Technology Development Fund (STDF), Ministry of Scientific Research, Egypt for partially funding this research through project ID 723 and greatly acknowledge Mrs. Mervat R. Diab for her technical efforts.

REFRENCES

Baum JA, Bogaert T, Clinton W, Heck GR, Feldmann P, Ilagan O, Johnson S, Plaetinck G, Munyikwa T, Pleau M, Vaughn T, Roberts J (2007). Control of coleopteran insect pests through RNA interference. Nat. Biotechnol. 25:1322-1326.

Bell RA, Joachim FG (1976). Techniques for Rearing Laboratory Colonies of Tobacco Hornworms and Pink Bollworms. Ann. Entomol. Soc. 69:365-373.

Berezikov E (2011). Evolution of microRNA diversity and regulation in animals. Nat. Rev. Genet. 12:846-860.

Beyenbach KW, Wieczorek H (2006). The V-type H^+ATPase: molecular structure and function, physiological roles and regulation. J. Exp. Biol. 209:577-589.

Bucher G, Scholten J, Klingler M (2002). Parental RNAi in *Tribolium* (Coleoptera). Curr. Biol. 12:R85-R86.

Chen J, Zhang D, Yao Q, Zhang J, Dong X, Tian H, Zhang W (2010). Feeding-based RNA interference of a trehalose phosphate synthase gene in the brown planthopper, *Nilaparvata lugens*. Insect Mol. Biol. 19:777-786.

Chen X, Tian H, Zaou L, Tang B, Hu J, Zhang W (2008). Disruption of *Spodoptera exigua* larval development by silencing chitin synthase gene with RNA interference. Bull. Entomol. Res. 98:613-619.

Dow JAT (1999). The Multifunctional *Drosophila melanogaster* V-ATPase is encoded by a multigene family. J. Bioenerg. Biomembr. 31:75-83.

Fire A, Xu SQ, Montgomery MK, Kostas SA, Driver SE, Mello CC (1998). Potent and specific genetic interference by double-stranded RNA in *Caenorhabtidis elegans*. Nature 39:806-811.

Forgac M (2007). Vacuolar ATPases: rotary proton pumps in physiology and pathophysiology. Nat. Rev. Mol. Cell Biol. 8:917-929.

Gordon KH, Waterhouse PM (2007). RNAi for insect-proof plants. Nat. Biotechnol. 25:1231-1232.

Gräf R, Harvey WR, Wieczorek H (1996). Purification and properties of a cytosolic V1-ATPase. J. Biol. Chem. 23:20908-20913.

Jin S, Singh ND, Li L, Zhang X, Daniell H (2015). Engineered chloroplast dsRNA silences *cytochrome p450 monooxygenase*, *V-ATPase* and *chitin synthase* genes in the insect gut and disrupts *Helicoverpa armigera* larval development and pupation. Plant Biotechnol. J. 13:435-446.

Kumar A, Sarin NB (2013). RNAi: A promising approach to develop transgenic plants against geminiviruses and insects. J. Plant Physiol. Pathol. 1:1-6.

Kwon DH, Park JH, Lee SH (2013). Screening of lethal genes for feeding RNAi by leaf disc-mediated systematic delivery of dsRNA in *Tetranychus urticae*. Pestic. Biochem. Physiol. 105:69-75.

Ky F, Guo WC, Lü FG, Liu XP, Li GQ (2014). Response of the vacuolar ATPase subunit E to RNA interference and four chemical pesticides in *Leptinotarsa decemlineata* (Say). Pestic. Biochem. Physiol. 114:16-23.

Li J, Chen Q, Lin Y, Jiang T, Wu G, Hua H (2011b). RNA interference in Nilaparvatalugens (Homoptera: Delphacidae) based on dsRNA ingestion. Pest Manage. Sci. 67:852-859.

Li X, Zhang M, Zhang H (2011a). RNA interference of four genes in adult *Bactrocera dorsalis* by feeding their dsRNAs. PLoS One 6:e17788.

Liu S, Ding Z, Zhang C, Yang B, Liu Z (2010). Gene knockdown by intro-thoracic injection of double-stranded RNA in the brown planthopper, *Nilaparvata lugens*. Insect Biochem. Mol. Biol. 40: 666–671.

Ma B, Xiang Y, An L (2011). Structural bases of physiological functions and roles of the vacuolar H^+-ATPase. Cell Signal. 23:1244-1256.

Mao YB, Cai WJ, Wang JW, Hong GJ, Tao XY, Wang LJ, Huang YP, Chen XY (2007). Silencing a cotton bollworm P450 monooxygenase gene by plant-mediated RNAi impairs larval tolerance of gossypol. Nat. Biotechnol. 25:1307-1313.

Miller SC, Brown SJ, Tomoyasu Y (2008). Larval RNAi in Drosophila?

Dev. Genes Evol. 218:505-510.
Mohammed A, Diab MR, Abd-Alla SMM, Hussien EHA (2015). RNA interference-mediated knockdown of vacuolar ATPase genes in pink bollworm, *Pectinophora gossypiella*. Int. J. Biol. Pharm. Allied Sci. 4:2641-2660.
Nelson N, Perzov N, Cohen A, Hagai K, Padler V, Nelson H (2000). The cellular biology of proton-motive force generation by V-ATPases. J. Exp. Biol. 203:89-95.
Osteresch C, Bender T, Grond S, Zezschwitz P, Kunze B, Jansen R, Huss M, Wieczorek H (2012). The binding site of the V-ATPase inhibitor apicularen is in the vicinity to those of bafilomycin and archazolid. J. Biol. Chem. 287:31866-31876.
Pietrantonio PV, Gill SS (1997). Ductin, a component of the V-ATPase, is developmentally regulated in *Heliothis virescens* midgut, and anti-ductin antibodies label lateral membranes. Cell Tissue Res. 289:97-108.
Price DR, Gatehouse JA (2008). RNAi-mediated crop protection against insects. Trends Biotechnol. 26:393-400.
Roignant JY, Carré C, Mugat B, Szymczak D, Lepesant JA, Antoniewski C (2003). Absence of transitive and systemic pathways allows cell-specific and isoform-specific RNAi in Drosophila. RNA 9:299-308.
Rong S, Li DQ, Zhang XY, Li S, Zhu KY, Guo YP, Ma EB, Zhang JZ (2013). RNA interference to reveal roles of *β*-N-acetyl glucosaminidase gene during molting process in *Locusta migratoria*. Insect Sci. 20:109-119.
Rosa C, Kamita SG, Falk BW (2012). RNA interference is induced in the glassy winged sharpshooter *Homalodisca vitripennis* by actin dsRNA. Pest Manage. Sci. 68:995-1002.
Sumner JP, Dow JAT, Earley FGP, Klein U, Jager D, Wieczorek H (1995). Regulation of plasma membrane V-ATPase activity by dissociation of peripheral subunit. J. Biol. Chem. 270:5649-2653.
Tamura K, Stecher G, Peterson D, Filipski A, Kumar S (2013). MEGA 6: Molecular evolutionary genetics analysis version 6.0. Mol. Biol. Evol. 30:2725-2729.
Terenius O, Papanicolaou A, Garbutt JS, Eleftherianos I, Huvenne H, Kanginakudru S, Albrechtsen M, An C, Aymeric JL, Barthel A, Bebas P (2011). RNA interference in Lepidoptera: An overview of successful and unsuccessful studies and implications for experimental design. J. Insect Physiol. 57:231-245.
Thakur N, Upadhyay SK, Verma PC, Chandrashekar K, Tuli R, Singh PK (2014). Enhanced whitefly resistance in transgenic tobacco plants expressing double stranded RNA of V-ATPase A gene. PLoS One 9:e87235.
Tian H, Peng H, Yao Q, Chen H, Xie Q, Tang B, Zhang W (2009). Developmental control of a lepidopteran pest *Spodoptera exigua* by ingestion of bacteria expressing dsRNA of a non-midgut gene. Plos One 4:e6225.
Tomoyasu Y, Denell RE (2004). Larval RNAi in Tribolium (Coleoptera) for analyzing adult development. Dev. Genes Evol. 214:575-578.
Upadhyay SK, Chandrashekar K, Thakur N, Verma PC, Borgio JF, Singh PK, Tuli R (2011). RNA interference for the control of whiteflies (*Bemisia tabaci*) by oral route. J. Biosci. 36:153-161.
Vitavska O, Wieczorek H, Merzendorfer H (2003). A novel role for subunit C in mediating binding of the H^+V-ATPase to the actin cytoskeleton. J. Biol. Chem. 278:18499-18505.
Vitavska O, Wieczorek H, Merzendorfer H (2005). The V-ATPase subunit C binds to polymeric F-actin as well as to monomeric G-actin and induces cross-linking of actin filaments. J. Biol. Chem. 280:1070-1076.
Whyard S, Singh AD, Wong S (2009). Ingested double-stranded RNAs can act as species specific insecticides. Insect Biochem. Mol. Biol. 39:824-832.
Wieczorek H, Grüber G, Harvey WR, Huss M, Merzendorfer H, Zeiske W (2000). Structure and regulation of insect plasma membrane H^+ V-ATPase. J. Exp. Biol. 203:127-135.
Xiong Y, Zeng H, Zhang Y, Xu D, Qiu D (2013). Silencing the *HaHR3* gene by transgenic plant-mediated RNAi to disrupt *Helicoverpa armigera* development. Int. J. Biol. Sci. 9:370-381.
Yao J, Rotenberg D, Afsharifar A, Barandoc-Alviar K, Whitfield AE (2013). Development of RNAi methods for *Peregrinus maidis*, the corn planthopper. PLoS One 8:e70243.
Zhang X, Zhang J, Zhu KY (2010). Chitosan/double-stranded RNA nano-particle mediated RNA interference to silence chitin synthase genes through larval feeding in the African malaria mosquito (*Anopheles gambiae*). Insect Mol. Biol. 19:683-693.
Zhao YY, Liu F, Yang G, You MS (2011). PsOr1, a potential target for RNA interference-based pest management. Insect Mol. Biol. 20:97-104.
Zhu F, Xu JJ, Palli R, Ferguson J, Palli SR (2011). Ingested RNA interference for managing the populations of the Colorado potato beetle, *Leptinotarsa decemlineata*. Pest Manage. Sci. 67:175-182.
Zhu JQ, Liu S, Ma Y, Zhang JQ, Qi HS, Wei ZJ, Yao Q, Zhang WQ, Li S (2012). Improvement of pest resistance in transgenic tobacco plants expressing dsRNA of an Insect-Associated gene EcR. PLoS One 7:e38572.
Zhu KY (2013). RNA interference: A powerful tool in entomological research and a novel approach for insect pest management. Insect Sci. 20:1-3.

SUPPLEMENTARY FIGURES

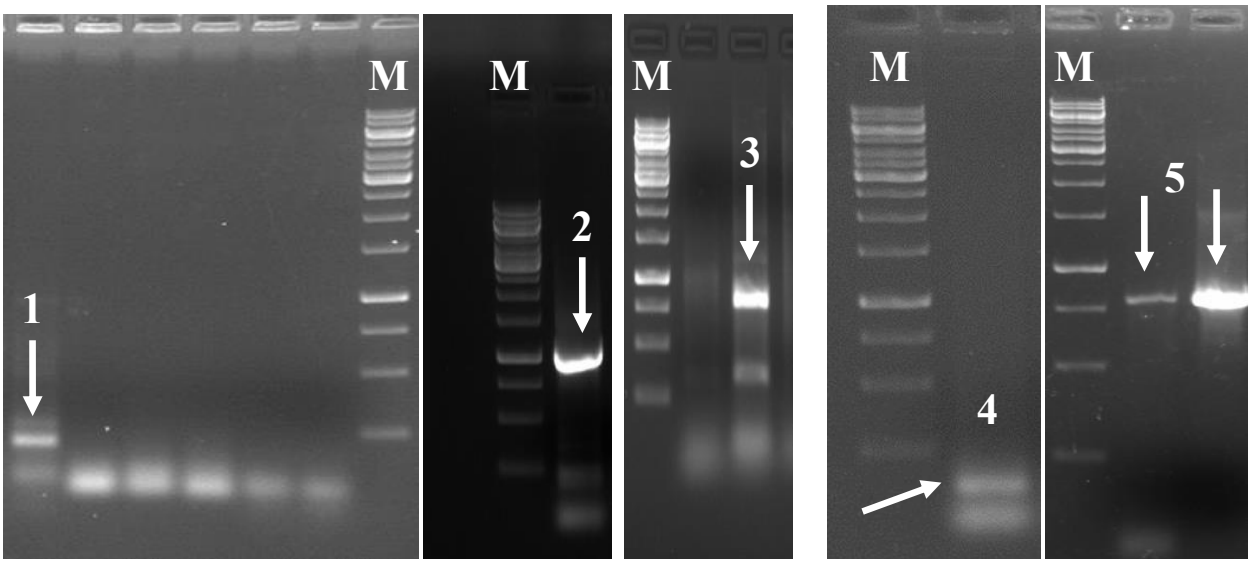

Figure S-1. Cloning of VATPase subunits a and c. PCR products of subunit a; (1) 220 bp using degenerate primer set (VATPavo2264FD/VATPavo2484RD), (2) 977 bp using degenerate/specific primers (VATPavo1439FD/VATPavo2416RS), (3) 783 bp using (VATPavo776FD/ VATPavo1559RS) and subunit c (4) 150 bp using degenerate primer set (VATPcvoFD/ VATPcvoRD), (5) 755 bp using degenerate/specific primers (VATPcvo146FD/ VATPcvo901RS). (M) 1 Kb DNA marker.

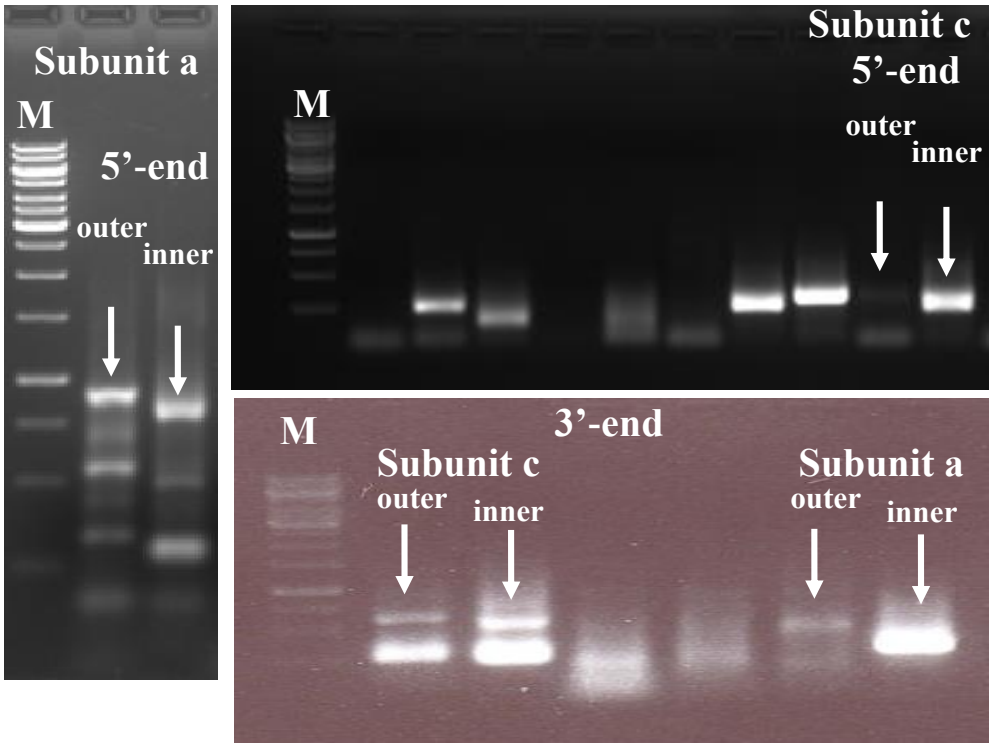

Figure S-2. RACE reactions; (1) 5'-end of subunit a was amplified using outer 5 prime supplied with the kit with VATPavo864RS specific primer followed by PCR reaction using inner 5 prime with VATPavo795RS specific primer. (2) 5'-end of subunit c was amplified using outer and inner prime with specific primers VATPcvo244RS and VATPcvo185RS, respectively. (3) 3'-end of both subunits a and c were synthesized using outer and inner 3 prime supplied with the kit with specific primers VATPcvo819FS and VATPcvo847FS for subunit c, and with specific primers VATPavo2265 FS and VATPavo2431FS for subunit a.

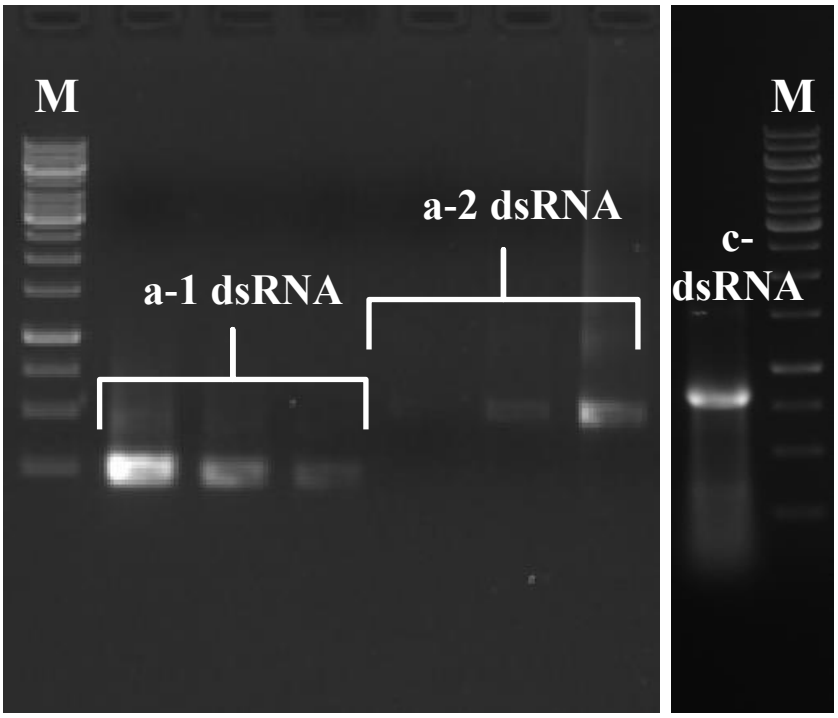

Figure S-3. Synthesis of dsRNA; a-1 dsRNA fragment of 220 bp using VATPavo2264F/ VATPavo2484R primer set; a-2 dsRNA fragment of 466 bp using VATPavo1950F/VATPavo2416R and c-dsRNA fragment of 740 bp using VATPcvo161F/ VATPcvo901R. (M) 1 Kb DNA marker.

academicJournals

Vol. 15(45), pp. 2558-2564, 9 November, 2016
DOI: 10.5897/AJB2016.15682
Article Number: 7F6708461543
ISSN 1684-5315

http://www.academicjournals.org/AJB

African Journal of Biotechnology

Full Length Research Paper

Genetic analysis of body weight of *Takifugu rubripes* at different developmental stages

Aijun Ma[1,2,3,4]* and Xin'an Wang[1,2,3,4]

[1]Yellow Sea Fisheries Research Institute, Chinese Academy of Fishery Sciences, China.
[2]Laboratory for Marine Biology and Biotechnology, Qingdao National Laboratory for Marine Science and Technology, Qingdao 266071, China.
[3]Key Laboratory of Sustainable Development of Marine Fisheries, Ministry of Agriculture, China
[4]Qingdao Key Laboratory for Marine Fish Breeding and Biotechnology, Qingdao 266071, China.

Received 20 September, 2016; Accepted 24 October, 2016

To elucidate the genetic mechanism of growth trait in *Takifugu rubripes* during ontogeny, developmental genetic analysis of body weight was conducted by mixed genetic model with additive-dominance effects, using complete diallel cross with three different strains of *T. rubripes* from Laizhou Shandong, Tangshan Hebei and Dalian Liaoning. Unconditional genetic analysis revealed that the unconditional dominance effects with very significant P<0.01 were detected during 8 to 20 months and the unconditional additive effects were detected only at 17 and 20 months. This suggests that the body weight trait was mainly controlled by dominance effects from 8 to 17 months and by both dominance and additive effects from 17 to 20 months. Conditional analysis showed that the net dominance effects were ascertained during growth from 0 to 8, 8 to 11, and 11 to 14 months, and the net additive effects were detected only during growth from 14 to 17 months. The following conclusions could be drawn from the results: the selection period should be considered during 14 to 17 months if the genetic improvement of *T. rubripes* is conducted using selective breeding, and the selection period should be considered during 8 to 14 months if cross breeding is used. The conditional genetic procedure is a useful method to elucidate the dynamics of genes action governing the variability of quantitative traits during ontogenetic development. In addition, the study is also highly important to determine the appropriate developmental period (*t*-1→*t*) for trait measurement in developmental quantitative genetic analysis in fish.

Key words: *Takifugu rubripes*, body weight, genetic parameters, gene effects.

INTRODUCTION

Takifugu rubripes belongs to teleost, Tetraodontiformers, Tetraodontoidei, Tetraodontidae, and Takifugu. It is distributed mainly in Japan of the Western North Pacific, the Korean Peninsula and China Coast (Wang et al.,

*Corresponding author. E-mail: maaj@ysfri.ac.cn.

2016). Due to its appealing taste, rich nutrition, low fat content and numerous trace elements, *T. rubripes* represents one of the fish species with high economic value (Wang et al., 2016). In recent years, T. rubripes are extensively farmed in Dalian, Qinhuangdao, Tangshan, and Tianjin regions, and have become the main cultured species of China puffer fishery. However, with the expansion of the scale of farming, serious germ plasm degeneration has appeared owing to lack of scientific and reasonable parent fish mating programmes, which has led to high mortality and retarded growth. Production of *T. rubripes* showed large fluctuations and the total yield decreased gradually, which severely restricted the development of *T. rubripes* aquaculture. Therefore, the genetic improvement of *T. rubripes* is necessary to sustain the development of the industry in a highly competitive aquaculture market.

For animal breeding, it is the foundation of the breeding work for studies on the genetic mechanism of breeding traits. These studies have important academic significance and application value to elucidate thoroughly the genetic mechanism of breeding traits and improve the predictability and selection efficiency of genetic breeding. In fish breeding, the genetic analysis of many quantitative traits was reported. Generally, these studies mostly utilized the data collected from one single time point to estimate the genetic effects (Gjerde et al., 1997; Martínez et al., 1999; Shikano, 2007; Tian et al., 2011; Liu et al., 2011, 2013; Zhang et al., 2014). However, the genetic mechanism of quantitative traits changes with temporal and spatial patterns (Zhu, 1995). Genes, based on developmental theory, are selectively expressed during the different growing stages in specific spatio-temporal patterns, and the mechanism that controls complex traits would be significantly changed in developmental process (Atchley, 1984; Cowle et al., 1992; Atchley et al., 1994; Atchley and Zhu, 1997). Clearly, the entire process of genetic regulation in the process of development cannot be disclosed using the data sampled at a particular point in time and the dynamics of gene expression need to be studied in different growth phases during ontogenetic development.

In the past, there were two common methods used for genetic analysis of developmental behavior: one by analyzing the phenotypic value at various periods; the other by using the difference ($y_{(d)}= y_{(t)}- y_{(t-1)}$) between two phenotypic values at time *t* and *t*-1. For quantitative traits, the genetic effects at time *t* were the sum of the genetic effects at time (*t*-1) and the extra genetic effects in the period (*t*-1) to *t* (Zhu, 1995). Obviously, the two methods ignored the dissimilar gene actions at different stages which is an important factor influencing the development of the quantitative traits and have not revealed the net genetic effects of gene expression during developmental stages. A conditional analysis method developed by Zhu (1995) can solve this problem well and can estimate the extra genetic effects in specific developmental intervals.

In recent years, genetic analysis for quantitative developmental traits has achieved important progress in terrestrial animals (Atchley, 1984, 1994; Atchley and Zhu, 1997; Cowley and Atchley, 1992) and plants (Zhu, 1995; Shi et al., 2001, 2002) based on the conditional analysis method. However, the aquatic organisms have attracted very limited attention (Wang et al., 2006). The objective of this study is to evaluate the developmental dynamics of genetic effects for body weight in *T. rubripes* at different growth periods based on the method and to explore the preliminary investigations on developmental quantitative genetics in fish.

MATERIALS AND METHODS

Cross mating and rearing conditions

During April 21 to 24 2011, a complete 3×3 diallel cross was conducted on three strains of *T. rubripes* collected from Laizhou Shandong, Tangshan Hebei and Dalian Liaoning in Laizhou Mingbo Fisheries Limited Company. Laizhou strain (LZ) came from Mingbo Fisheries Limited Company in Laizhou Shandong; Tangshan strain (TS) came from Tanghai Nanpu Salt Farm in Tangshan Hebei; Dalian strain (DL) came from Tianzheng Industrial Limited Company in Dalian Liaoning. The cross mating experiments were performed in nine concrete tanks filled with air-pumped circulating seawater with five females and five males in each tank. The quantity of fish and the environment were standardized to obtain similar rearing conditions for all cross combinations at the early breeding stage. After hatching at 15, 30, 60, and 120 days, the quantity of larvae or juveniles in each cross combination was standardized using random samples of 15000, 8000, 5000, and 2000, respectively. At 6 months of age, 400 samples were randomly selected from each stocking tank for tagging using Visible Implant Fluorescent Elastomer (VIE) tags. Polyculture was used with two parent fish and their reciprocal cross combinations in one tank (72 m^3 each); for example, the parents Laizhou and Tangshan and their reciprocal hybrids Laizhou(♀)×Tangshan(♂) and Tangshan(♀)×Laizhou(♂) with 300 fish each were combined in a single tank with a total of 1200 fish. Clearly, 3 kinds of polycultures were obtained by diallel crossing resign of 3×3. Nine of such tanks were used in this study with three replicates for each polyculture. Thus, a total of 10800 fish were initially tagged using VIE tags. The environmental conditions were standardized for the different rearing stages. During the larval-culture period, water temperature, salinity, illumination intensity, pH, ammonia nitrogen, nitrite-nitrogen, and dissolved oxygen were 5 to 22°C, 25 to 32, 500 to 1000 lx, 7.8 to 8.3, ≤1 mg/L, ≤0.4 mg/L, and 5 to 10 mg/L, respectively. During the juvenile- and adolescent-culture period, the above seven indices were 22 to 24°C, 15 to 32, 500 to 1000 lx, pH 7.8 to 8.3, ≤1 mg/L, ≤0.4 mg/L and ≥6 mg/L, respectively.

From 8 to 20 months, the body weights (BW) of all fish in each tank were measured every three months. Each data collection was synchronous with moving ponds. Body weights were measured using an electronic balance with a precision of 0.01 g. More than 90% survival rates were obtained for each tank due to well-maintained culture conditions.

Genetic analysis methods

The statistical analysis model including additive and dominance genetic effects was adopted to calculate the genetic components of additive (V_A) and dominance variance (V_D) of body weights of *T.*

Table 1. Estimates of unconditional variance components and their proportions to phenotype variance for body weight in *Fugu rubripes* at different growth stages.

Months	Unconditional variance components			Proportions of unconditional variance components	
	V_A	V_D	V_p	V_A/V_p	V_D/V_p
8	0	102.626**	1312.09*	0	0.0782156
11	0	1238.52**	9109.13**	0	0.135965
14	0	1890.38**	11472.8**	0	0.1647*
17	1331.02**	2307.09**	19834.7**	0.0671054	0.116316+
20	1490.4**	3474.56**	20490.7**	0.0727356	0.169568*

V_A, unconditional additive variance; V_D, unconditional dominance variance; V_p, unconditional phenotypic variance; +, * and ** are significant at 0.10, 0.05 and 0.01 levels, respectively. The means of abbreviations and symbols in Tables 2, 3 and 4 are the same as those in Table 1.

rubripes. The unconditional genetic analysis model can be written as (Zhu, 1995; Atchley and Zhu, 1997; Wang et al., 2006):

$$Y_{ij(t)} = u_{(t)} + A_{i(t)} + A_{j(t)} + D_{ij(t)} + e_{ij(t)}$$

where $Y_{ij(t)}$ is the unconditional phenotypic value of the individual from maternal line i × paternal line j at time t;$u_{(t)}$ is the unconditional population mean at time t; $A_{i(t)}$ or ($A_{j(t)}$) is the unconditional additive effect from maternal line i (or paternal line j) at time t, $A_{i(t)} \sim (0, \sigma^2_{A_{i(t)}})$, $A_{j(t)} \sim (0, \sigma^2_{A_{j(t)}})$; $D_{ij(t)}$ is the unconditional dominance effect from the cross of line i ×j at time t, $D_{ij(t)} \sim (0, \sigma^2_{D_{(t)}})$; and $e_{ij(t)}$ is the unconditional residual error at time t, $e_{ij(t)} \sim (0, \sigma^2_{e_{(t)}})$.

For body weight, genetic effect at time t includes cumulative genetic effects at time (t-1) and added genetic effects in the period (t-1 → t) (Zhu, 1995; Atchley and Zhu, 1997; Wang et al., 2006). The measured values at time t were conditioned on measured values at time t – 1. Thus, the conditional genetic model can be written as follows (Zhu, 1995; Atchley and Zhu, 1997; Wang et al., 2006):

$$Y_{ij(t|t-1)} = u_{(t|t-1)} + A_{i(t|t-1)} + A_{j(t|t-1)} + D_{ij(t|t-1)} + e_{ij(t|t-1)}$$

where $Y_{ij(t|t-1)}$, $u_{(t|t-1)}$, $A_{i(t|t-1)}/A_{j(t|t-1)}$, $D_{ij(t|t-1)}$ and $e_{ij(t|t-1)}$ is the conditional measured value of the individual from female parent fish i ×male parent fish j at time t, the conditional population mean value at time t, the conditional additive effect from female parent fish i / male parent fish j at time t, the conditional dominance effect from the hybridization of line i × j at time t and the conditional residual error at time t, respectively, $A_{i(t|t-1)} \sim (0, \sigma^2_{A_{i(t|t-1)}})$, $A_{j(t|t-1)} \sim \sigma^2_{A_{j(t|t-1)}}$, $D_{ij(t|t-1)} \sim (0, \sigma^2_{D_{(t|t-1)}})$ and $e_{ij(t|t-1)} \sim (0, \sigma^2_{e_{(t|t-1)}})$.

According to the estimated unconditional and conditional variance components, phenotypic unconditional and conditional variance can be obtained by $V_{P(t)} = V_{a(t)} + V_{d(t)} + V_{e(t)}$ and $V_{P(t|t-1)} = V_{a(t|t-1)} + V_{d(t|t-1)} + V_{e(t|t-1)}$, respectively. The unconditional ($V_{A(t)}$ and $V_{D(t)}$) / conditional ($V_{A(t|t-1)}$ and $V_{D(t|t-1)}$) variance components were estimated using the MINQUE(1) method (Rao, 1970, 1971; Zhu, 1995; Wang et al., 2006) with 1 for all prior components (Zhu, 1993; Zhu and Weir, 1996; Wang et al., 2006). The Jackknifing re-sampling method (Miller, 1974; Zhu and Weir, 1996) was employed to estimate the standard errors of variance components. The t-test was applied to test the significance of all estimated parameters. All data were calculated and analyzed using the statistical programs supplied by Zhu (Zhu, 1995).

RESULTS

Unconditional and conditional variance components

The unconditional genetic variances for body weight including V_A and V_D (The genetic variances for body weight at a fixed age) showed that the unconditional additive variances can be significantly detected only at 17 and 20 months and the value at 17 months was greater than that at 20 months (Table 1); and the unconditional dominance variances with very significant P<0.01 can be detected from 8 to 20 months; it appears that there was systematically increased trends with the development of *T. rubripes* (range: 102.626-3474.56). The proportions of unconditional additive/dominance variance showed that, the changes of the proportions of unconditional additive variance were basically identical to those of unconditional dominance variance except for a lower proportion at 17 months, and the proportions of unconditional dominance variance were greater than that of the unconditional additive variance at 17 and 20 months (Table 1). This indicates that the phenotypic variability of body weight was controlled by dominance effects from 8 to 14 months and controlled by both additive and dominance effects from 8 to 20 months.

For body weight, the genetic effect at time t includes both cumulative genetic effects at time (t-1) and added genetic effects within the period (t-1 → t) (Zhu, 1995; Wang et al., 2006). In the present paper, the unconditional genetic effects described earlier at different months of age were the cumulative genetic effects of many genes expressed at specific age periods from the initial month to the month when the body weights were measured. The unconditional genetic analysis can estimate the cumulative but cannot estimate the added genetic effects in a certain

Table 2. Estimates of conditional variance components and their proportions to phenotype variance for body weight in *Fugu rubripes* at different growth stages.

Month interval	Conditional variance components			Proportions of conditional variance components	
	$V_{A\ (t\mid t-1)}$	$V_{D\ (t\mid t-1)}$	$V_{p\ (t\mid t-1)}$	$V_{A\ (t\mid t-1)} / V_{p\ (t\mid t-1)}$	$V_{D\ (t\mid t-1)} / V_{p\ (t\mid t-1)}$
8 | 0	0	102.626**	1312.09*	0	0.0782156
11 | 8	0	646.951**	6166.78**	0	0.104909
14 | 11	0	791.852**	2372.14**	0	0.333813**
17 | 14	539.608**	0	3412.21**	0.15814**	0
20 | 17	0	0	2228.55**	0	0

$V_{A(t\mid t-1)}$, conditional additive variance; $V_{D(t\mid t-1)}$, conditional dominance variance; $V_{e(t\mid t-1)}$, conditional residual variance; $V_{p(t\mid t-1)}$, conditional phenotypic variance.

Table 3. Unconditional and conditional additive effects for body weight in *Fugu rubripes* parents at different growth stages.

Months	Unconditional additive effects			Month interval	Conditional additive effects		
	$A_{(TS)}$	$A_{(DL)}$	$A_{(LZ)}$		$A_{(TS)\ (t\mid t-1)}$	$A_{(DL)\ (t\mid t-1)}$	$A_{(LZ)\ (t\mid t-1)}$
8	0	0	0	8 | 0	0	0	0
11	0	0	0	11 | 8	0	0	0
14	0	0	0	14 | 11	0	0	0
17	25.615422	-25.975728	0.359682	17 | 14	14.579467	-17.796248+	3.215729
20	23.328032	-30.023141	6.694391	20 | 17	0	0	0

$A_{(TS)}$, unconditional additive effects of TS parents; $A_{(DL)}$, unconditional additive effects of DL parents; $A_{(LZ)}$, unconditional additive effects of LZ parents; $A_{(TS)\ (t\mid t-1)}$, conditional additive effects of TS parents; $A_{(DL)\ (t\mid t-1)}$; conditional additive effects of DL parents; $A_{(LZ)\ (t\mid t-1)}$; conditional additive effects of LZ parents.

period; the conditional genetic analysis developed by Zhu (1995) provides a useful method to elucidate the dynamics of genes action governing the variability of quantitative traits during ontogenetic development (Zhu, 1995; Atchley and Zhu, 1997) and could estimate the extra genetic effects. The conditional genetic variances showed that the conditional dominance variances with very significant $P<0.01$ were detected only at the intervals of 0 to 8, 8 to 11 and 11 to 14 months, and the conditional additive variances only at the intervals of 14 to 17 months (Table 2). Obviously, the net additive/ dominance genetic variances (conditional genetic variance) at different developmental stages were different and detected only at some time intervals. It is very difficult to elucidate these genetic characteristics using traditional genetic analysis methods.

Conditional and conditional genetic effects

The additive effects of *T. rubripes* parents and dominance effects of their cross combinations are different at different growth stages (Tables 3 and 4). The results indicated that the genetic effects at different developmental stages were different; therefore, the traditional genetic analysis (unconditional) using the phenotypic values measured at a fixed age cannot reveal the differences of the genetic effects in specific development intervals. But, the differences can be clearly elucidated using developmental genetic analysis method and the optimal parents and optimal mating combinations could be selected for genetic improvement.

The unconditional and conditional additive effects of parents at different growth stages are summarized in Table 3. The unconditional additive effects of three *T. rubripes* parents can be detected only at 17 and 20 months, but the two values were not statistically significant ($P>0.10$). The unconditional additive effect value of TS parents was the largest and that of DL parents was the lowest. The conditional additive effects can be only detected at the intervals of 14 to 17 months and the new expression of additive effect genes was turned-off at other four development intervals.

The unconditional and conditional dominance effects of different mating combinations at different growth stages are summarized in Table 4. The unconditional dominance effects of different mating combinations can all be detected at five development intervals and were not statistically significant ($P>0.10$), but the three sets values showed different change trends, that is, the unconditional

Table 4. Unconditional and conditional dominance effects for body weight in *Fugu rubripes* crosses at different growth stages.

Months	Unconditional dominance effects			Month interval	Conditional dominance effects		
	$D_{(TS\times DL)}$	$D_{(TS\times LZ)}$	$D_{(DL\times LZ)}$		$D_{(TS\times DL)\ (t\mid t-1)}$	$D_{(TS\times LZ)\ (t\mid t-1)}$	$D_{(DL\times LZ)\ (t\mid t-1)}$
8	12.531387	-6.894688	11.535862	8 | 0	12.531387	-6.894688	11.535862
11	59.224261	-33.516730	-14.718509	11 | 8	30.433316	-17.150900	-34.844647
14	45.838099	-67.665930	10.208108	14 | 11	-18.260171	-38.848113+	29.084396*
17	48.592290	-71.303413	10.043455	17 | 14	0	0	0
20	77.881972+	-73.870438	-3.207248	20 | 17	0	0	0

$D_{(TS\times DL)}$, unconditional dominance effects of TS×DL mating combination; $D_{(TS\times LZ)}$, unconditional dominance effects of TS×LZ mating combination; $D_{(DL\times LZ)}$, unconditional dominance effects of DL×LZ mating combination; $D_{(TS\times DL)\ (t\mid t-1)}$, conditional dominance effects of TS×DL mating combination; $D_{(TS\times LZ)\ (t\mid t-1)}$, conditional dominance effects of TS×LZ mating combination; $D_{(DL\times LZ)\ (t\mid t-1)}$, conditional dominance effects of DL×LZ mating combination.

dominance effects of TS×DL, TS×LZ and DL×LZ mating combinations showed increasing, decreasing and fluctuant change, respectively. The conditional dominance effects of different mating combinations can be detected only at the intervals of 0 to 8, 8 to11, and 14 to 17 months, but the three values were not statistically significant (*P*>0.10). The net dominance effects of both TS×DL and DL×LZ mating combinations have two positive and one negative value and that of TS×LZ mating combination has three decreasing negative values. The conditional dominance effects cannot be detected at the intervals of 14 to 17 and 17 to 20 months, and the new expression of dominance effect genes was turned-off at the two development intervals.

DISCUSSION

The body weight at a time point, as a typical quantitative trait, depends on the genes expression, regulation and their interactions during growth and development. The genetic analysis using the body weight measured at a specific moment in time can only reflect the accumulative genetic effects of multiple genes controlling body weight, but cannot reveal the extra genetic effects in specific development intervals. Therefore, it is necessary to study the differences in gene expression for body weight in specific development intervals, which can deeply understand the genetic architecture of quantitative traits and provide more detailed theory evidences for the genetic improvement of body weight (Zhu, 1995). In this study, the developmental genetic analysis was conducted for body weight in *T. rubripes* by using the statistical methods of the conditional genetic variance component estimation and conditional genetic effect prediction (Zhu, 1995). This method can overcome the drawback of the traditional genetic analysis that cannot estimate the extra genetic effects in specific development intervals and was widely applied in terrestrial animals (Atchley, 1984; Cowley and Atchley, 1992; Atchley et al., 1994; Atchley and Zhu, 1997) and plants (Zhu, 1995; Ye and Zhu, 2000; Fan et al., 2000; Shi et al., 2001). But, little research in this field has been conducted in fish (Wang et al., 2006).

The unconditional genetic variances for body weight at different developmental stages in *T. rubripes* showed that the unconditional additive variances can be significantly detected only at 17 and 20 months, and the unconditional dominance variances can be significantly detected during all stages and appeared systematically increased trends with the development of *T. rubripes*. The conditional genetic variances showed that the conditional additive variances only at the intervals of 14 to 17 months and the conditional dominance variances which were very significant (P<0.01) were detected only at the intervals of 0 to 8, 8 to 11 and 11 to 14 months. Obviously, the genetic effects of controlling body weight at some developmental stages displayed alternative expressions. The following conclusions could be drawn from the results described earlier: the selection period should be considered during 14 to 17 months if the genetic improvement of *T. rubripes* is conducted using selective breeding, and the selection period should be considered during 8 to 14 months if using cross breeding.

The unconditional additive effects of three *T. rubripes* parents at different growth stages showed that it can be detected only at 17 and 20 months and that of TS, LZ and DL parents were the largest, larger and negative, respectively. The conditional additive effects showed that it can be only detected at the intervals of 14 to 17 months and the new expression of additive effect genes was turned-off at other development intervals. The unconditional dominance effects of different mating combinations at different growth stages showed that it can all be detected at five development intervals, and the change trends of the dominance effects of TS×DL, TS×LZ and DL×LZ mating combinations showed increasing, decreasing and fluctuating changes, respectively. The conditional dominance effects of different mating combinations showed that it can be detected only at the intervals of 0 to 8, 8 to 11 and 14 to 17 months, and that of both TS×DL and DL×LZ mating combinations have two positive and one negative values

and that of TS×LZ mating combination three decreasing negative values. The results described earlier showed that the preferred parents should be from TS and LZ strains if the genetic improvement of *T. rubripes* is conducted using selective breeding and the preferred mating combinations should be TS×DL and DL×LZ if using cross breeding, whereas DL strain and TS×LZ mating combination were unsuitable for selective breeding and cross breeding.

Using conditional genetic analysis method can obtain the net genetic effects between two development periods, investigate the dynamic genetic expression of a certain period under condition of eliminating early interference, and further explain the results of unconditional analysis (Ye and Zhu, 2000). For conditional genetic analysis, the test interval (t-k) plays an important role in investigating the gene activity of quantitative traits at various stages. Previous studies showed that the genetic effects of opposite direction counteracted each other and were not detected due to a long test interval when the intensity of gene activity varied from weak to strong (Ye and Zhu, 2000). The developmental genetic analysis of body weight in T. rubripes was conducted using the data measured during 8 to 20 months. Obviously, the developmental interval used in this study is in the period that the intensity of gene activity varied from weak to strong, and the fast-growth is likely to continue for some time after 20 months. In this study, the unconditional and conditional genetic effects (additive and dominance effects) cannot be significantly detected except for the conditional additive effects of DL parents at the intervals of 14 to 17 months and the conditional dominance effects of TS×LZ and DL×LZ mating combination at the intervals of 11 to 14 months. This could be because the test interval of 3 months is too long for the genetic analysis of body weight in *T. rubripes ; it is* not an optimal interval.

From breeding viewpoint, the studies on the genetic mechanism of breeding traits provided the necessary background to determine the best selection strategy (for example, determining breeding method, clarifying breeding period, identifying the best individuals for mating and predicting response to selection, etc.) to be adopted in the genetic improvement program in order to allow the selection response and efficient advancement predicted. In addition, it could also provide some basis for quantitative trait loci (QTLs) analysis and marker assisted selection (MAS) of *T. rubripes* quantitative traits improvement at different developmental stages.

Conclusion

The following conclusions could be drawn from the results described earlier: the selection period should be considered during 14 to 17 months if the genetic improvement of *T. rubripes* is conducted using selective breeding and the selection period should be considered during 8 to 14 months if cross breeding is used.

Conflicts of Interests

The authors have not declared any conflict of interests.

ACKNOWLEDGEMENTS

The authors are grateful for the financial support provided by the Earmarked Fund for the Special Fund for Basic Scientific Research Business of Central Public Research Institutes (20603022012005) and Daliang Xinzhou Research Program (2012-B1-012), China.

REFERENCES

Atchley WR (1984). Ontogeny, timing of development and genetic variance-covariance structure. Am. Nat. 123(4):519-540.

Atchley WR, Zhu J (1997). Developmental quantitative genetics, conditional epigenetic variability and growth in mice. Genetics 147(2):765-776.

Atchley WR，Xu SZ, Vogl C (1994). Developmental quantitative genetic models of evolutionary change. Dev. Genet. 15(1):92-103.

Cowley DE, Atchley WR (1992). Quantitative genetic models for development, epigenetic selection and phenotypic evolution. Evolution 46(46):495-518.

Fan LJ, Shi CH, Wu JG, Zhu J, Wu P (2000). Developmental genetic analysis of brown rice thickness of indica rice (*Oryza sativa* L.). Acta Genet. Sin. 27(10):870-877.

Gjerde B, Røer JE, Lein I, Stoss J, Refstie T (1997). Heritability for body weight in farmed turbot. Aquac. Int. 5(2):175-178.

Liu XD, Zhao GT, Cai MY, Wang ZY (2013). Estimated genetic parameters for growth-related traits in large yellow croaker Larimichthys crocea using microsatellites to assign parentage. J. Fish Biol. 82(1):34-41.

Liu YX, Wang GX, Wang YF, Si F, Sun ZH (2011). Estimation of genetic parameters for growth traits of Japanese flounder Paralichthys olivaceus using an animal model. Fish. Sci. 77(1):87-93.

Martínez V, Neira R, Gall GAE (1999). Estimation of genetic parameters from pedigreed populations: lessons from analysis of alevin weight in Coho salmon *Oncorhynchus kisutch*. Aquaculture 180(3-4):223-236.

Miller RG (1974). The jackknife: a review. Biometrika 61(1):1-15.

Rao CR (1970). Estimation of heteroscedastic variances in linear model. J. Am. Stat. Assoc. 65(329):161-172.

Rao CR (1971). Estimation of variance and covariance components-MINQUE theory. J. Multivar. Anal. 1(3):257-275.

Shi CH, Wu JG, Fan LJ, Zhu J, Wu P (2001). Developmental genetic analysis of brown rice weight under different environmental conditions in indica rice. Acta Bot. Sin. 43(6):603-609.

Shi CH, Wu JG, Lou XB, Zhu J, Wu P (2002). Genetic analysis of transparency and chalkiness area at different filling stages of rice (*Oryza sativa* L.). Field Crops Res. 76(1):1-9.

Shikano T (2007). Quantitative genetic parameters for growth-related and morphometric traits of hatchery-produced Japanese flounder *Paralichthys olivaceus* in the wild. Aquac. Res. 38(12):1248-1253.

Tian YS, Xu TJ，Liang Y, Chen SL (2011). Estimates of genetic and phenotypic parameters for weight and length in Paralichthys olivaceus (Temminck et Schlegel). Acta Oceanol. Sin. 30(6):58-64.

Wang CH, Li SF, Liu ZG, Xiang SP, Wang J (2006). Developmental quantitative genetic analysis of body weight and morphological traits in red common carp, *Cyprinus carpio* L.. Aquaculture 251(2):219-230.

Wang QL, Zhang HT, Ren YQ, Zhou Q (2016). Comparison of growth parameters of tiger puffer Takifugu rubripes from two culture systems in China. Aquaculture 453(13):49-53.

Ye ZH, Zhu J (2000). Genetic analysis on flowering and boll setting in upland cotton (*Cossypium hirsutum* L.). III. Genetic behavior at different developing stages. Acta Genet. Sin. 27(9):800-809.

Zhang TS, Kong J, Liu BS, Wang QY, Cao BX., Luan S, Wang WJ (2014). Genetic parameter estimation for juvenile growth and upper

thermal tolerance in turbot (*Scophthalmus maximus* Linnaeus). Acta Oceanol. Sin. 33(8):106-110.
Zhu J (1993). Methods of predicting genotype value and heterosis for offspring of hybrids. J. Biomath. 8(1):32-44.
Zhu J (1995). Analysis of conditional genetic effects and variance components in developmental genetics. Genetics 141(141):1633-1639.
Zhu J, Weir BS (1996). Mixed model approaches for diallel analysis based on a bio-model. Genet. Res. 68(3):233-240.

academicJournals

Vol. 15(45), pp. 2565-2571, 9 November, 2016
DOI: 10.5897/AJB2016.15553
Article Number: C9941D461545
ISSN 1684-5315

http://www.academicjournals.org/AJB

African Journal of Biotechnology

Full Length Research Paper

Diversity of growth hormone gene and its relation with average daily gain in Simmental cattle in West Sumatera Province, Indonesia

Hary Suhada[1], Sarbaini Anwar[2], Arnim[2], Hendri Maulana[2] and Dan Yurnalis[2]*

[1]Directorate General animal Husbandry and animal Health, Ministry of Agriculture, Indonesia.
[2]Faculty of Animal Husbandry, Andalas University, Indonesia.

Received 30 June, 2016; Accepted 24 October, 2016

This study was aimed to analyse the genetic polymorphism of Growth Hormone (GH) polymorphism of Simmental cattle using polymerase chain reaction-restriction fragment length polymorphism (PCR-RFLP) method and its relation to average daily gain. The research was conducted in the Padang Mangatas Breeding Centre, Limapuluh Kota district, West Sumatera Province and Biotechnology Laboratory of Faculty of Animal Husbandry, Andalas University. The research used 100 Simmental calves. DNA were isolation from blood sample using DNA purification Kit from Pomega. The PCR procedure was used to amplify 591-bp of bGH exon 1 (GH1) and 694-bp exon 2 (GH2). The PCR product were digested by restriction enzymes *Msp*I and *Alu*I. Digestion of 591-bp GH gen PCR product with enzyme restriction *Msp*I reveal allele A(+) and B(-) with frequency 0.875 and 0.125 respectively and digestion with restriction enzyme *Alu*I revealed allele C(+) and D(-) with frequency 0.95 and 0.05 respectively and. Digestion of 694-bp PCR product by *Msp*I represent allele P(+) and Q(-) with frequency 0.88 and 0.12 respectively and digestion with *Alu*I enzyme represent allele R(+) and S(-) with frequency 0.94 and 0.06 respectivly. The observed heterozygosity, effective allele numbers and polymorphism information content of GH1/MspI, GH2/MspI, GH1/*Alu*I, and GH2-*Alu*I were 0.11/0.1948, 0.04/0.1889, 0.00/0.0927, and 0.00/0,1096 respectively. Using GLM, there was no relation between these polymorphic and avarage daily gain of calve.

Key words: Simmental cattle, growth hormone (GH) gene, polymorphism, avarage daily gain growth.

INTRODUCTION

Growth traits are extremely important to animal husbandry. With the development of molecular biology and biotechnology, more accurate and efficient selection goal can be achieved through marker assisted selection (MAS). Growth hormone (GH) is an anabolic hormone synthesized and secreted by the somatotroph cells of the anterior lobe of the pituitary in a circadian and pulsatile manner (Ayuk and Sheppard, 2006), the pattern of which

*Corresponding author. E-mail: yurnalisunand@yahoo.com.

Table 1. Primers used for PCR analysis of GH gene.

Fragment	Primer sequence	Location	*Size* (bp)
GH1F	5'CCAGTGGTCCTTGCATAAATGT-3'	554/1144	591
GH1R	5'CTCGGGAGCTTACAAACTCTTT-3'		
GH2F	5'-ATGTCCTTGTCCGGCCTG-3'	1048/1741	694
GH2R	5'-CTGGATGAGGAGCAGTGAGAT-3'		

Table 2. Characteristics of restriction enzyme MspI and AluI.

Enzyme	Sequences identified	Intersection	t°C Incubation
*Msp*I	5'...C↓C G G...3'	976,1059,1084,1375,1438,1547	37°
*Alu*I	5'..A G↓C T… 3'	81,415,701,709,729,803,928,1105, 1137,1327,1538,1712	37°

plays an important role in postnatal longitudinal growth and development, tissue growth, lactation, reproduction, as well as protein, lipid, and carbohydrate metabolism (Akers, 2006; Ayuk and Sheppard, 2006; Thidar et al., 2008; Musa et al., 2013). Effects of GH on growth are observed in several tissues, including bone, muscle and adipose tissue. Therefore is a great interest in using GH gene as a promising candidate for selection purposes in breeding program of animals (Grochowska et al., 2002). GH gene in cattle is located on chromosome 19 consisting an arranged 191 amino acids (Hediger et al., 1990; Schlee et al., 1994), it has 2856 bp of nucleotide and consists of five exons and four introns (Woychik et al., 1982; Gordon et al., 1983; Vukasinovic et al., 1999). The sequence variations in the *GH* gene are well documented (Lucy et al., 1993; Yao et al., 1996; Hetch and Geldermann, 1996; Lagziel et al., 2000; Lagziel et al., 1996; Ferraz et al., 2006; Yurnalis et al., 2013).

Relationships between several polymorphic sites in *GH1* and milk production traits have been much investigated, particularly, the Leu/Val polymorphism (at residue 127) in exon five and polymorphic *Msp*I restriction site (TC/G insertion/transition) in the third intron. In beef production, Oka et al. (2007) reported that the carcass weight of the Leu/Leu the Val/Val group, while Barendse et al. (2006) found the Val variant to be associated with lower marbling. It has been reported that the restriction fragment length polymorphisms (RFLPs) of GH-*Taq*I were associated with body weight at 7 and 13 months of age in Belgian White Blue bulls (Sneyers et al., 1994). Significant effects were found for bGH genotype on yearling weight, with positive effects associated with the LV (leucine/valine) genotype in the Canchim beef cattle (Pereira et al., 2005). Regarding the effects of the polymorphic *Msp*I restriction site, Hoj et al. (1993), Lagziel et al. (1996), Lee et al. (1993) and Falaki et al. (1996) found that the allele lacked a functional *Msp*I site (*Msp*I[-]) to be associated with higher fat and protein yield and percentage in different dairy cattle breeds. In contrast, Yao et al. (1996) found the *Msp*I [-] allele to be associated with a statistically significant decrease in milk, fat and protein yield. The present study was carried out to detect allelic variants of the GH gene in relation to growth traits in Simmental cattle breeds.

MATERIALS AND METHODS

Blood samples and DNA extraction

Blood samples were collected from 100 Simmental cattle from Padang Mangatas Breeding centre, Lima Puluh Kota distric, West Sumatera Province, Indonesia. DNA was extracted using DNA purification Kit from Promega, following manufacturer instructions. Two regions of the GH gene (591 and 694 bp) were amplified from bovine genomic DNA using two primer pairs that designed using online primer3 program base on GH gene sequence from GenBank access number M57764.1 (Table 1).

Both PCR reactions were performed in a 25 µl mixture containing 2 ul of 10 pmol each primers, 12.5 ul master mix from thermo scientific, 6.5 ul nuclease free water, and 2 ul of 50 ng genomic DNA as template. The PCR cycling conditions included an initial denaturation step of 94°C for 5 min followed by 94°C for 1 min, 58°C for 1 min and elongation at 72°C for 1 min. After 35 cycles, a final extension was given at 72°C for 5 min. Samples were held at 4°C until further use. To check fragment integrity PCR products were electrophoresed at 150 V in a 1.5% agarose gel containing 0.5 µg ethidium bromide/mL along with a DNA molecular size marker. The gels were visualized and documented with the Gel documentation system (Gel doc 1000, Bio-Rad, USA).

The 591 and 694 bp amplicon was treated using *Msp*I and *Alu*I restriction enzyme to identify polymorphisms at the GH gene. A volume of 20 mL of PCR product was digested with 5 U *Msp*I and *Alu*I enzyme and the digested product was separated through ethidium bromide staining in 2% of agarose gel (Table 2).

Genotypic frequencies of different PCR-RFLP patterns were estimated from the combinations of various alleles generated based on presence or absence of one or more restriction sites. Allelic frequencies were calculated from genotypic frequencies using standard methods. The mean expected heterozygosity and deviations from Hardy-Weinberg equilibrium were calculated. Chi-square test was carried out to evaluate allelic and genotypic frequency differences across the investigated cattle breeds.

Analysis of the data is used as follows.

Table 3. Mean and standard deviation of Post weaning live weight gain simmental heifers and steers in Animal Breeding Center and forage Padang Mengatas.

No.	Source	Number	Post weaning live weight gain (kg)
1	Steers	71	0.36± 0.15
2	Heifers	29	0.24± 0.11
	Population	100	0.33± 0.15

Frequency of genotype

Genotype frequency was calculated based on the number of genotypes divided by the number of samples (N) with the equation as follows:

$$F_1 = \frac{\sum X_i}{N}$$

Xi = the observed genotype and N = the number of animals analyzed.

Frequency of allele

Alel frequency of GH gene is obtained from PCR analysis that was calculated by sum of all alels divided by twice the number of samples (2N):

$$F_1 = \frac{\sum X_i}{2N}$$

Xi = the observed allele and N = the number of animals analyzed.

Diversity of genetic (genetic variabability)

Diversity of genetic was obtained by estimating the frequency of heterozygosity observations (Ho) and heterozygosity expectations (He) and calculated by using formula (Nei, 1987; Weir, 1996) as follows:

$$H_o = \sum_{i \neq j} \frac{N_{1\,ij}}{N}$$

H_o = the frequency of observations heterozygosity; N_{1ij} = number of individuals heterozygous at the locus to-I, and N = number of individual analyzed.

$$H_e = 1 - \sum_{1=i}^{n} P_{1i}^2$$

H_e = frequency of heterozygosity expectations; P_{1ij} = frequency of allele to-i on the locus to-1^t, and n = number of allel on locus to-i^t.

Polymorphic informative content (PIC)

Information level for an alel is calculated using a value approach of Polymorphic Informative Content (PIC) (Botstein et al., 1980). PIC value can also be used to determine whether there is a polymorphic alel aside from being based on the value of heterozigisitas.

$$PIC = 1 - \sum_{I=1}^{N} P_i^2 - \sum_{i=1}^{n-1} \sum_{j=i+1}^{n} 2P_1^2 P_j^2$$

Pi = alel frequency to-I; n = number of allele on each marker.

Hardy - Weinberg equilibrium

Estimation of heterozygosity values is useful to get an idea of the genetic diversity of a livestock population (Marson et al., 2005). The balance of gene in Simmental cattle population (Hardy - Weinberg equilibrium) was tested using chi-square (χ^2) test (Hart and Clark, 1997) as follow:

$$\chi^2 = \sum \frac{(O_{IJ} - E_{IJ}).^2}{E_{ij}}$$

χ^2 = Chi-Squere test; O_{ij} = number of genotype observed to-i in group to-j; E_{ij} = number of genotype expectation i to group-j

The correlation of genotype fragment GH gene with post-weaning growth

Analysis of the correlation genotype of fragment GH gene with post-weaning growth of Simmental cattle in BPTU HPT Padang Mengatas was done by using *General Linear Model* as follow:

$Y_{ij} = \mu + G_i + Hi + E_{ij}$

Yij = Value Observation due to genetic influences to-I; μ = Mean common; Gi = Effect of sex I;
Hj = Effect of genotype to-I; Eijk = Effect of error experiment.

RESULTS AND DISCUSSION

Post weaning live weight gain

Mean and standard deviation of Post weaning live weight gain Simmental heifers and steers during the interval from 177 to 582 days of age are presented in Table 3.

Interactions between heifers and steers were significant sources of variation ($t < 0.05$), indicating heifers of the different sex studied responded not similarly. These results reflect the bull has higher than the cow. These results is lower than Suhada (2008) that claimed Post weaning live weight gain Simmental is 0.42 ± 0.10 kg. Sawyer et al. (1991) post weaning live weight gain Simmental heifer in southwest Australia could be 1.07 kg/day. Speer (2016) average of weight gains of

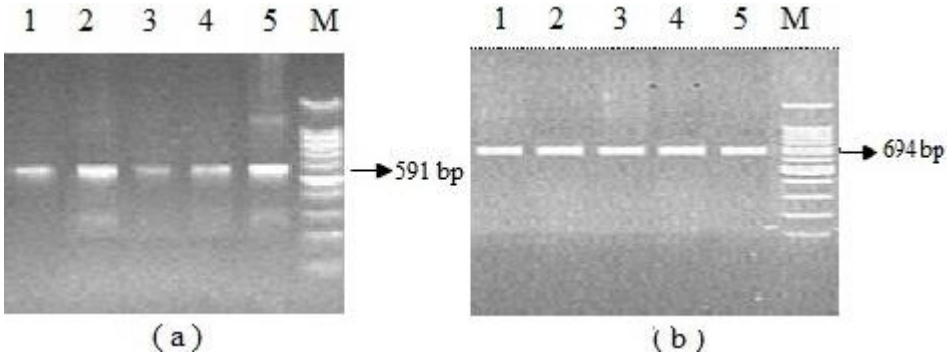

Figure 1. (a) Electrophoresis resulted of PCR product bGH with bGH-1; (b) Electrophoresis resulted of PCR product bGH with bGH-2. M: Marker (DNA ladder 100 bp), 1, 2, …etc = Number of sample.

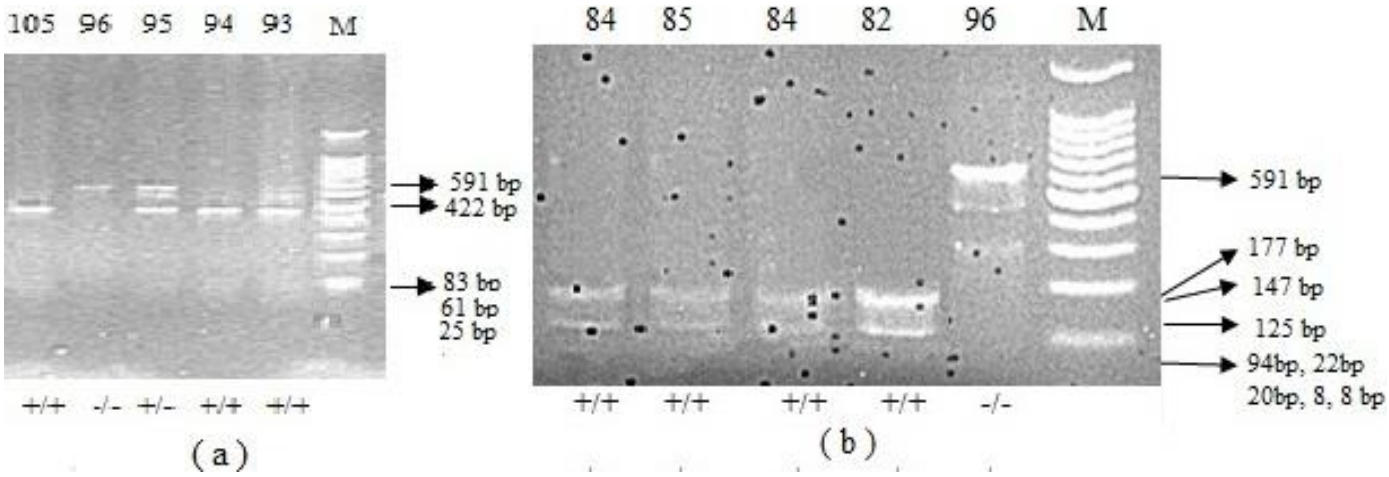

Figure 2. Different genotypes resulted from bGH-1 and bGH-2 with *Msp*I and *Alu*I endonuclease enzym restriction (a) b GH-1 *Msp*I (b) bGH-1 *Alu*I. M: marker (DNA ladder 100 bp), 93, 94,…etc = number of sample. +/+,+/-,-/- = genotype.

Simmental which treatments in feddlot for 1.51 kg/day.

These differences can be expected because of cattle adaptation capability to climate changing of Indonesia which is not optimal yet. Livestock production appearance can be affected by some factors, genetic, feed, management, eradication and prevention of disease and environment factors. Of the many possible influences operating to affect weaning weight the nutritional status of the calf is undoubtedly a most important one. The variation in weaning weight may be accounted for by differences in the milk production of the dams.

Genotyping genotype and allele frequency

The amplified bGH-1 resulted in a DNA fragment with 591 bp and bGH-2 resulted in a DNA fragment with 694 bp (Figure 1). Different genotypes resulted from bGH-1 and bGH-2 with MspI and AluI endonuclease enzym restriction (Figures 2 and 3).

bGH-1 MspI polymorphisms

In homozygous animals either a unique band (591 bp, -/- genotype), or four-band (422, 83.61 and 25 bp, +/+ genotype) patterns were observed. Heterozygous animals gave a five-band (591, 422, 83, 61 and 25 bp, +/- genotype), or four-band (422, 83, 61 and 25 bp, +/+ genotype) patterns were observed) pattern (Figure 2). Considering the 71 sterrs and 29 heifers analysed, the overall genotype frequencies were 0.82 for (+/+), 0.11 for (+/-) and 0.07 for (-/-). Gene frequencies of alleles (+) and (-) were 0.875 and 0.125 respectively (Table 4).

bGH-1 AluI polymorphisms

In homozygous animals either a unique band (591 bp, -/- genotype) or eight-band (177, 147, 125, 94, 22, 20, 8 and 8 bp, +/+ genotype) patterns were observed (Figure 2). Considering the 71 sterrs and 29 heifers analysed, the

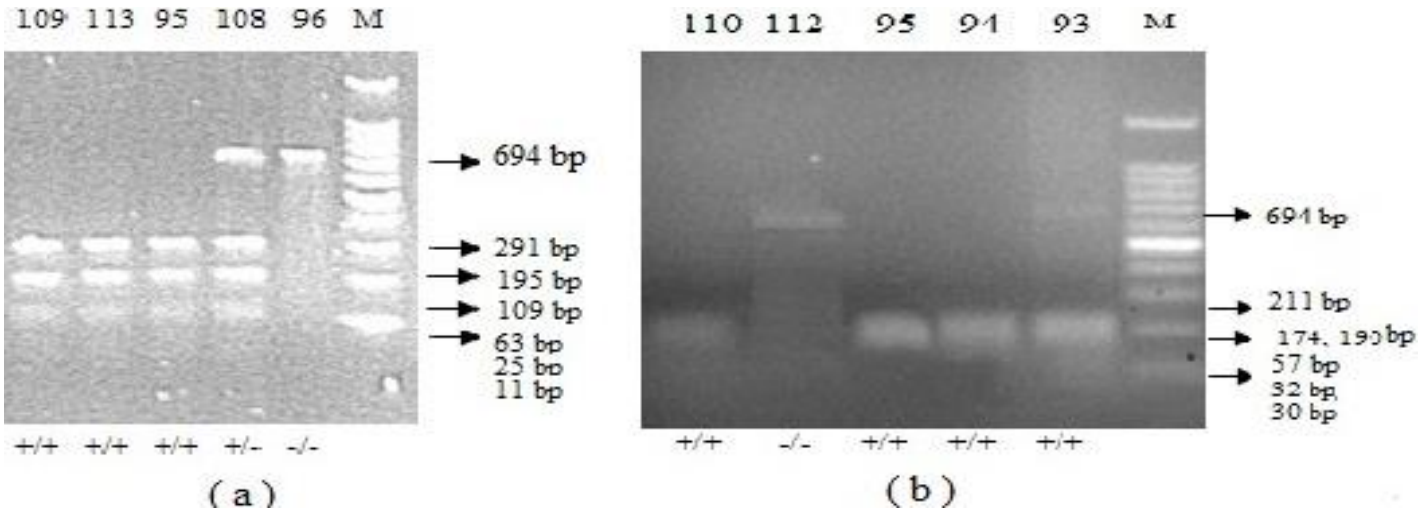

Figure 3. Different genotypes resulted from bGH-1 and bGH-2 with *Msp*I and *Alu*I endonuclease enzym restriction (a) b GH-2 *Msp*I (b) bGH-2 *Alu*I. M: Marker (DNA ladder 100 bp), 93, 94,…etc = number of sample (+/+,+/-,-/-) = genotype.

Table 4. Distribution of genotype frequencies and Allele frequencies (%) of RFLP polymorphism at the *Msp*I and *Alu*I loci in the bGH gene of Simmental.

Primer	Enzyme	Number of sample	Genotype frequency			Allele frequency	
			(+/+)	(+/-)	(-/-)	(+)	(-)
GH1	*Msp*I	100	0.82	0.11	0.07	0.875	0.125
	*Alu*I	100	0.95	0	0,05	0.95	0.05
GH2	*Msp*I	100	0.86	0,04	0.10	0.88	0.12
	*Alu*I	100	0.94	0	0.06	0.94	0.06

overall genotype frequencies were 0.95 for (+/+) and 0.05 for (-/-). Gene frequencies of alleles (+) and (-) were 0.95 and 0.05 respectively (Table 4).

bGH-2 MspI polymorphisms

In homozygous animals either a unique band (694 bp, -/- genotype), or six-band (291, 195, 109, 63, 25 and 11 bp, +/+ genotype) patterns were observed. Heterozygous animals gave a seven-band (694, 291, 195, 109, 63, 25 and 11 bp, +/+ genotype) patterns were observed (Figure 3). Considering the 71 sterrs and 29 heifers analysed, the overall genotype frequencies were 0.86 for (+/+), 0.04 for (+/-) and 0.10 for (-/-). Gene frequencies of alleles (+) and (-) were 0.88 and 0.12 respectively (Table 4).

bGH-2 AluI polymorphisms

In homozygous animals either a unique band (694 bp, -/- genotype) or six-band (211, 190, 174, 57, 32 and 30 bp, +/+ genotype) patterns were observed (Figure 3). Considering the 71 sterrs and 29 heifers analysed, the overall genotype frequencies were 0.95 for (+/+) and 0.05 for (-/-). Gene frequencies of alleles (+) and (-) were 0.94 and 0.06 respectively (Table 4).

Table 4 suggests that the genotype and allele frequency range of the MspI and AluI for Simmental cattle breeds of Aniamal Breeding Centre and Forage Indonesia. The Simmental cattle have genotype frequency (++) higher than other genotype frequency and allele frequency (+) of Simmental cattle is higher than alel frequency (-). This condition described that population of Simmental have alleles that are polymorphic, where in one population has more than one allele. An allele is said to be polymorphic if one alelnya less than 99% (Nei and Kumar, 2000). The frequency of allele (-) in this breed is lower than some of the reported Allele frequencies of GH variant (-) were: 0.32 in Bavarian Simmental bulls by Schlee et al. (1994), 0.44 in Slovak Simmental bulls by Chrenek et al. (1998).

Hardy-Weinberg equilibrium

The animals considered in this study have deviated from a Hardy-Weinberg equilibrium (Table 5), the overall chi-

Table 5. Equilibrium testing of GH1 and GH2 gene are restricted with the enzyme MspI and AluI.

Primer	Enzyme	Number	$(\chi^2)_{test}$
GH1	*MspI*	100	24.667**
	AluI	100	90.811**
GH2	*MspI*	100	65.706**
	AluI	100	90.92**

Table 6. The observations heterozygosity value (Ho) and expectations heterozygosity (He) GH gene are restricted with the enzyme MspI and AluI.

Gene fragment		Number sample (n)	$H_{observed}$ (Ho)	$H_{expected}$ (He)
GH1	*Msp*I	100	0.11	0.2188
	*Alu*I	100	0.00	0.0950
GH2	*Msp*I	100	0.04	0.2112
	*Alu*I	100	0.00	0.1128

square value for GH-1*Msp*I and GH-1 *Alu*I were 24,667 and 90,811 respectively. GH-2 *Msp*I and GH-2 *Alu*I were 24,667 and 90,811, respectively. This genetically unbalanced condition could be caused the main purpose of keeping Animal Breeding Center and Forage Padang Mengatas is livestock breeds production and the livestock kept in imported from Australia which has been selected beforehand.

Heterozygosity value

The observed heterozygosity was found to be less than expected in growth hormone gene locus in the whole investigated group of animals as well as in Simmental cattle (Table 6). The expectation value of heterozygosity (He) was bigger than the observations of heterozygosity (Ho). If the expectations of heterozygosity values bigger than the value of the observation of heterozygosity (Ho <He) identifies that the sample population had a degree of endogamy (marriage within the group) as a result of an intensive selection process (Machado et al., 2003).

The relationship of polymorphism GH gene with post weaning live weight gain

The relationship of growth hormone genotypes on growth traits are of great interest for their breeders. The results analysis of relationship polymorphism GH gene with post weaning live weight gain Simmental heifers and steers in Animal Breeding Center and Forage Padang Mengatas was observed as non-significant (P > 0.05). These matters showed the variation in each group is homogeneous. This caused by the nature of production is a trait that is controlled by many genes (polygenes) and environmental influences are very large (Warwick et al., 1983; Falconer and Macay, 1996).

In conclusion, it may be stated that growth hormone gene is low polymorphic and non-significant relationship between the genotypes polymorphic GH gene *Ms*pI and *Alu*I with post weaning live weight gain in the Simmental Cattle. The present study is the first report on GH genotyping of Simmental in Indonesia and has to be considered as a preliminary study. A larger number of observations are needed to establish or deny the existence of an association between GH genotypes and quantitative traits in those breeds.

Conflicts of Interests

The authors have not declared any conflict of interests.

ACKNOWLEDGMENT

This study contains some data from the author's dissertation work.

REFERENCES

Akers RM (2006). Major advances associated with hormone and growth factor regulation of mammary growth and lactation in dairy cows. J. Dairy Sci. 89:1222-1234.

Ayuk J, Sheppard MC (2006). Growth hormone and its disorders. Postgrad. Med. J. 82:24-30.

Barendse W, Bunch RJ, Harrison BE, Thomas MB (2006).The growth hormon 1 GH1:c.457C>G mutation is associated with intramuscular

and rump fat distribution in a large sampel of Australian feedlot cattle. Anim. Genet. 37:211-214.
Botstein D, White RL, Skolnick M, Davis RW (1980). Contruction of a genetic linkage map in human using restriction fragment length polymorphisms. Am. J. Hum. Genet. 32:314-331.
Chrenek P, Kmef J, Sakowski I, Va_icek D, Huba Jand Chrenek J. (1998). Relationships of growth hormone genotypes with meat production traits of Slovak Pied bulls. Czech J. Anim. Sci. 43:541-544.
Falaki M, Gengler N, Sneyers M, Prandi A, Massart S, Formigoni A, Burny A, Portetelle D, Renaville R (1996). Relationships of polymorphism for growth hormone and growth hormone receptor genes with milk production traits for Italian Holstein-Friesian bulls. J. Dairy Sci. 79:1446-1453.
Falconer DS, Mack Y (1996). Introduction to Quantitative Genetics. Fourth Ed. Loungman Inc., New York.
Ferraz AL. J, Bortolossi JC, Curi RA, Ferro MIT, Ferro JA, Furlan LR (2006). Identification and characterization of polymorphisms within the 5′ flanking region, first exon and part of first intron of bovine GH gen. J. Anim. Breed. Genet. 123:208-212.
Gordon DF, Quick DP, Erwin RC (1983). Nucleotide sequence of the bovine growth hormone chromosomal gene. Mol. Cell Endocrinol. 33(1):81-95.
Grochowska R, Gajewska A, Snochowski M, Zwierchovski L (2002). Ligand-binding activity of growth hormone receptor (GHR) in bulls of different breeds with identified GHR genotypes. J. Anim. Feed Sci. 11:223-236.
Hart DL, Clark AG (1997). Principle of Population Genetic.Sinauer Associates. Inc, Sounderland, Massachusetts.
Hediger R, Johnson SE, Barendse W, Drinkwater RD, Moore SS, Hatzel J (1990). Assignment of the growth hormone gene locus to 19q26-gter in cattle and to 11q25-qter in sheep by in situ hybridization. Genome 8:171-174.
Hoj, S, Fredholm M, Larsen NJ, Nielsen VH (1993). Growth hormone gene polymorphism associated with selection for milk fat production in lines of cattle. Anim. Genet. 24:91-95.
Lagziel A, DeNise S, Hanotte O, Dhara S, Glazko V, Broadhead A, Davoli R, Russo V, Soller M (2000). Geographic and breed distributionof an *Msp*I PCR-RFLP in the bovine growth hormone (bGH) gene. Anim. Genet. 31:210-213.
Lagziel A, Lipkin E, Soller M (1996). Association between SSCP haplotypes at the bovine growth hormon gene and milk production traits. Genetics 142:945-951.
Lee BK, Lin GF, Crooker BA, Murtaugh MP, Hansen LB, Chester-Jones H (1993). Association of somatotropin (bst) gene polymorphism at selection for milk yield in Holstein cows. Dairy Sci. 76(Suppl 1):149.
Lucy MC, Hauser SD, Eppard PJ, Krivi GG, Clark JH, Bauman DE, Collier RJ (1993). Variants of somatotropin allele in cattle: Gene frequencies in major dairy breeds and associated milk production. Dom. Anim. Endocrinol. 10:325-333.
Machado MA, Schuster I, Martinez ML, Campos AL (2003). Genetic diversity of four cattle breeds using microsatellite markers. Rev. Bras. Zootec. 32(1):93-98.
Marson EP, Ferraz JB, Meirelles FV, Balieiro JC, Eler JP, Figueiredo LG, Mourão GB (2005). Genetic characterization of European-Zebu composite bovine using RFLP markers. Genet. Mol. Res. 4(3):496-505.
Musa LMA, Reissman M, Ishag IA, Rahamtalla SA, Brockmann G. dan Peters JK (2013). Characterization of growth hormone Gene (GH1) in Sudanese Kanana and Butana Cattle Breeds. J. Anim. Prod. 3(2):28-34
Nei M, Kumar S (2000). Molecular Evolution and Phylogenetics. Oxford University Press. New York.
Nei M (1987). Molecular Evolutionary Genetics. Columbia University Press. New York.
Oka A, Iwaki F, Iwamoto E, Tatsuda K (2007). Effects of growth rate during the early fattening period on growth, carcass characteristics and circulating hormones in the different growth hormone genotypes of Japanese black steers. Anim. Sci. J. 78:142-150.
Pereira AP, Alencar De, De MM, Oliveira HN, de Regitano LC (2005). Association of GH and IGF-1 polymorphisms with growth traits in a synthetic beef cattle breed. Genet. Mol. Biol. 28:230-236.
Sawyer GJ, Barker DJ, Morris RJ (1991) Performance of young breeding cattle in commercial herds in the south-west of Western Australia. 2. Liveweight, body condition, timing of conception and fertility in first-calf heifers. Aust. J. Exp. Agric. 31(4):431-441.
Schlee P, Grami R, Rottmann O, Pirchner F (1994). Infulence of growth hormone genotypes on breeding value os simmental bulls. J. Anim. Breed. Genet. 111:253-256.
Sneyers M, Renaville R, Falaki M, Massart S, Devolder A, Boonen F (1994). TaqI restriction fragment length polymorphisms for growth hormone in bovine breeds and their association with quantitative traits. Growth Regul. 4:108-112.
Speer P (2016). Simmental High Performers in Feedlot Study. Australian Simmental Breeder Association. Available at: http://www.wsff.info/files/simbeef_info_kit/simm_feedlot.pdf.Accessed at 19 February 2016
Suhada H (2008). Estimasi Parameter Genetik Sifat Produksi Sapi Simmental di Balai Pembibitan Ternak Unggul Sapi Potong Padang Mengatas,. Tesis. Program Pascasarjana Universitas Gadjah Mada, Yogyakarta.
Thidar M, Yoshida H, Ito HT, Inoue He MH, Kuwayama H (2008). Combined administration of ghrelin and GHRH synergistically stimulates GH release in Holstein pre-weaning calves. Domest. Anim. Endocrinol. 34:118-123.
Vukasinovic N, Denise SK, Freeman AE (1999). Association of growth hormone loci with milk yield traits in Holstein bulls. J. Dairy Sci. 82:788-794.
Warwick EJ, Astuti JM, dan Hardjosubroto W (1990). Pemuliaan Ternak. Gadjah Mada University Press, Yogyakarta.
Weir BS (1996). Genetic Data Analysis: Method for Discrete Population Genetic Data. Second ed. Sinauer Assosiates. Sunderland, MA USA.
Woychik RP, Camper SA, Lyons RH (1982). Cloning and nucleotide sequencing of the bovine growht hormone gene. Nucleic Acid Res. 10:7197-7210.
Yao J, Aggrey SE, Zadworny D, Hayes JF, Kiihnlein U (1996). Sequence Variations in the Bovine Growth Hormone Gene Characterized by Single-Strand Conformation Polymorphism (SSCP) Analysis and Their Association with Milk Production Traits in Holsteins. J. Genet. 144:1809-1816.
Yurnalis Y, Sarbaini S, Arnim A, Jamsari J, Nellen W (2013). Identification of single nucleotide polymorphism of growth hormone gene exon 4 and intron 4 in Pesisir cattle, local cattle breeds in West Sumatera Province of Indonesia. Afr. J. Biotechnol. 12(3):249-252.

academicJournals

Vol. 15(45), pp. 2572-2577, 9 November, 2016
DOI: 10.5897/AJB2016.15715
Article Number: 9DB546361547
ISSN 1684-5315

http://www.academicjournals.org/AJB

African Journal of Biotechnology

Full Length Research Paper

Hesperidin effects on behavior and locomotor activity of diabetic Wistar rat

Doria Amina Bensaoula[1]*, Nadia Boukhris[2] and Abdelkrim Tahraoui[1]

[1]Laboratory of Applied Neuro-endocrinology, Department of Biology, Faculty of Sciences, University Badji Mokhtar Annaba, Algeria.
[2]Department of Internal Medicine, Ibn Sina University Hospital Center, Annaba, Algeria.

Received 6 October, 2016; Accepted 27 October, 2016

Today, there are sufficient validated scientific data that support the existence of relations between diabetes and certain neuropsychiatric disorders, such as behavioral disorders, anxiety, cognitive decline and depression. The objective of this work was to investigate the effect of a natural bioflavonoid, the antioxidant hesperidin on the neuro behavioral alterations and locomotor function in streptozotocine diabetic wistar rats. Twenty eight male rats were divided equally into four groups; control, and treated series (hesperidin, streptozotocine and hesperidin+ streptozotocine) then exposed to open field test, where animals were individually placed in the center of the compartment for a period of 5 min. Results of the open field test showed high level of anxiety and a slowdown in locomotion and mental flexibility on diabetic rats. Treatment with hesperidin, significantly module these disorders of the animals related to diabetes. Thus, our results confirm the capacity of hesperidin as an antioxidant, to correct neurobehavioral and locomotion disorders related to diabetes and its complications by neutralizing free radicals generated by this metabolic disease.

Key words: Diabetes, oxidative stress, hesperidin, streptozotocine.

INTRODUCTION

Diabetes mellitus is a complex endocrine metabolic disorder and that is multifactorial (Permutt et al., 2005). It causes adverse changes in the central nervous system causing behavioral disorders, depression and cognitive dysfunction (Anderson et al., 2002; Alvarez et al., 2009; Reijmer et al., 2011). Diabetes affect stress response as shown by an increased activity of the hypothalamic-pituitary-adrenal (Saravia et al., 2001; Chan et al., 2003) and also an alterations in vessels, eyes and peripheral nerves, as evidenced by the frequency of neuropathic pain in diabetics (Schwarz et al., 2009).

The earliest observations have reported the presence of a peripheral neurological deficit, induced by a neuronal degeneration and slowing down the nerve impulses (Gispen and Biessels, 2000). Today it is possible to associate diabetes with psychiatric manifestations; such as depression (Schwarz et al., 2009), behavioral disorders and anxiety (Oldroy et al., 2005), cognitive

*Corresponding author. E-mail: bensaoula.doria.amina@live.com.

dysfunction (Adeghate et al., 2006; Sima et al., 2009), a slower speed and mental flexibility (Ramanathan et al., 1998; Brands et al., 2005). Therefore the anxious behavior of high level diabetics was highlighted by an open field tests, as well as in the elevated plus-maze (Adeghate et al., 2006; Miyata et al., 2007).

Although the pathogenesis of defects in learning and memory in diabetics is not well understood, but however it involves several factors, such as metabolic disorders, vascular complications and accumulation of free radicals (Biessels et al., 2007; Kucukatay et al., 2007; Tuma, 2007). It is now accepted that high levels of glucose in the extra and intracellular environments induce stress, which has been defined as an imbalance between pro-oxidant and antioxidant, highlighted in experimental diabetes in animals and patients with type1 (Northam et al., 2006) and type2 (Stewart and Liolitsa, 1999). Oxidative stress has been involved in the past two decades as the main insidious in the genesis of various chronic diseases and degenerative complications (diabetes, atherosclerosis, cancer, rheumatoid arthritis, Alzheimer's disease, and asthma). It is induced either by excessive production of reactive oxygen species, reactive nitrogen species or a depletion of antioxidant defense capabilities (Schaalan et al., 2009), so an antioxidant supplementation has been considered as adjuvant therapy (Favier, 2003). Therefore it is hypothesized that, administration of antioxidants to animals could reduce the risk of developing behavioral and cognitive disorders in diabetic patients.

According to the present literatures, it is hypothesized that the administration of antioxidants reduces the risk of developing behavioral and cognitive disorders in diabetic patients. To confirm this hypothesis it is been assessed that, contribution of an antioxidant in the prevention of abnormal locomotors, behavioral and cognitive functions in diabetic rats has been injected with streptozotocin and later treated with hesperidin.

This is a natural bioflavonoid that possesses a very good antioxidant property which has been proved to be very effective in various neurobehavioral diseases (Maridonneau-Parini et al., 1986). Therefore this present work was conducted by the application of an open field test (Sáenz et al., 2006) that allowed the evaluation of rat basal activity and its behavioral evolution.

MATERIALS AND METHODS

Experimental protocol

Wistar male rats weighing 200 ± 20 g were obtained from Pasteur Institute, Algiers. The rats were reared in the rearing house of the Department of Biology, University of Annaba inside polyethylene cages with a mean temperature of 25 ± 2°C, standardized photoperiod and humidity. Rats were supplied with water and fed on standard diet made up in the form of rods produced by, local food factory (SPA, Bouzareah, Algiers).

Mode of treatment

Twenty eight rats were divided into equal four groups; control vehicle (CV), treated control (rat) with hesperidin (CHS), diabetic inducted with streptozotocine considered as diabetic vehicle (DV) and rats treated with hesperidin + streptozotocine represented as (DHS).

Control rat (CV) received daily saline solution of Nacl 0.9% at 1 ml/kg. Hesperidin group (CHS) rats received hespiridin at dose 50 mg/kg daily during 21 days diluted in 1 ml/kg of Nacl 0.9%. Induction of diabetes in the rats (DV) was done by a single intraperitoneal injection of streptozotocin [Sigma ST Lowis, Mo] at the dose of 60 mg/kg body weight, with a volume of 1 ml/kg. Streptozotocin was prepared extemporaneously in a citrate buffer 0.1 M (pH 4.5).

Diabetes appears in rats after 48 h. Diabetes was checked by measurement of fasting glucose in blood and confirmed by the presence of glycosuria in urine using dipstick bili labstix®. However, after 72 h of inducting diabetes (DHS), hesperidin (50 mg/kg) was dissolved in NaCl and was given by stomach tube to animals for a period of 21 days.

The open field test

The open field test (OF) was developed in order to measure differences in emotional reactivity of rodents (Sáenz et al., 2006). Therefore the OF evaluates the ambulatory behavior and the environmental neophobie of the tested animals. The structure OF is a Plexiglas unit comprising of (70 X 70 cm) base, surrounded by parapets Plexiglas with a height of 40 cm. The floor of this unit is divided into two areas, central and peripheral area, each measuring 35 cm length divided in squares (1square=1cm^2). The central zone is defined as the opened, deems and the peripheral area borders of the walls. This test consists of, introducing the individual rats in the center of the unit and left for five minutes. The test parameters measured were, locomotor activities, standing position, the time of permanence and entry in the center and edge.

All rat movements were recorded by a high resolution camera, thereby recording the number of squares crossed and the time spent in each area, respectively reflecting the locomotor activity and the anxious behavior. The anxiety level is estimated by, the reference to the displacements in two surfaces. It is considered that, when the spent time in the central area is higher the rat's anxiety level will be lower. In general an anxious animal will tend to prefer the peripheral zone, while avoiding entering the central zone. The device is wiped off after each session with an alcoholic solution, to overcome the polarizing effects due to the odors left by the previous rat.

The results were expressed in mean ± SEM and was compared to control which was analysed using Student's t-test, at $P<0.05$.

RESULTS

Effect on glycemia

The rats were subjected to treatment in order to induct diabetes. Glycemia increased significantly ($p<0.001$) for a period of 21 days in comparison to the control. However, this hyperglycemic state decreased significantly after treatment of these animals with hesperidin (Figure 1).

Open field tests

The open field tests were evaluated by the spent time of

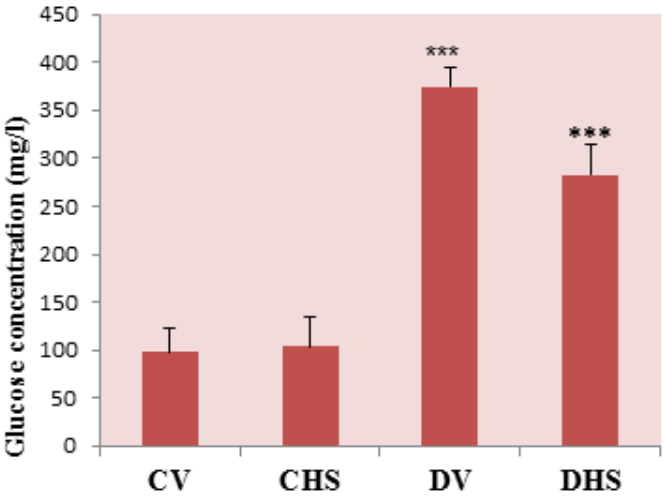

Figure 1. Concentration of blood glucose (mg/l) of the four rat groups; control vehicle (CV), treated control with hesperidin (CHS), diabetic vehicle (DV) and treated with hesperidin + streptozotocine (DHS). (***= p <0.01).

Table 1. Parameters of the open field test (OF) of the control and treated rat groups.

Group of rats	The open field test parameters		
	Spent time (s) in the center	Spent time (s) in the periphery	Traversed distance (cm)
Control vehicle (CV) Nacl 0.9% 1 ml/kg	10.4 ±0.74[a]	289.6±3.14[a]	421.3±20.14[a]
Treated control with hesperidin (CHS) 50 mg/kg	15±3.54[b]	285.4±4.07[a]	550.6±21.33[b]
Diabetic vehicle (DV) 60 mg/kg	3.6±0.84[c]	297.75±2.83[b]	202.3±19.33[c]
Treated streptozotocine and hesperidin (DHS)	4.3±0.90[c]	295.75±3.83[b]	380.16±19.67[d]

For each group, mean values followed by the same letter are not significantly different (P< 0.05).

the rats in the center, periphery and running distance. The results of the different series are represented in Table 1.

Treatment effects on time spent in the center and in the edge

Results show that the group treated rats with hesperidin (CHS) spent less time (second) in the central part and more time in the edge of the device as compared to the control (CV) (15 ± 0.73 against 10.4 ± 0.74) and (285 ± 6.70 against 289.6 ± 3.14) (Table 1). These statistical analyses showed that the differences are significant (P < 0.05) (Figure 2A).

These group of diabetic (DV and DHS) spent less time in the central part and more time in the edge of this device than that of the control group (3.6 ± 0.84 and 4.3 ± 0.90 s against 10.4 ± 0.74s) and (296.4 ± 4.07 s and 295.75 ± 2.83 s against 289.6 ± 3.14 s) (Table 1) with highly significant differences (P < 0.001) (Figure 2B). In the group of treated diabetic rats (DHS), the spent time (second) in the center was slightly higher than the diabetic control (DV) (4.3 ± 0.90 against 3.6 ± 0.84) (Table 1) and consequently, the treated diabetic rats spent less time in the edge than that of diabetic control (295.75 ± 2.83 s against 4.07 ± 296.4 s), but the statistical analysis of these results was not significant (Figure 2A and B).

Treatment effects on the distance traversed

The results of the running distance test by the different groups of rats are shown in Table 1. The assay showed that the number of squares (cm) traversed by rats treated with hesperidin was significantly (P < 0.01) (Figure 2C) higher than that traversed by the control (54.75 ± 4.07 cm against 43 ± 5.23 cm). Conversely, diabetic control and treated rats traversed fewer tiles than that of diabetic control (21 ± 3.88 cm and 37.2 ± 3.24 against 43 ± 5.23 cm) (Table1). The analysis of these results show a highly

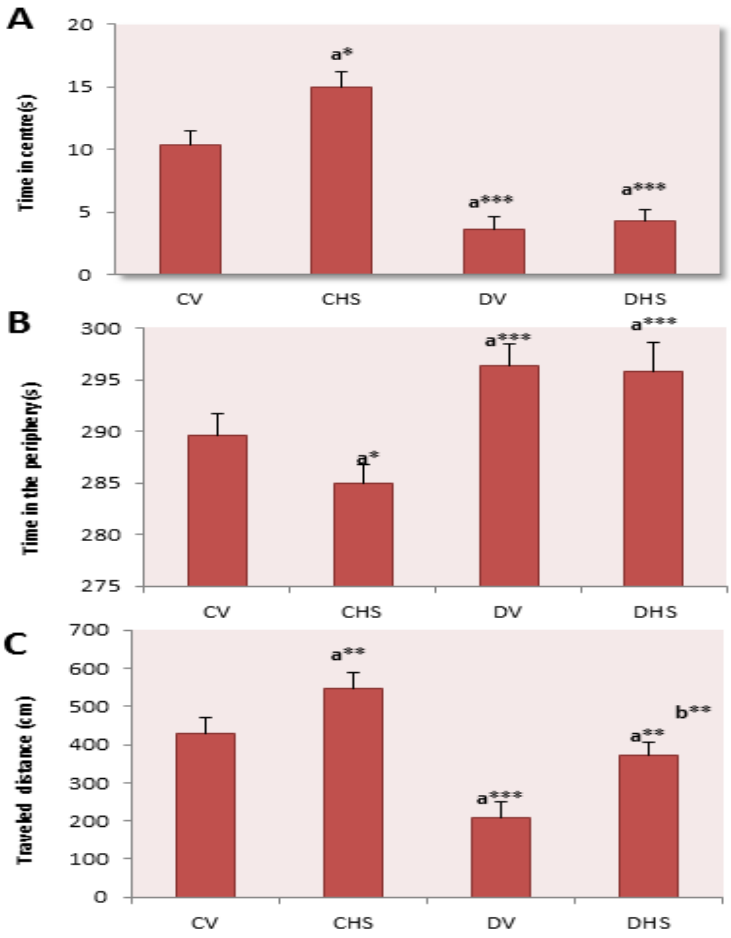

Figure 2. Parameters of the open field test of the four groups. **(A)** The spent time (s) in the center. **(B)** The spent time (s) in the unit edge (periphery). **(C)** Number of squares (cm) traversed. [Treated rats (CV, CHS, DHS) a: compared to the control (CV), b: compared to diabetic rats (DV)]. *= $p< 0.05$, **= $p< 0.01$, ***= $p< 0001$.

significant difference for diabetic rats ($P < 0.001$) and another significant difference for the diabetic rats treated with hesperidin ($P < 0.01$) (Figure 2C). Indeed, for the treated diabetics, the number of crossed tiles was significant ($P < 0.01$) and higher than that traversed by the diabetic control (37.2 ± 3.24 against 21 ± 3.88 cm).

DISCUSSION

Oxidative stress is considered as the main insidious of various chronic diseases and degenerative complications, like diabetes. (Brands et al., 2005; Alp et al., 2012; Moree et al., 2013). It is induced either by the excessive production of reactive oxygen species or reactive nitrogen species or a depletion of antioxidant defense capabilities. In the present study, diabetes was confirmed by the recorded increase of glucose in blood and urine and this was due to the injected streptozotocin which has certainly destructed pancreatic β cells, and led to impaired glucose stimulated insulin release and insulin resistance. Elevation of blood glucose may be attributed to the reduced entry of glucose to peripheral tissues, muscle and adipose tissue which increased glycogen breakdown, gluconeogenesis and hepatic glucose production (Bouhali et al., 2015). Such results agree with the previously published data (Schuster and Duvuri, 2002).

The OF parameters measured in the current investigation were the locomotor activity, standing permanent and entry time in the center and the edge, the time of permanence and entries close to walls. The analysis of these results traduced by the level of anxiety, locomotor function and mental flexibility, showed an increase in time and number of entry in the edge of diabetic and diabetic treated rats. Similar results were obtained when male wistar rats were treated with natural flavonoid like Quercetin (Bouhali et al., 2015). This

demonstrates a high level of anxiety and a slowdown in motor function (Brands et al., 2005). It was reported that music is used as a therapy that modulates a combined predator and noise stress which induced anxiety-like behavior in male wistar rat (Attoui et al., 2015).

In terms of the distance traveled by crossed squares, data analysis showed a clear and significant difference in both diabetic and treated diabetic rats with hesperidin. In diabetic rats injected with hesperidin, the number of crossed squares was significantly ($P < 0.001$) higher than that of the control. Blood glucose in the presence of this antioxidant has returned to normal level as that of the control which confirmed the test results carried out by Ahmed et al. (2010). Similar results have been reported after treatment of *Ruta graveolens* and *rutin* with nicotinamide/streptozotocin diabetic rats (Gispen and Biessels, 2000).

After treating with hesperidin, there was an increase in the anxiety level which improved locomotor activity and recovery time during testing in open field. The same remark was made for treated diabetics (CHS) compared to control.

Hesperidin was reported to ameliorate the behavioral and biochemical indicators of mice thereby modulating the nitrergic pathway (Viswanatha et al., 2012). These results support the findings of previous studies which showed an improvement in the number of entry and the time spent in the open arms of the treatment after repeated hesperidin. It is concluded that the present study showed a high level of anxiety, and a slowdown in locomotion and mental flexibility. Treatment with an antioxidant remarkably module the disorders related to diabetes (Bouhali et al., 2015). Thus our results confirm the capacity of hesperidin as an antioxidant which corrects neurobehavioral disorders as related to diabetes and its complications by neutralizing free radicals, of cell aging and apoptosis.

Conclusion

The obtained results of the open field tests on diabetic rats showed an increase in anxiety and a decrease in locomotion activity. The supplementation of hesperidin has controlled the neuro-degenerative symptoms. It is therefore suggested that, hesperidin can be used as a therapeutic complement against neuro-behavior disorders of stressed diabetic rats.

Conflict of Interests

The authors have not declared any conflict of interests.

REFERENCES

Adeghate E, Schattner P, Dunn E (2006). An update on the etiology and epidemiology of diabetes mellitus. Ann. N Y. Acad. Sci. 10(84):1-29.

Ahmed OM, Abdel-Moneim A, Abulyazid I, Mahmoud AM (2010). Anti hyperglycemic, anti hyperlipidemic and antioxidant effects and the probable mechanisms of action of *Ruta graveolens* and rutin in nicotinamide/streptozotocin diabetic albino rats. Diabetol. Croat. 39:15-32.

Alp HS, Varol MM, Celik M, Altas O, Evliyaoglu O, Tokgoz MH, Tanrýverdi E, Uzar J (2012). Protective effects of beta glucan and gliclazide on brain tissue and sciatic nerve of diabetic rats induced by streptozosin. Exp. Diabetes Res. 7:243-247.

Alvarez EO, Beauquis J, Revsin Y, Banzan AM, Roig P, De Nicola AF, Saravia F (2009). Cognitive dysfunction and hippocampal changes in experimental type 1 diabetes. Behav. Brain Res. 198:224-230.

Anderson RJ, Grisby A, Freedland KE, de Groot M, McGill JB, Clouse RE (2002). Anxiety and poor glycemic control: a meta-analytic review of literature. Int. J. Psychiatry Med. 32(3):235-247.

Attoui N, Bouhali IE, Tayaa H, Habbachi W, Bairi A, Tahraoui A (2015). Music Therapy Modulates Combined Predator and Noise Stress Induced Anxiety-Like Behavior in Male Wistar Rat. Middle East J. Sci. Res. 23(3):374-377.

Biessels GJ, Kerssen A, de Haan EH, Kappelle LJ (2007). Cognitive dysfunction and diabetes: Implications for primary care. Prim. Care Diabetes 1:187-193.

Bouhali, IE, Tayaa H, Tahraoui A (2015). Quercetin, a Natural Flavonoid, Mitigates Fenthion Induced Locomotor Impairments and Brain Acetylcholinesterase Inhibition in Male Wistar Rat. Middle East J. Sci. Res. 23(1):55-58.

Brands AM, Biessels GJ, De Haan EH, Kappelle LJ, Kessels RP (2005). The effects of type1diabetes on cognitive performance: A meta-analysis. Diabetes Care 28(3):726-735.

Chan O, Inouye K, Riddell MC, Vranic M, Matthews SG (2003). Diabetes and the hypothalamo-pituitary adrenal (HPA) axis. Minerva Endocrinol. 28:87-102.

Favier A (2003). Le stress oxydant Intérêt conceptuel et expérimental dans la compréhension des mécanismes des maladies et potentiel thérapeutique. Laboratoire de recherche, lésions des acides nucléiques et département de biologie intégrée au CHU de Grenoble, France 2:50-136.

Gispen WH, Biessels GJ (2000). Cognition and synaptic plasticity in diabetes mellitus. Trends Neurosci. 23(11):542-548.

Kucukatay V, Agar A, Gumuslu S, Yargicog˘lu P (2007). Effect of sulfur dioxide on active and passive avoidance in experimental diabetes mellitus: Relation to oxidant stress and antioxidant enzymes. Int. J. Neurosci. 117:1091-1107.

Maridonneau-Parini I, Braquet P, Garay RP (1986). Heterogenous effect of flavonoids on K+ loss and lipid peroxidation induced by oxygen-free radicals in human red cells. Pharm. Res. Comm. 18(1):61-72.

Miyata S, Yamada, N, Hirano, S, Tanaka, S, Kamei J (2007). Diabetes attenuates psychological stress-elicited 5-HT secretion in the prefrontal cortex but not in the amygdala of mice. Brain Res. 1147:233-239.

Moree SS, Kavishankar GB, Rajesha J (2013). Antidiabetic effect of secoisol ariciresinol diglucoside in streptozotocin induced diabetic rats. Phytomedicine 20(3-4):237-245.

Northam E, Rankins D, Cameron FJ (2006). Therapy insight: the impact of type 1 diabetes on brain development and function. Nat. Clin. Pract. Neurol. 2:78-86.

Oldroy dJ, Banerjee G, Heald A, Cruickshank A (2005). Diabetes and ethnic minorities. Postgrad. Med. J. 81:486-490.

Permutt MA, Wasson J, Cox N (2005). Genetic epidemiology of diabetes. J. Clin. Investig. 115:1431-1439.

Ramanathan M, Jaiswal AK, Bhattacharya SK (1998). Differential effects of diazepam on anxiety in streptozotocin induced diabetic and non-diabetic rats. Psychopharmacology 135(4):361-367.

Reijmer YD, Van Den Berg E, De Bresser J (2011). Accelerated cognitive decline in patients with type 2 diabetes: MRI correlates and risk factors. Diabetes Metab. Res. Rev. 27(2):195-202.

Sáenz JCB, Villagro OR, Trias JF (2006). Factor analysis of Forced Swimming test, Sucrose Preference test and Open Field test on enriched, social and isolated reared rats. Behav. Brain Res. 169:57-65.

Saravia FE, Gonzalez SL, Roig P, Alves V, Homo-Delarche F, De Nicola AF (2001). Diabetes increases the expression of hypothalamic neuropeptides in a spontaneous model of type I diabetes, the nonobese diabetic (NOD) mouse. Cell. Mol. Neurobiol. 21:15-27.

Schaalan M, El-Abhar HS, Barakat M, El-Denshary ES (2009). Westernized-like-diet-fed rats: effect on glucose homeostasis, lipid profile and adipocyte hormones and their modulation by rosiglitazone and glimepiride. J. Diabetes Complications 23:199-208.

Schuster DP, Duvuri V (2002). Diabetes mellitus. Clin. Pediatr. Med. Surg. 19(1):79-107.

Schwarz PE, Li J, Lindstrom J, Tuomilehto J (2009). Tools for predicting the risk of type 2 diabetes in daily practice. Horm. Metab. Res. 41:86-97.

Sima AA, Zhang W, Muzik O, Kreipke CW, Rafols JA, Hoffman WH (2009). Sequential abnormalities in type 1 diabetic encephalopathy and the effects of C-Peptide. Rev. Diabet. Stud. 6(3):211-222.

Stewart R, Liolitsa D (1999). Type 2 diabetes mellitus, cognitive impairment and dementia. Diabet. Med. 16:93-112.

Tuma I (2007). Diabetes mellitus and cognitive impairments. Vnitrni Lekarstvi 53:486-488.

Viswanatha GL, Shylaja H, Sandeep, Rao VR, Santhosh K, Jagadeesh M (2012). Hesperidin Ameliorates Immobilization-Stress Induced Behavioral and Biochemical Alterations and Mitochondrial Dysfunction in Mice by Modulating Nitrergic Pathway. ISRN Pharmacology Volume 2012, Article ID 479570, 8 p.

academicJournals

Vol. 15(45), pp. 2578-2586, 9 November, 2016
DOI: 10.5897/AJB2016.15621
Article Number: E80C6C361549
ISSN 1684-5315

http://www.academicjournals.org/AJB

African Journal of Biotechnology

Full Length Research Paper

Optimization of humidifying procedure in controlled environment for indoor cultivation of *Pleurotus pulmonarius*

Tariqul Islam[1], Zarina Zakaria[2]*, Nasrul Hamidin[3] and Mohd Azlan Bin Mohd Ishak[4]

[1]School of Bioprocess Engineering, Universiti Malaysia Perlis (UniMAP), 02600 Arau, Perlis, Malaysia.
[2]Faculty of Engineering Technology, Universiti Malaysia Perlis (UniMAP), 02100 Padang Besar, Perlis, Malaysia.
[3]School of Environmental Engineering, Universiti Malaysia Perlis (UniMAP), 02600 Arau, Perlis, Malaysia.
[4]Faculty of Applied Sciences, Universiti Technology MARA (UiTM), 02600 Arau, Perlis, Malaysia.

Received 21 August, 2016; Accepted 28 October, 2016

This study investigated mushroom cultivation in controlled indoor environment. For this, the environmental factors including humidity and temperature were controlled by humidifier and ventilation. Four ventilations were installed on tops to bring the air from inside to outside and four small ventilations were installed on side wall along with black filter to bring the air from outside to inside. Four humidifiers were placed in four different positions inside the cultivation house. A single unit of humidifier was applied along with two top ventilations and two side ventilation to optimize the humidifying duration for 80 to 90% humidity. In this process 15 min humidifying duration was optimized to retain 80 to 90% humidity. Then the four units of humidifier were applied for 15 min by one combined application and five individual applications to optimize the configuration to ensure the 80 to 90% humidity in the whole cultivation room with tolerable temperature. Finally, the individual application as 15 min interval period by following after every 15 min humidifying treatment from four different points had been optimized and applied for the cultivation of method. During cultivation 28.60±1.02°C temperature, 87.96±2.26% humidity, 0.035±.005% CO_2 and 34.53±19.003 lux light intensity had recorded. The total 261.8 kg mushroom was harvested from the controlled cultivation system, a fairly good production of mushroom was harvested till 7 flushes within 3 months of cultivation. This method of humidifying optimization and configuration procedure may ensure the continuous mushroom production throughout the years.

Key words: Indoor, cultivation, model, mushroom, environment, optimization.

INTRODUCTION

Mushroom has been considered as human diet since 200 years for its taste, nutritional and medicinal properties in the world. The demand of mushroom is increasing by times but in Malaysia, the number of cultivators and production is decreasing (Haimid et al., 2013). This is due to the inconsistent environmental condition with high temperature (32-35°C) and low humidity (60-70%). *Pleurotus* species can grow in ranges of 25 to 30°C temperature and 80 to 90% humidity (Chang and Miles 2004; Uddin et al., 2011).

Jang et al. (2003) investigated the morphological differences of *Pleurotus ostreatus* grown in the artificial

environmental conditions .They controlled temperature and humidity from 13°C to above 16°C and from 60% to above 80% to cultivate P. ostreatus by using air cooler, over pressure ventilation system and under pressure ventilation system. In the humidity in excess of 80% at 13 to 16°C temperature, the best morphology and yield of *P. ostreatus* was investigated. In other conditions, *P. ostreatus* generally showed the morphology closing to malformation. Another study of Yang et al. (2013) in china was investigated the morphology and yield of *Pleurotus eryngii* in indoor controlled environment. The temperature and humidity were controlled from 14 to 18°C and from 89 to 97% by using air conditioners, humidifiers and fans. The maximum yield was found in the growing room from 16 to 18°C and 93% or above respectively.

Pleurotus sajor-caju was cultivated indoor house with electronic coolinics Model CTG 250 Yamamota and found the highest yield from 20 to 25°C temperature verified by farmers in local area (Seung et al., 1984). Pink Oyster mushroom was successfully cultivated in the artificially mushroom cultivation chamber at 23 to 25°C (Subramanian et al., 2014). Thepa et al. (1999) found that the combination of evaporative cooling and continuous ventilation system provided maximum yield and a suitable environmental condition for growing *Lentinula edodes*. Veena and Pandey (2012) was cultivated Tramete versicolor in 25±2°C temperature and 80 to 85% humidity and kept open the door of the cultivation room three times in a day for 30 min to supply fresh air. Generally outdoor cultivation provides lower yields and longer production times compare with indoor cultivation (Barney, 2000). Recently a study reported that humidifying treatment had influenced the mushroom growth in different stages of production but no optimized condition had identified (Islam et al., 2016).

In the environmental profile of Malaysia, it must need to apply any artificial system to provide optimum growing environment for mushroom. Although, some researches had performed on controlling and maintaining environmental factors to find out optimum range of humidity and temperature which are expensive and not suitable for convention commercial cultivation. So, this study has investigated to develop a new method and way of controlling the indoor environmental condition for commercial cultivation which ensure the continuous mushroom production throughout the years in Malaysia and other similar ecological regions.

MATERIALS AND METHODS

Model and design of indoor cultivation room

The indoor cultivation room was measured at 5.8 L×4.57 W×2.74 H m^3 in size inside a concrete building located at Taman Pauh Indah, Arau, Perlis. The wall was made by bricks at one side and by gypsum board on the rest of the walls. The roof of the room was build up by also gypsum board under the main concrete roof. The room was installed with four rows of racks; each rack contained four iron bars distance by 15 cm from each other and 55 cm distance between the racks. Roof ventilation, light and side ventilation were installed inside the room in order to facilitate fresh air and maintain proper light intensity respectively. The roof ventilations was installed with top roof to bring air from inside to outside and the side ventilations was installed at bottom of the wall with black filter to bring air outside to inside.

The bags were arranged horizontally through the racks by using nylon rope and made it tight by cable tie and hanged vertically. Twelve bags were arranged in one column of rope by 3 bags in together in 4 parts. The columns of rope were arranged at 25 cm distance from each other in every rack so that the air and humidity can easily flow through the spaces between the bags, preventing the temperature of the bags from increasing. Mushroom mycelia emitted heat during incubation, so the bags can be easily overheated if they touch each other (Curvetto et al., 2004). The distance of the top end bag from the ceiling was 76 cm and the down end bag from the floor was 30 cm. The humidifiers (TAY-RING TL-3600) were placed between the two columns of bags where the distance of humidifier from the opening part of the bags (front view) was 25 to 30 cm; from the side view of bags was 20 to 25 cm and from the back view of bags was 10 to 15 cm. The Hygro-thermometers (EXTECH 445703), Luxmeters (HI 97500) and CO_2 meter (Drager Pac 7000) were installed in different positions inside the cultivation room to monitor temperature, humidity, light intensity and CO_2 level during the experimental procedure. The design and indoor cultivation model is followed as in Figure 1.

Optimized humidifying duration

In this method, four humidifiers were placed in four different points as surrounding 2.9×2.29 (m^2) inside the room where the distance among the humidifier positions was 2 to 2.5 (m) from each other's as shown in Figure 2. The duration of humidifying was optimized in order to maintain the humidity values ranging between 80 and 90% in the surrounding 2.9×2.29 (m^2) by using single unit of humidifier and two units of continuous roof and side ventilation. Here, side ventilation was applied since the room was closed and two roof ventilation was running continuously which had a strong tends to bring air out, so it is important to use an air incoming ventilation along with air out ventilation which also helps to proper air circulation and reduce the indoor temperature. For this, the humidifier and ventilation was run to achieve maximum humidity from initial range to higher than 90%. After that, the humidifying process was stopped and ventilation was still running. Then, the humidity was monitored until the reading dropped to lower than 80%. The changes of humidity with time were measured at 5 min interval. The same procedure was used in all 4 replicates. The data of increasing humidity from all replicates were analysed and a graph was plotted using duration of humidifying (Min) on the X-axis while the percentages of humidity (%) value on the Y-axis to obtain the equation for by which optimized the duration of humidifying for maintaining 80 to 90% of humidity.

Optimized humidifiers configuration

Then the four humidifiers were configured in two different ways of

*Corresponding author. E-mail: zarinaz@unimap.edu.my. Tel: +60175487772. Fax: +604 9798755.

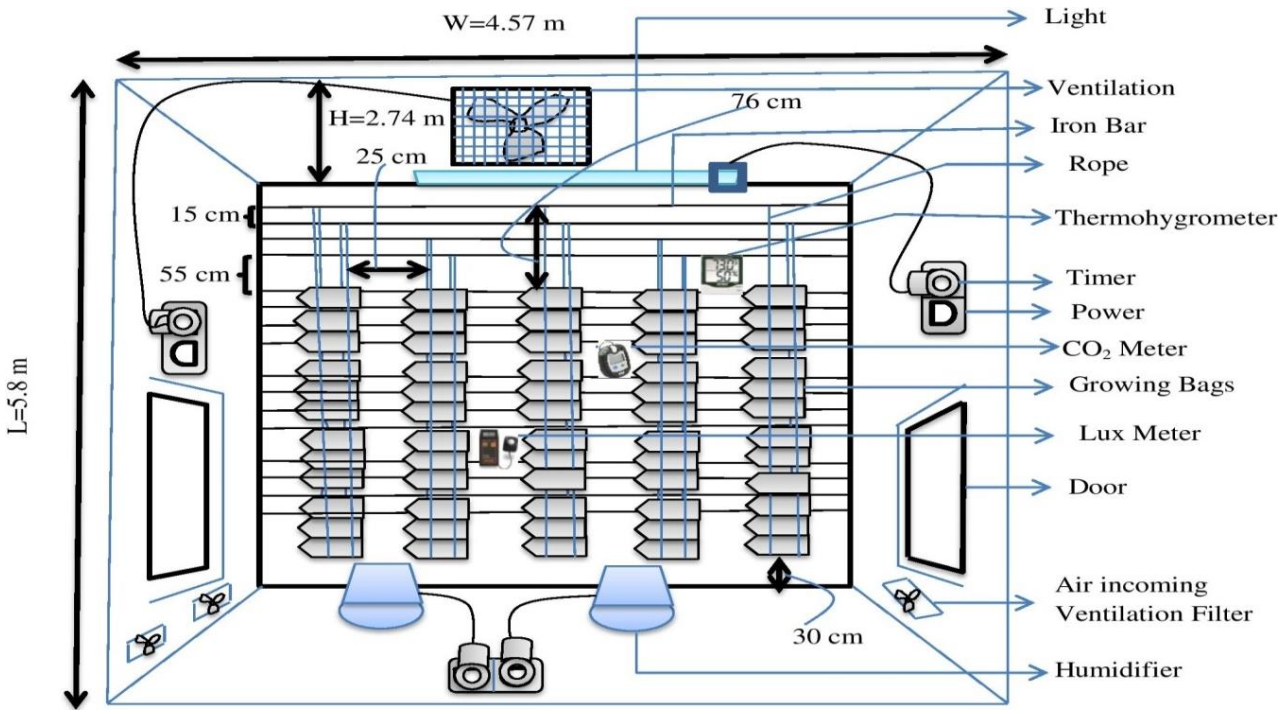

Figure 1. Floor plan and design of indoor mushroom cultivation house with bags.

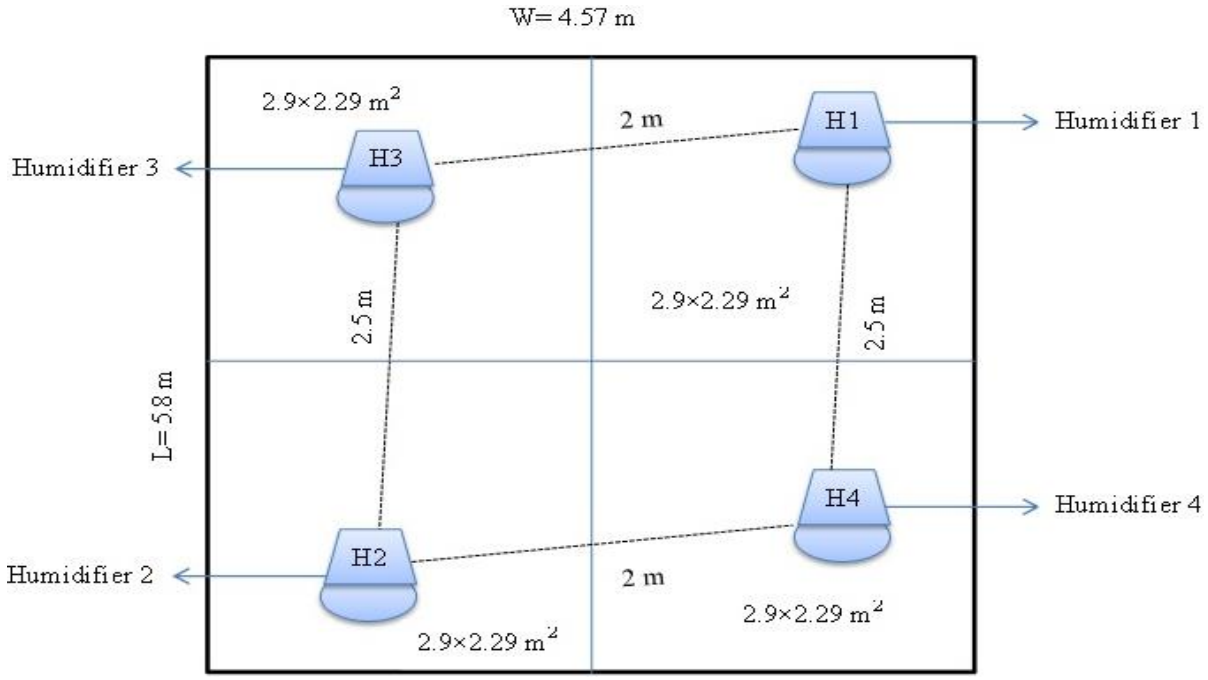

Figure 2. Configuration of humidifier position in different points inside the growing house.

application for 15 min optimized duration obtained from the result section (Optimize Humidifying Duration) in order to ensure 80 to 90% humidity. First one was “Combined Application” and another one was “Individual Application”.

Combined application

Combined application was followed by applying four units of humidifier in together for 15 min optimized duration with 2 units of

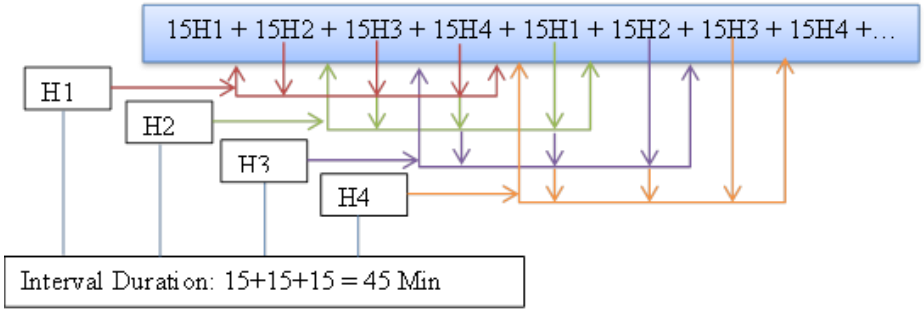

Figure 3. Humidifying configuration 2 for individual application.

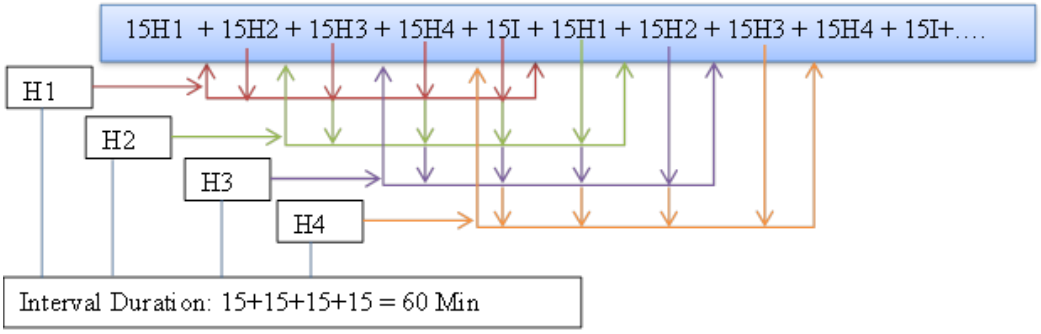

Figure 4. Humidifying configuration 2 for individual application.

continuous roof and side ventilation. All humidifiers were applied in together for 15 min by 45 min interval from four different parts of the room. The procedure was continued for 24 h with 4 replicates. The changes of humidity and temperature with time were measured at 5 min interval. The data from all replicates were analysed and made a profile for combined application of humidifiers.

Individual application

The individual application was followed by applying humidifier one after another with or without interval along with 2 units of continuous roof and side ventilation. Then the four humidifiers were configured by the optimized humidifying duration to ensure 80 to 90% humidity in whole the growing room. Four humidifiers were fixed by 15 min optimized duration as following the five configurations to optimize the procedure and environmental condition that able to provide optimum humidity and corresponding tolerable temperature for mushroom cultivation.

Configuration 1

In this procedure, the four humidifiers were configured as 15 min running one after another without any interval among them and followed the process for 24 h. For this, every humidifier had to run after 45 min left as in Figure 3. Ventilations process was running continuously throughout the whole procedure. This procedure was controlled by fixing with electrical timer and the changes of humidity with time were measured at 5 min interval. The same procedure was used in all 4 replicates. The data from all replicates were analysed and made a profile for humidity with corresponding temperature.

Configuration 2

In this procedure, the four humidifiers were configured as 15 min running one after another with one 15 min interval between humidifier 4 (H4) and humidifier 1 (H1) and followed the process for 24 h. For this, every humidifier had to run after 60 min left as in Figure 4. Ventilations process was running continuously throughout the whole procedure. This procedure was controlled by fixing with electrical timer and the changes of humidity with time were measured at 5 min interval. The same procedure was used in all 4 replicates. The data from all replicates were analysed and made a profile for humidity with corresponding temperature.

Configuration 3

In this procedure, the four humidifiers were configured as 15 min running one after another with two 15 min interval, one was between humidifier 2 (H2) and humidifier 3 (H3) and another one was between humidifier 4 (H4) and humidifier 1 (H1) and followed the process for 24 h. For this, every humidifier had to run after 75 min left as in Figure 5. Ventilations process was running continuously throughout the whole procedure. This procedure was controlled by fixing with electrical timer and the changes of humidity with time were measured at 5 min interval. The same procedure was used in all 4 replicates. The data from all replicates were analysed and made a profile for humidity with corresponding temperature.

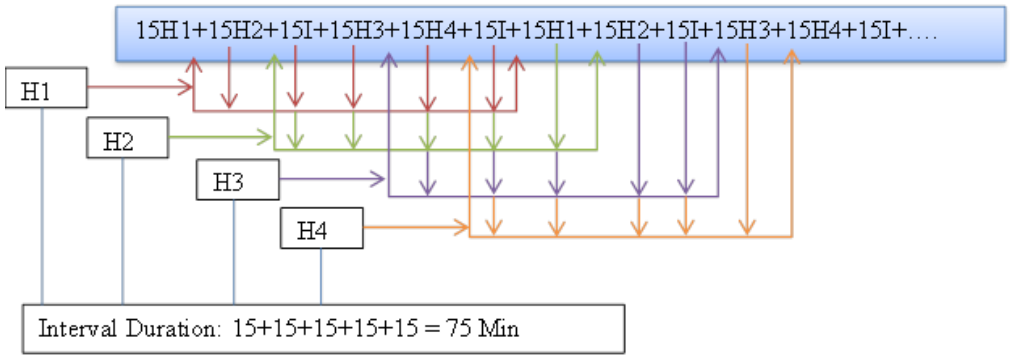

Figure 5. Humidifying configuration 3 for individual application.

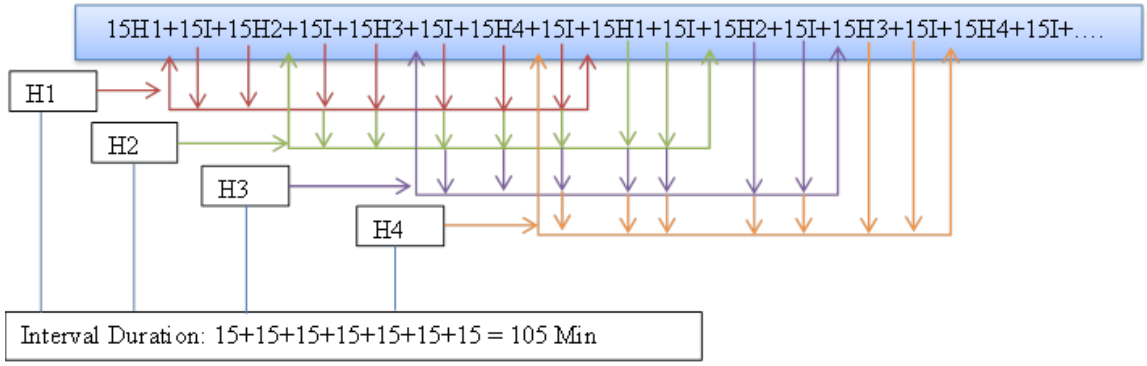

Figure 6. Humidifying configuration 4 for individual application.

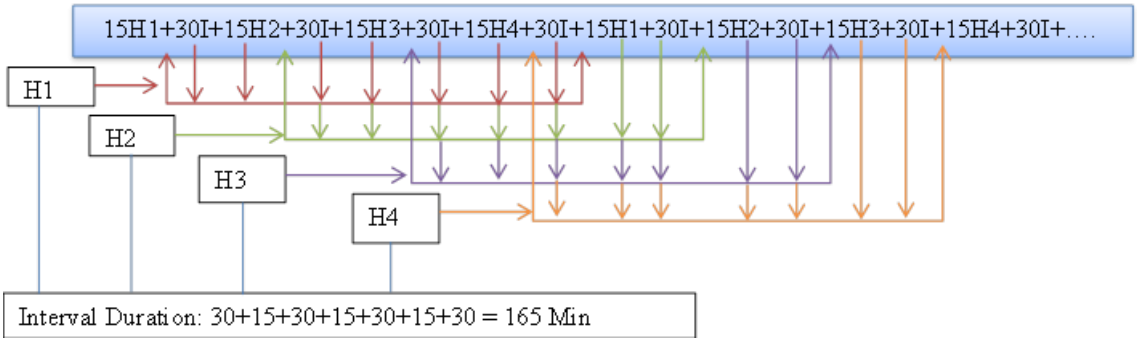

Figure 7. Humidifying configuration 5 for individual application.

Configuration 4

In this procedure, the four humidifiers were configured as 15 min running one after another with 15 min interval after each 15 min humidifying procedure. For this, every humidifier had to run after 105 min left as in Figure 6. Ventilations process was running continuously throughout the whole procedure. This procedure was controlled by fixing with electrical timer and followed 24 h with 4 replicates. The changes of humidity and temperature were measured at 5 min interval. The data from all replicates were analysed and made a profile for humidity with corresponding temperature.

Configuration 5

In this procedure, the four humidifiers were configured as 15 min running one after another with 30 min interval after each 15 min humidifying. For this, every humidifier had to run after 165 min left as in Figure 7. Ventilations process was running continuously throughout the whole procedure. This procedure was controlled by fixing with electrical timer and followed 24 h with 4 replicates. The

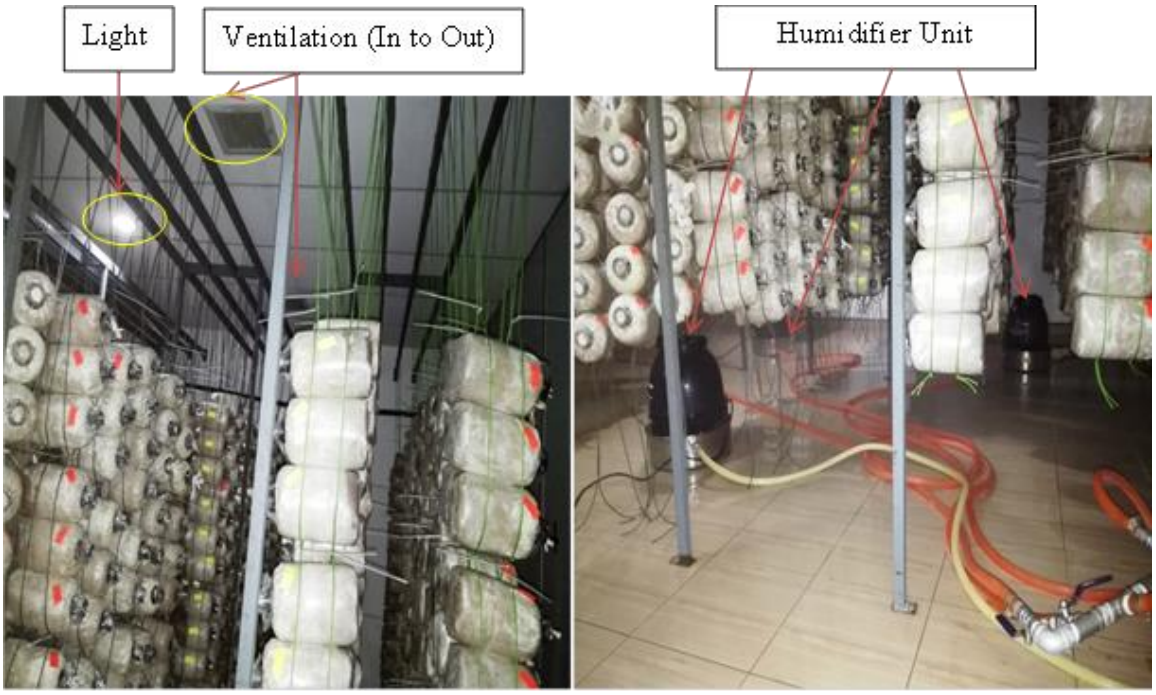

Figure 8. Side view of indoor mushroom cultivation in optimized condition.

changes of humidity and temperature were measured at 5 min interval. The data from all replicates were analysed and made a profile for humidity with corresponding temperature.

Cultivation in optimized procedure

After optimized the configuration procedure, 1200 complete colonized bags were transferred into the growing room and arranged as shown in Figure 1. The mushroom growing bags were prepared by mixing saw dust, rice barn and hydrated lime in sterilization process. In this treatment, the indoor environment was artificially maintained by humidifying and continuous ventilation process. The humidifier and ventilation was operated at duration suggested from optimized results obtained from optimization process mentioned in result section (Optimized Humidifier Configuration). The four units of humidifier were controlled by fixing with timer at 15 min running one after another with 15 min interval after each 15 min humidifying process. A light was applied from the centre of the roof only for 6 h from 12 to 6 am. Light also tends to increase indoor temperature due to heat. So, light was applied from midnight to early morning since that period considered as low temperature (Wafi et al., 2011) compared than other periods. Temperature, humidity, light intensity and CO_2 level of the room were recorded at every 1 h interval within 24 h and continued to record until production of fruit body throughout the cultivation period. Data for environmental factor and mushroom yield was recorded. Figure 8 showed the side view of indoor cultivation system.

Data collection and analysis

Environment factors

Environmental factors including temperature, humidity, light intensity and CO_2 level were regularly monitored throughout all the investigation system. The maximum and minimum of indoor temperature and humidity were regularly recorded on daily basis during the cultivation.

Total yield

The total yield was determined by the sum of total mushroom harvested from all flushes throughout the cultivation period and calculated by the following Equation 1 (Shen and Royse, 2001):

$$Total\ Yield\ (Kg) = \sum \text{Weight in all flashes} \quad (1)$$

Statistical analysis

Descriptive statistics was applied to determine the maximum, minimum, mean, median and standard deviation (SD) executed using SPSS 17.0.

RESULTS AND DISCUSSION

Optimize humidifying duration

The data from the humidifying process were plotted using duration of humidifying (Min) on the X-axis while the percentages of humidity (%) value on the Y-axis (Figure 9).

For increasing humidity, a graph equation was obtained as Equation 2 with the correlation coefficient, R2 of 0.9919 which is acceptable as the value closed to Equation.

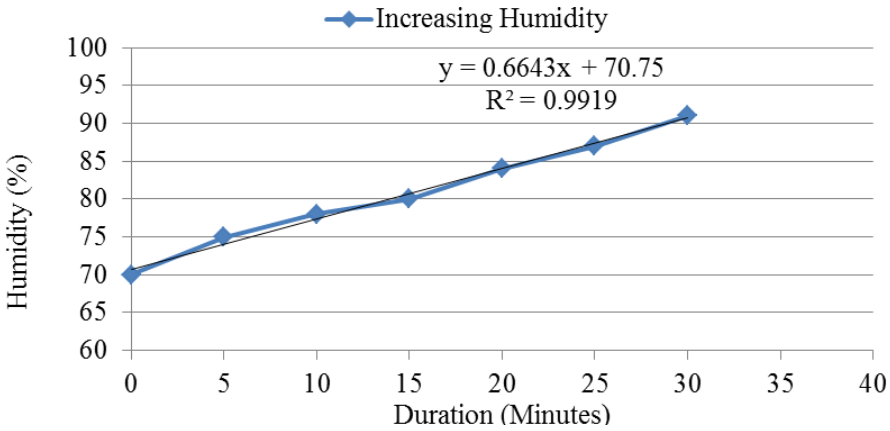

Figure 9. Duration optimization for increasing humidity in indoor controlled environment. Values are mean of 4 replicates.

Table 1. Descriptive of humidity and temperature in different ways of humidifier configuration.

Ways of humidifier configuration	Humidity			Temperature		
	Mean±Std. Dev.	Min.	Max.	Mean ±Std. Dev.	Mini.	Max.
Combined application	87.6±3.7	80.00	94.00	31.1±1.1	29.00	32.50
Configuration 1	93.2±3.7	87.00	99.00	28.1±1.1	26.50	30.50
Configuration 2	92.5±3.3	84.00	97.00	28.3±1.0	27.00	30.60
Configuration 3	90.4±4.8	83.00	97.00	28.4±.98	27.50	30.60
Configuration 4	87.1±3.5	80.00	92.00	28.6±1.02	27.50	30.80
Configuration 5	74.2±8.8	62.00	90.00	30.2±.87	28.50	31.40

*Values are mean of 4 replicates.

$$y = 0.6643x + 70.75 \quad (2)$$

Where y is the value of humidity (%) and x is the duration of humidifying (min).

From the Equation 2, the humidifying duration for 90% humidity was calculated 28.98 min and for 80% humidity was calculated 13.92 min. For increasing from 80 to 90% humidity the duration of humidifying was 15.06 min. So, for this System, the humidifying procedure for increasing humidity had optimized as 15 min for surrounding 2.9×2.29 (m^2) by using single unit of humidifier and two units of continuous roof and side ventilation.

Optimized humidifier configuration

In the configuration of combined application the maximum humidity 94% was found where the mean was 87.6±3.7% and the maximum temperature 32.5°C was found where the mean was 31.1±1.1°C (Table 1). In this configuration, although the maximum humidity was found 94% but the mean was within the optimum range for mushroom cultivation. On the other hand, the maximum and mean temperature was found higher than the optimum range. Sarker et al. (2008) reported that *Pleurotus* species able to grow till 30°C. Here although the four units of humidifier were run in together for 15 min but the temperature was higher than optimum since the interval period was 45 min. When the humidifiers were running the temperature was start to decrease but its needed to stop after 15 min to maintain optimum humidity, after that 45 min needed to wait for next humidifier application and the temperature was increased since 45 min was long interval period. Moreover a lot of vapour was produced within the 15 min application by four units of humidifier in together and after stopping, all the vapours condensed on the floor within very few min because the concentration of vapour inside the room was high which was mixed to each other and converted into small water which is heavier than vapour and condense on floor very quickly. So, this study not recommended this combined application of humidifier for ensuring optimum environmental condition during indoor cultivation.

The mean value of humidity 93.2±3.7, 92.5±3.3 and 90.4±4.8% had found in configuration 1, 2 and 3 respectively where the maximum humidity were 99 and 97%. The mean temperature 28.1±1.1, 28.3±1.0 and

Table 2. Overview of environmental factors (temperature, humidity, CO_2 and light) during the optimized cultivation of system.

Environmental factors	Mean	Std. Dev.	Std. Error	Minimum	Maximum
Temperature (°C)	28.60	1.02	0.038	26.00	30.80
Humidity (%)	87.96	2.26	0.085	80.00	92.00
Carbon dioxide (%)	0.035	0.005	0.0005	0.03	0.04
Light (lux)	34.53	19.003	1.09	5.00	65.00

28.3±1.0°C were found in the configuration of 1, 2 and 3 respectively where the maximum was 30.5°C and 30.6°C (Table 1). In these three configurations, the mean temperature was within the optimum range for mushroom cultivation but the maximum and mean humidity was too high rather than optimum range. Kong (2004) reported that *P. ostreatus*, *P. florida*, *P. sajor-caju* reach their optimum growth at 25 to 30°C temperature. Yang et al. (2013) reported that, during the fruiting period, the suitable air relative humidity can be as high as 85 to 90%.

In these three configurations (1, 2 and 3), the humidity were found too high since there were without or very short interval period within the humidifier application. A single unit of humidifier was run one after another for 15 min without any interval period (Configuration 1), only 15 min interval between Humidifier 4 and Humidifier 1 (Configuration 2) and 15 min interval Humidifier 2 and Humidifier 3 and 2nd 15 min interval between Humidifier 4 and Humidifier 1 (Configuration 3). Among the three configurations, the highest mean value of humidity was found in Configuration 1 and the lowest was found in Configuration 3. So, the mean value of humidity was started to decrease with the increasing interval frequency. Deacon (2013) reported that excessive water or humidity surrounding the environment can cause diseases, contamination and poor quality of mushrooms. So, this study had also rejected these three procedures of humidifier configuration to ensure optimum environmental condition during indoor cultivation of *Pleurotus pulmonarius*.

In Configuration 4, although the maximum 92% humidity was found but the mean value was 87.1±3.5% which was within the optimum range of mushroom cultivation. On the other hand, the maximum 30.80°C temperature was found with mean value 28.6±1.02°C (Table 1) which was also within the optimum range (Kong, 2004; Sarker et al., 2008). Here the mean humidity and temperature were within the optimum range since 15 min interval period was followed after every 15 min humidifying treatment.

In Configuration 5, the mean 74.2±8.8% humidity was found which was lower than optimum ranges. Jang et al. (2003) showed that, 80% or more relative humidity is suitable for the formation of highest cap size and individual weight of the *P. ostreatus* and the cap size and stipe thickness started to decrease at lower than 80% and decreased severely at 60% or less relative humidity. The mean 30.2±.87°C temperature was found in configuration 5 which was higher than the optimum ranges (Table 1). In this configuration the low mean humidity and high mean temperature were found since there was 30 min interval period was followed after every 15 min humidifying treatment.

Among the configurations, configuration 4 was able to provide optimum environmental condition with optimum ranges of humidity and temperature. So, humidifier configuration 4 was followed in the experimental indoor controlled mushroom cultivation.

Environmental conditions during indoor cultivation

The maximum 30.8°C and minimum 26°C temperature had found throughout the cultivation period where the mean temperature was 28.60±1.02°C which was within the tolerable ranges of mushroom fruiting temperature. The maximum 92% and minimum 80% temperature had found throughout the cultivation period where the mean humidity was 87.96±2.26 which was within the optimum ranges of mushroom fruiting requirements. Another two environmental factors including CO_2 and light intensity had also found within the optimum ranges as 0.035±.005% and 34.53±19.003 lux respectively (Table 2).

Total yield

A total of 261.8 kg mushroom was harvested from the controlled cultivation System, a fairly good production of mushroom was harvested till 7 flushes within 3 months, Bano and Rajarathnam (1982) reported that increasing temperature and lower humidity had shortened spawn run and longer fruiting period which is also similar to the observation of Chang and Miles (2004). The highest 59.2 kg mushroom had harvested from the first flash and the production started to decrease after first flash. The lowest 17.3 kg mushroom had collected from the 7th harvesting flash (Figure 10). Although the production was decreasing by increasing flushes but the total production had found maximum similar to other studies (Jiskani et al., 1999; Dundar et al., 2008; Sharma et al., 2013).

Based on the result of current study, it could be concluded that humidifying and ventilation system

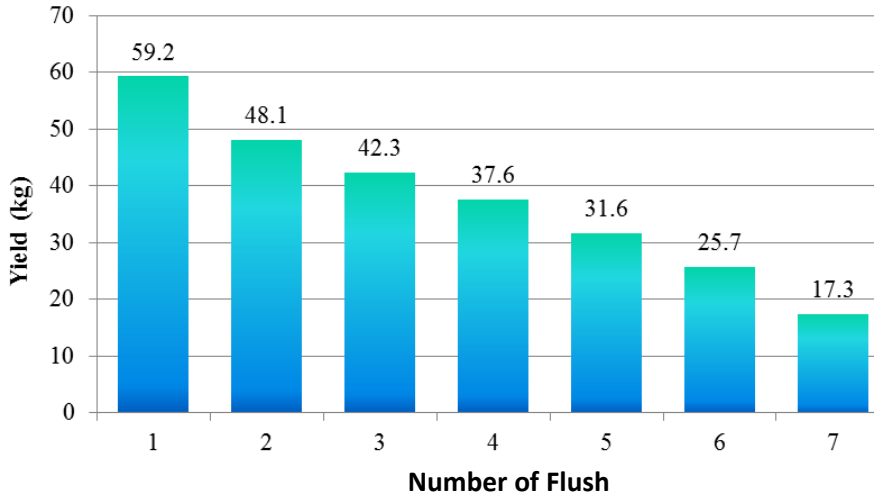

Figure 10. Total yield performance in the optimized cultivation of system.

influenced the indoor mushroom cultivation. It is very well known that low temperature and high humidity favoured the mushroom cultivation by many researches. This study showed the way of controlling indoor environment for commercial mushroom cultivation. The optimized procedure for humidifying able to maintain optimum humidity with tolerable temperature which may ensure the continuous production of mushroom all over the years by independent of weather.

Conflict of Interests

The authors have not declared any conflict of interests.

REFERENCES

Bano Z, Rajarathnam S (1982). Studies on the cultivation of *Pleurotus sajor-caju*. Mushroom J. 1:243-246.

Barney DL (2000). Growing Mushrooms Commercially: Risks and Opportunities. University of Idaho, College of Agriculture, Cooperative Extension System, Agricultural Experiment Station.

Chang ST, Miles PC (2004). Cultivation, Nutritional Value, Medicinal Effect and Environmental Impact of Mushrooms. CRC Press, Bora Raton, London, New York, Washington DC.

Curvetto NR, Gonzalez Matute R, Figlas D, Delmastro S (2004). Oyster mushroom cultivation. MushWorld. China.

Deacon J (2013). Fungal Biology. 4th Edition. Blackwell publishing, UK.

Dundar A, Acay H, Yildiz A (2008). Yield performances and nutritional contents of three oyster mushroom species cultivated on wheat stalk. J. Biotechnol. 7:3497-3501.

Haimid MT, Rahim H, Dardak RA (2013). Understanding the mushroom industry and its marketing strategies for fresh produce in Malaysia. Econ. Technol. Manage. Rev. 8:27-37.

Islam MT, Zakaria Z, Hamidin N, Ishak MABM (2016). Characteristics of Indoor Mushroom Cultivation of Grey Oyster (*Pleurotus pulmonarius*) by Different Stages of Humidifying Treatment. World Appl. Sci. J. 34:1066-1075.

Jang KY, Jhune CS, Park JS, Cho SM, Weon HY, Cheong JC, Choi SG, Sung JM (2003). Characterization of fruitbody morphology on various environmental conditions in *Pleurotus ostreatus*. Mycobiology 31:145-150.

Jiskani MM, Pathan MA, Wagan KH (1999). Yield performance of oyster mushroom *Pleurotus florida* (strain PK, 401) on different substrates. Pak. J. Agric. Eng. Vet. Sci. 15:26-29.

Kong W-S (2004). Descriptions of commercially important Pleurotus species. Oyster mushroom Cultiv Part II Oyster mushrooms Seoul Heineart Inc. pp. 54-61.

Sarker NC, Hossain MM, Sultana N, Mian IH, Karim AJ, Amin SM (2008). Relationship between Nutrient Content in substrates and Economic Yield of Oyster Mushroom (*Pleurotus ostreatus*). Bangladesh J. Mushroom 2:27-33.

Seung Joo Go, Byun MO, You CH, Park YH (1984). Selection of Pleurotus sajor-caju as Suitable Species for Cultivation under Summer Climatic Conditions in Korea. Korea J. Mycol. 12:53-58.

Sharma S, Kailash R, Yadav P, Pokhrel CP (2013). Growth and Yield of Oyster mushroom (*Pleurotus ostreatus*) on different substrates. J. New Biol. Rep. 2:3-8.

Shen Q, Royse D (2001). Effects of nutrient supplements on biological efficiency, quality and crop cycle time of maitake (*Grifola frondosa*). Appl. Microbiol. Biotechnol. 57:74-78.

Subramanian K, Shanmugasundaram K, Muthu N (2014). Spawn Production And Cultivation Strategies For *Pleurotus eous* (Pink Oyster Mushroom). World J. Pharm. Pharm. Sci. 3:915-924.

Thepa S, Kirtikara K, Hirunlabh J, Khedari J (1999). Improving indoor conditions of a Thai-style mushroom house by means of an evaporative cooler and continuous ventilation. Renew. Energy 17:359-369.

Uddin MN, Yesmin S, Khan MA, Tania M, Moonmoon M, Ahmed S (2011). Production of Oyster Mushrooms in Different Seasonal Conditions of Bangladesh. J. Sci. Res. 3:161-167.

Veena SS, Pandey M (2012). Physiological and cultivation requirements of Trametes versicolor, a medicinal mushroom to diversify Indian mushroom industry. Indian J. Agric. Sci. 82:672-675.

Wafi SR, Ismail MR, Ahmed EM (2011). A Case Study of the Climate Factor on Thermal Comfort for Hostel Occupants in Universiti Sains Malaysia (USM), Penang, Malaysia. J. Sustain. Dev. 4:50-57.

Yang J, Zhao J, Yu H, Wang Y, Wang R, Tang L (2013). Mathematical Study of the Effects of Temperature and Humidity on the Morphological Development of *Pleurotus eryngii* Fruit Body. In. Computer and Computing Technologies in Agriculture VI. Springer, pp. 312-323

African Journal of Biotechnology

Related Journals Published by Academic Journals

- *Biotechnology and Molecular Biology Reviews*
- *African Journal of Microbiology Research*
- *African Journal of Biochemistry Research*
- *African Journal of Environmental Science and Technology*
- *African Journal of Food Science*
- *African Journal of Plant Science*
- *Journal of Bioinformatics and Sequence Analysis*
- *International Journal of Biodiversity and Conservation*

academicJournals